In search of retinal biomarkers for HIV related neurodegeneration

Demirkaya, N.

Nazlı Demirkaya

In search of retinal biomarkers for HIV related neurodegeneration:

The AGE$_h$IV and NOVICE studies

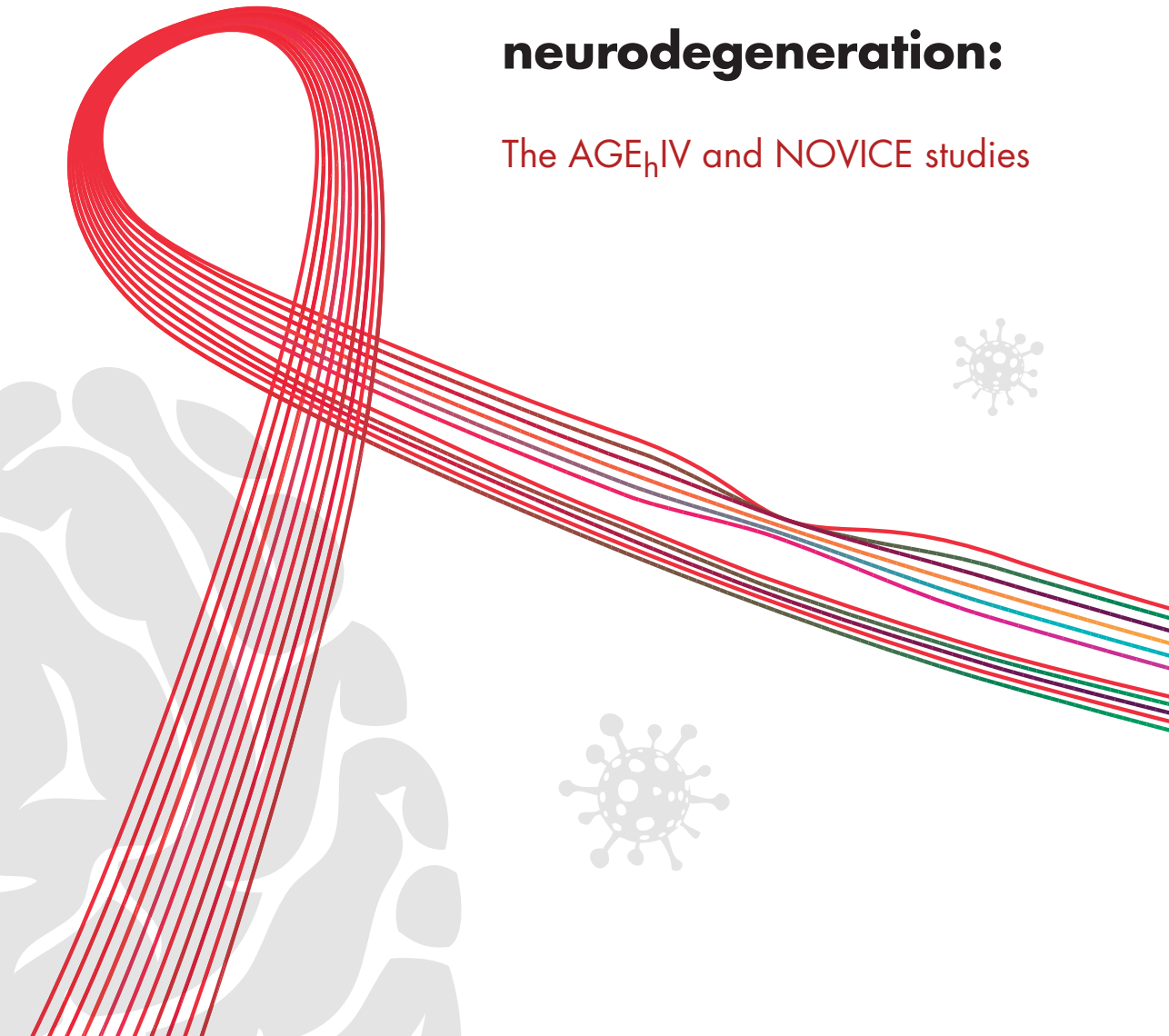

Nazlı Demirkaya

In search of retinal biomarkers for HIV related neurodegeneration:

The AGE$_h$IV and NOVICE studies

ISBN: 978-94-6361-097-1

Layout and printed by: Optima Grafische Communicatie (www.ogc.nl)

Funding: The research described in this thesis (based on the AGE$_h$IV and NOVICE studies) was supported by The Netherlands Organisation for Health Research and Development (ZonMW) (grant nr 300020007), AIDS Fonds (grant nrs 2009063 and 2012033), The Emma Foundation (grant 11.001), Foundation Nuts Ohra, Boehringer Ingelheim (unrestricted grant) and Bayer Healthcare (Global Ophthalmology Awards Program 2012).

Publication of this thesis was financially supported by Oculenti and Bayer Healthcare.

In search of retinal biomarkers for HIV related neurodegeneration: the AGE$_h$IV and NOVICE studies

ACADEMISCH PROEFSCHRIFT

ter verkrijging van de graad van doctor
aan de Universiteit van Amsterdam
op gezag van de Rector Magnificus
prof.dr.ir. K.I.J. Maex
ten overstaan van een door het College voor Promoties ingestelde commissie,
in het openbaar te verdedigen in de Agnietenkapel
op dinsdag 29 mei 2018, te 10 uur

door
Nazlı Demirkaya

geboren te Schiedam

PROMOTIECOMMISSIE

Promotor	Prof. Dr. R.O. Schlingemann	
Copromotores	Dr. F.D. Verbraak	AMC-UvA
	Dr. F.W.N.M. Wit	AMC-UvA
Overige leden	Prof. Dr. C.J.F. Boon	AMC-UvA
	Prof. Dr. C.C.W. Klaver	Erasmus Universiteit Rotterdam
	Prof. Dr. P. Portegies	AMC-UvA
	Prof. Dr. J.M. Prins	AMC-UvA
	Prof. Dr. L. Reneman	AMC-UvA
	Dr. H.J. Scherpbier	AMC-UvA
	Prof. Dr. J.R. Vingerling	Erasmus Universiteit Rotterdam

Faculteit der Geneeskunde

Ter nagedachtenis aan mijn vader
Babamın anısına

TABLE OF CONTENTS

CHAPTER 1 Thesis outline

INTRODUCTION

Since combination antiretroviral therapy (cART) became widely accessible in developed countries, the incidence of Human Immunodeficiency Virus (HIV)-associated dementia and other severe central nervous system abnormalities, as well as HIV-related retinal disease, such as cytomegalovirus retinitis, has decreased dramatically.[1-3] Nevertheless, even in cART-treated HIV-patients both subtle brain and retinal functional and (micro) structural alterations have been reported, which have been termed *HIV-associated neurocognitive disorder* (HAND) and *HIV-associated neuroretinal disorder* (HIV-NRD), respectively.[4,5] As neuroretinal tissue can be considered to be an extension of the brain,[6] these abnormalities may have a shared pathophysiology, which could include direct HIV neurotoxicity, HIV-induced immune activation and neuro-inflammation.[4,5,7-12]

The availability of objective, reliable non-invasive biomarkers offers great advantages in assessing central nervous system (CNS) involvement and monitoring disease progression in patients with sustained suppression of HIV on cART. Current state-of -the-art MRI techniques enable detailed non-invasive investigation of brain structure and physiology in vivo. For example, Diffusion Tensor Imaging (DTI) is a highly sensitive MRI-based neuro-imaging technique, which captures subclinical white matter structure alterations by measuring molecular diffusion of water.

Although brain MRI markers are now widely used to study HIV-related neurodegeneration,[9,13-16] undergoing MRI scanning is time-consuming, expensive and not applicable for some patients due to MRI-contra-indications.

Unlike the brain, direct visualization of the retina is relatively simple and rapid with non-invasive high-resolution optical imaging techniques, in particular optical coherence tomography (OCT), which enables the visualization of retinal structures with a depth resolution of approximately 5 µm, and a lateral resolution of 15 µm.

In recent years, several combined OCT/MRI studies have explored retinal thickness (RT) as a potential proxy for brain structural damage and dysfunction in several neurodegenerative conditions, as well as healthy aging.[6,17-19] Similar comparative imaging studies on HIV-related neuroretinal degeneration and brain abnormalities are lacking; to our knowledge, we are the first to report on this subject **(this thesis;[20]).**

STUDY POPULATION

AGE$_h$IV study

The results of the research described in **Chapters 4 and 5** of this thesis are part of the neuro(retinal)- imaging substudy of the AGE$_h$IV cohort study. The AGE$_h$IV cohort study is a longitudinal observational comparative study on the prevalence, incidence and risk factors for age-associated comorbidities and organ dysfunction in HIV-infected patients aged 45 years or older and HIV-uninfected but otherwise similar controls.[21] The HIV-infected patients were recruited from the HIV-outpatient clinic of the Academic Medical Center in Amsterdam and the HIV-uninfected controls were recruited at the sexual health clinic of the Public Health Service in Amsterdam. The two groups shared a similar socio-demographic background and life-style.

The neuro(retinal)-imaging substudy of the AGE$_h$IV cohort study was initiated to gain further insight into the HIV-related effects on cognitive impairment, brain structure and retinal functional and structural alterations.[9,14,15,22-24]

NOVICE study

As in HIV-infected adults, the prevalence of severe CNS abnormalities in HIV-infected children, such as HIV-encephalopathy, has decreased dramatically since the introduction of cART.[25] Nevertheless, cART- treated HIV-infected children still encounter neurological and cognitive problems with macro- and microstructural cerebral damage that can be present subclinically.[26,27] In addition, retinal abnormalities have been described in perinatally HIV-infected children on cART.[28,29]

The NOVICE study (which can be considered to be the pediatric counterpart of the AGE$_h$IV study) was designed to evaluate neurological and neurocognitive disorders, neuroradiological and retinal alterations in perinatally HIV-infected children (aged 8-18 years) as compared to age, sex, ethnicity and socio-economic status (SES) matched healthy controls in the Netherlands.[30,31] In **Chapters 6 and 7** we describe the ophthalmic findings of this study.[20,32]

GENERAL AIM AND THESIS OUTLINE

The main goal of this thesis was to assess whether HIV-infected patients (adults and children respectively), receiving long-term cART with systemically well-controlled infection, are still at risk for retinal neurodegeneration, and to determine the value of

retinal thickness (measured with spectral-domain (SD)-OCT) as a potential biomarker for brain alterations in HIV-infected patients.

As a general introduction, in **Chapter 2**, we provide an overview of studies investigating HIV-NRD in HIV patients on cART without a history of opportunistic ocular infections, and try to elucidate underlying mechanisms and associated risk factors.[5]

When studying changes over time in retinal thickness, it is essential to distinguish disease processes from normal age-related changes. In **Chapter 3** we evaluate the associations of age with the thickness of individual retinal layers, measured with SD-OCT, in a population of healthy individuals.[33]

Neuroretinal changes in HIV-infected adults

In **Chapter 4** we assess the prevalence and risk factors of retinal structural and functional loss in HIV-infected adult patients with prolonged suppressed viremia on cART as compared to HIV-uninfected controls[24]; subsequently, in **Chapter 5** we investigate associations between retinal thickness and both white matter (WM) integrity and cerebral volume, by means of SD-OCT and advanced MRI techniques (DTI) (manuscript in preparation).

Neuroretinal changes in HIV-infected children

Chapter 6 describes functional and structural retinal differences between a group of perinatally HIV-infected children and matched healthy controls.[32] In **Chapter 7** we explore associations between retinal thickness and cerebral abnormalities in the same study population.[20]

Finally, in **Chapter 8**, we summarize and review the main findings of this thesis.

REFERENCES

1. McArthur JC, Hoover DR, Bacellar H, et al. Dementia in AIDS patients: incidence and risk factors. Multicenter AIDS Cohort Study. *Neurology.* 1993;43(11):2245-2252.
2. d'Arminio Monforte A, Cinque P, Mocroft A, et al. Changing incidence of central nervous system diseases in the EuroSIDA cohort. *Ann Neurol.* 2004;55(3):320-328.
3. Port AD, Orlin A, Kiss S, Patel S, D'Amico DJ, Gupta MP. Cytomegalovirus Retinitis: A Review. *J Ocul Pharmacol Ther.* 2017;33(4):224-234.
4. Schouten J, Cinque P, Gisslen M, Reiss P, Portegies P. HIV-1 infection and cognitive impairment in the cART era: a review. *AIDS.* 2011;25(5):561-575.
5. Demirkaya N, Wit F, Schlingemann R, Verbraak F. Neuroretinal Degeneration in HIV Patients Without Opportunistic Ocular Infections in the cART Era. *AIDS Patient Care STDS.* 2015;29(10):519-532.
6. London A, Benhar I, Schwartz M. The retina as a window to the brain-from eye research to CNS disorders. *Nat Rev Neurol.* 2013;9(1):44-53.
7. Joseph J, Colosi DA, Rao VR. HIV-1 Induced CNS Dysfunction: Current Overview and Research Priorities. *Curr HIV Res.* 2016;14(5):389-399.
8. Deeks SG. HIV infection, inflammation, immunosenescence, and aging. *Annu Rev Med.* 2011;62:141-155.
9. Su T, Caan MW, Wit FW, et al. White matter structure alterations in HIV-1-infected men with sustained suppression of viraemia on treatment. *AIDS.* 2016;30(2):311-322.
10. Abdulle S, Mellgren A, Brew BJ, et al. CSF neurofilament protein (NFL) -- a marker of active HIV-related neurodegeneration. *J Neurol.* 2007;254(8):1026-1032.
11. Eden A, Fuchs D, Hagberg L, et al. HIV-1 viral escape in cerebrospinal fluid of subjects on suppressive antiretroviral treatment. *J Infect Dis.* 2010;202(12):1819-1825.
12. Xu H, Chen M, Forrester JV. Para-inflammation in the aging retina. *Prog Retin Eye Res.* 2009;28(5):348-368.
13. Thompson PM, Jahanshad N. Novel Neuroimaging Methods to Understand How HIV Affects the Brain. *Curr HIV/AIDS Rep.* 2015;12(2):289-298.
14. Su T, Mutsaerts HJ, Caan MW, et al. Cerebral blood flow and cognitive function in HIV-infected men with sustained suppressed viremia on combination antiretroviral therapy. *AIDS.* 2017;31(6):847-856.
15. Su T, Wit FW, Caan MW, et al. White matter hyperintensities in relation to cognition in HIV-infected men with sustained suppressed viral load on combination antiretroviral therapy. *AIDS.* 2016;30(15):2329-2339.
16. van Zoest RA, Underwood J, De Francesco D, et al. Structural Brain Abnormalities in Successfully Treated HIV Infection: Associations With Disease and Cerebrospinal Fluid Biomarkers. *J Infect Dis.* 2017;217(1):69-81.
17. Mutlu U, Bonnemaijer PWM, Ikram MA, et al. Retinal neurodegeneration and brain MRI markers: the Rotterdam Study. *Neurobiol Aging.* 2017;60:183-191.
18. Liu S, Ong YT, Hilal S, et al. The Association Between Retinal Neuronal Layer and Brain Structure is Disrupted in Patients with Cognitive Impairment and Alzheimer's Disease. *J Alzheimers Dis.* 2016;54(2):585-595.
19. Pietroboni AM, Dell'Arti L, Caprioli M, et al. The loss of macular ganglion cells begins from the early stages of disease and correlates with brain atrophy in multiple sclerosis patients. *Mult Scler.* 2017:1352458517740214.

20. Blokhuis C, Demirkaya N, Cohen S, et al. The Eye as a Window to the Brain: Neuroretinal Thickness Is Associated With Microstructural White Matter Injury in HIV-Infected Children. *Invest Ophthalmol Vis Sci.* 2016;57(8):3864-3871.
21. Schouten J, Wit FW, Stolte IG, et al. Cross-sectional comparison of the prevalence of age-associated comorbidities and their risk factors between HIV-infected and uninfected individuals: the AGEhIV cohort study. *Clin Infect Dis.* 2014;59(12):1787-1797.
22. Schouten J, Su T, Wit FW, et al. Determinants of reduced cognitive performance in HIV-1-infected middle-aged men on combination antiretroviral therapy. *AIDS.* 2016;30(7):1027-1038.
23. Su T, Schouten J, Geurtsen GJ, et al. Multivariate normative comparison, a novel method for more reliably detecting cognitive impairment in HIV infection. *AIDS.* 2015;29(5):547-557.
24. Demirkaya N, Wit FW, van Den Berg TJ, et al. HIV-Associated Neuroretinal Disorder in Patients With Well-Suppressed HIV-Infection: A Comparative Cohort Study. *Invest Ophthalmol Vis Sci.* 2016;57(3):1388-1397.
25. Patel K, Ming X, Williams PL, Robertson KR, Oleske JM, Seage GR, III. Impact of HAART and CNS-penetrating antiretroviral regimens on HIV encephalopathy among perinatally infected children and adolescents. *AIDS.* 2009;23(14):1893-1901.
26. Blokhuis C, Kootstra NA, Caan MWA, Pajkrt D. Neurodevelopmental delay in pediatric HIV/AIDS: current perspectives. *Neurobehavioral HIV Medicine.* 2015.
27. Hoare J, Ransford GL, Phillips N, Amos T, Donald K, Stein DJ. Systematic review of neuroimaging studies in vertically transmitted HIV positive children and adolescents. *Metab Brain Dis.* 2014;29(2):221-229.
28. Moschos MM, Margetis I, Markopoulos I, Moschos MN. Optical coherence tomography and multifocal electroretinogram study in human immunodeficiency virus-positive children without infectious retinitis. *Clin Exp Optom.* 2011;94(3):291-295.
29. Moschos MM, Mostrou G, Psimenidou E, Spoulou V, Theodoridou M. Objective analysis of retinal function in HIV-positive children without retinitis using optical coherence tomography. *Ocul Immunol Inflamm.* 2007;15(4):319-323.
30. Cohen S, Caan MWA, Mutsaerts H, et al. Cerebral injury in perinatally HIV-infected children compared to matched healthy controls. *Neurology.* 2015.
31. Cohen S, Ter Stege JA, Geurtsen GJ, et al. Poorer cognitive performance in perinatally HIV-infected children versus healthy socioeconomically matched controls. *Clin Infect Dis.* 2015;60(7):1111-1119.
32. Demirkaya N, Cohen S, Wit FW, et al. Retinal Structure and Function in Perinatally HIV-Infected and cART-Treated Children: A Matched Case-Control Study. *Invest Ophthalmol Vis Sci.* 2015;56(6):3945-3954.
33. Demirkaya N, van Dijk HW, van Schuppen SM, et al. Effect of age on individual retinal layer thickness in normal eyes as measured with spectral-domain optical coherence tomography. *Invest Ophthalmol Vis Sci.* 2013;54(7):4934-4940.

CHAPTER 2

General introduction: Neuroretinal degeneration in HIV patients without opportunistic infections in the cART era

Nazli Demirkaya
Ferdinand W. Wit
Reinier O. Schlingemann
Frank D. Verbraak

Published in: AIDS Patient Care and STDs, 2015 Oct;29(10):519-32.

ABSTRACT

Subtle structural and functional retinal abnormalities, termed 'HIV-associated Neuroretinal Disorder (HIV-NRD)', have been reported in HIV patients receiving combination antiretroviral therapy (cART), without infectious retinitis or any apparent fundus abnormalities otherwise.

In this review, we provide an overview of studies investigating HIV-NRD in HIV patients without opportunistic ocular infections in the cART era, and try to elucidate underlying mechanisms and associated risk factors.

Most studies focused on patients with severe immune-deficiency and demonstrated that patients with nadir CD4 counts <100 cells/µl are most at risk for neuroretinal damage, with a thinner retinal nerve fiber layer, subtle loss of color vision and/or contrast sensitivity, visual field deficits and subnormal electrophysiological responses. In contrast, alterations in retinal vascular calibers and retinal blood flow were not associated with nadir CD4 counts, but instead with detectable viremia, suggesting a role for (chronic) inflammation in microvascular damage.

Although the alterations in visual function are subtle, they can lead to difficulties in activities, such as reading or driving, thereby affecting quality of life. Since HIV has become a chronic disease, its long-term effects with respect to visual function loss become more important, as is recently emphasized by a longitudinal study, reporting that AIDS patients with HIV-NRD have higher risks of developing bilateral visual impairment and even blindness than patients without HIV-NRD.

The question remains whether patients with high (>350 cells/µl) nadir CD4 counts and well-suppressed HIV infection on cART remain at risk for HIV-NRD, as this group constitutes a growing part of the ageing HIV-infected population.

Key words: HIV-neuroretinal disorder, visual function, retinal nerve fiber layer thickness, optical coherence tomography, retinal vascular calibers, Pelli-Robson contrast sensitivity

INTRODUCTION

The introduction of combination antiretroviral therapy (cART) has altered the spectrum of HIV-related retinal disease, with a major decline in incidence of opportunistic infections such as cytomegalovirus retinitis, and an increased risk for non-infectious age-related retinopathies (e.g. diabetic retinopathy and glaucoma),[1] the consequence of a considerably higher life-expectancy of cART-treated patients.

Furthermore, in the last few years, subtle subclinical retinal abnormalities have been reported in HIV patients, treated with cART, without infectious retinitis and any visible fundus abnormalities. Several studies demonstrated decreased visual function in HIV patients without retinitis, such as a subtle loss of color vision and/or contrast sensitivity, visual field deficits and subnormal electrophysiological responses.[2-12] Structural studies showed a thinner peripapillary retinal nerve fiber layer thickness, especially in patients with nadir CD4 counts<100 cells/µl, using several techniques, such as optical coherence tomography and scanning laser polarimetry (GDx).[2,5,13-17] In addition, changes in retinal vascular calibers have been reported in these patients, as well as ocular hemorheological abnormalities.[18-25]

These findings are thought to be part of an 'HIV-associated Neuroretinal Disorder' (HIV-NRD) and may be associated with a broader spectrum of neurological abnormalities reported in cART-treated HIV patients, including HIV-associated neurocognitive disorder (HAND),[26] subtle brain alterations[27,28] and autonomic dysfunction.[29] The pathophysiology underlying both the neuroretinal and central nervous system (CNS) changes is largely unknown, but may be mediated by similar processes, such as a long-standing (micro)vasculopathy,[18-24,30] direct damage of neural tissue by HIV and/or cART,[31] chronic immune activation and inflammation[32,33] and accelerated/accentuated biological aging of the HIV-infected population.[34,35]

In this review we describe and compare studies investigating HIV-NRD in HIV patients without (prior) opportunistic ocular infections, specifically in the cART era, and try to elucidate the possible underlying mechanisms and associated risk factors. Since HIV has become a chronic disease, it is important to preserve the quality of life of HIV patients as they age, which may be affected by a decrease in contrast sensitivity and color vision, by an impaired reading speed,[36] and by disturbed visual function, resulting in for example difficulties in driving.[37,38]

Studies are categorized in 6 sections: functional, structural, structure and function combined, vascular and genetic studies exploring HIV-NRD. A separate section addresses the possible mechanisms and pathophysiology of HIV-NRD.

FUNCTIONAL STUDIES

Multifocal electroretinography

Multifocal electroretinography (mfERG) is used to measure ERG activity in small areas of the retina, in the posterior pole, localizing focal retinal damage occurring in a variety of diseases, including diabetes **(Figure 1)**. Parameters of the mfERG can be separately related to the function of the outer retina or the inner retina. Special computational programs are provided with the recording system for multifocal ERG to extract the first- and second-order kernels. The first-order kernel (FOK) response reflects mainly outer retinal function (receptor cells and bipolar cells) with little contribution by ganglion cells, while the second-order kernel (SOK) parameters are thought to reflect early changes in adaptive retinal mechanisms and inner retina cell function (ganglion cells).

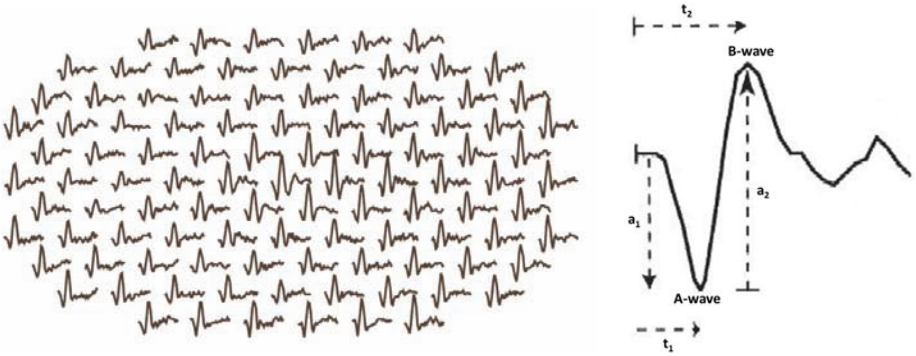

FIGURE 1. The multifocal electroretinogram (mfERG) technique allows local ERG responses to be recorded simultaneously (left). The ERG waveform consists of a negative a-wave followed by a positive b-wave (right). Parameters measured are: 1) the amplitude from the baseline to the negative trough of the a-wave (a_1) and the amplitude of the b-wave measured from the trough of the a-wave to the following peak of the b-wave (a_2); and 2) the ''implicit times'': time from flash onset to the trough of the a-wave (t_1) and the time from flash onset to the peak of the b-wave (t_2).

In an early pilot study by Falkenstein et al.[3] using mfERG (RETIscan, Version 3.1) analyzing the FOK, no differences in amplitudes and implicit times between groups were found, although this study consisted of only a small number of patients (15 HIV patients and 15 controls). Also there was no correlation between local visual field defects (Humphrey VFA; 6 of 10 studied eyes) and mfERG responses in corresponding areas.

These results suggest inner retinal damage (visual field defects) in HIV patients without infectious retinitis, while the outer retina is spared (normal mfERG FOK responses).

In a second study by Falkenstein et al.,[4] three groups of patients were evaluated by mfERG: 50 HIV patients with a nadir CD4 count above 100 cells/mm^3, 56 HIV patients whose nadir CD4 count was less than 100 cells/mm^3 for at least 6 months and a group consisting of 41 HIV-negative controls. Although there were no significant differences in amplitudes between the groups in both kernels, widespread delays in implicit times were found in both kernels, especially in the patients with low nadir CD4 counts. These findings reflect subtle functional changes before noticeable diminished amplitudes or clinically relevant vision loss.

A subsequent study,[12] using support vector machine (a machine learning classifier) to analyze the SOK response of mfERG, confirmed the presence of mfERG SOK abnormalities in HIV patients; more specifically, delayed implicit times were found. The new finding in this study was the comparable severity of the delay in implicit times in both low and high nadir CD4 groups. The authors concluded that the support vector machine was more sensitive in detecting mfERG abnormalities than standard linear classifiers. A limitation of these studies is the lack of information on (current) CD4 counts, viral load levels or cART.

Visual fields

Machine learning classifiers were also used in a study by Kozak et al.[8] to analyze visual field defects (Humphrey Visual Field Analyzer, model 620) in 35 HIV patients with CD4 counts <100 cells/µl at some point during their medical history for at least 6 months, 38 HIV patients with nadir CD4 counts >100 cells/µl, and 52 HIV-negative individuals. All HIV patients were treated with cART prior to and at the time of examination; data on current CD4 counts and viral load levels was not described. Patients in the low CD4 group had visual field defects, especially in the visual field superiorly near the blind spot, implying more pronounced damage to the retina inferiorly near the optic disc. Although most visual fields appeared normal in the group of patients with higher CD4 counts, the machine learning classifiers were able to distinguish these eyes from normal eyes, whereas human experts rated most of these visual fields as normal. The locations of the visual field defects in the high CD4 group followed no specific pattern.

Visual field results are generally expressed as mean deviation (MD) and pattern standard deviation (PSD). The MD gives an overall value of the total amount of visual field loss, and the MD value becomes more negative as the overall field worsens. The PSD is

designed to highlight localized defects by accounting for generalized visual field loss (likely due to a cataract). A high PSD indicate a non-uniform sensitivity loss.

Freeman et al.[6] also used the Humphrey Field analyzer (model 600/700) to asses visual field function in 1336 patients diagnosed with AIDS (without ocular opportunistic infections), participating in the prospective Longitudinal Study of Ocular Complications of AIDS (LSOCA). The study population consisted mainly of males (80%), approximately 80% of the patients were on cART during the time of examination, with a median current CD4 count of 180 (quartiles: 71,328) cells/µl and a median HIV viral load of 1518 (200,56957) copies/ml. Median nadir CD4 count was 42 (13-106) cells/µl and median time since AIDS diagnosis was 4.1 (1.7-6.9) years.

Since there was no control group, visual field results were compared with published visual field data from a healthy population of the Diagnostic Innovations in Glaucoma Study (DIGS). Thirty-nine percent of the examined eyes had an abnormal mean deviation defined as less than the lowest 2.5 percentile (-2.63 decibels [dB]) from the expected distribution of DIGS controls with normal vision, and 33% of the eyes had an abnormal pattern standard deviation (higher than the upper 2.5 percentile (2.57 dB) from the expected distribution of DIGS controls with normal vision). Risk factors for visual field loss included race (higher risk for Blacks and Hispanics versus Whites), intravenous drug use, anemia, lower Karnofsky score and lack of private health insurance, reflecting a higher disease severity and/or less access to care for HIV disease. Although there was no internal control group in this study, the results show that there is a large percentage of patients with an AIDS diagnosis with reduced visual field function.

Color vision and contrast sensitivity

Several studies examined contrast sensitivity and/or color vision in HIV- infected subjects. Shah et al.[11] evaluated contrast sensitivity (CS; Pelli-Robson chart) and color vision (Farnsworth-Munsell 100-Hue color test; FM-100) among 71 HIV patients, with 65 patients having nadir CD4 counts<200 cells/µl (who were also co-enrolled in the LSOCA study). cART was being administered to 55 subjects, median current CD4 counts were 330 (range; 9-998) cells/µl and median HIV viral load was 509 (range; 19-441.661) copies/ml. The results were compared with published values for normal populations. Seven percent of the patients had reduced contrast sensitivity (<1,5 log CS; >2 SD below the mean score for a healthy population described by Myers et al.[39]) and 9,9% had abnormal color vision (> 2 SD above the mean score for a healthy population aged 40-49 years described by Verriest et al.[40]). No relationship was found between impaired CS and impaired color vision. Associations with HIV-related factors were likewise not detected.

Freeman et al.[6] also assessed Pelli-Robson values among 1330 HIV patients diagnosed with AIDS who were participating in the LSOCA study. Approximately 12% of the examined eyes had low contrast sensitivity values (defined as <1,5 log CS). Risk factors for low CS included intravenous drug use, lower education levels and lower current CD4 counts. Discrepancies in the association between CS and CD4 counts in this study compared with the previous study by Shah et al.[11] could be explained by the much smaller sample size of the study by Shah et al.

Follow-up LSOCA study[41]

A recent report by the LSOCA study group[41] describes the incidence, risk factors and long-term outcomes of HIV-associated neuroretinal disorder (HIV-NRD; defined as having a Pelli Robson contrast sensitivity value <1.5 log units) among 1822 patients with AIDS (80% male), having median CD4 counts of 198 (IQR 81-362) cells/µl at enrollment, median nadir CD4 counts of 41 (IQR 13-109) cells/µl and median HIV viral load levels of 2.68 (IQR 1.74-4.59) $\log_{10}$ copies/ml at enrollment. Of the 1822 AIDS patients (of whom 85% were on cART), 294 (16%) had HIV-NRD at enrollment, which was found to be significantly associated with being female, African-American, having lower CD4 counts at enrollment and a positive hepatitis C antibody status. In addition, a significantly lower percentage of patients with HIV-NRD used cART (at present or past) compared to patients without HIV-NRD (79% vs 86%). Patients with HIV-NRD at enrollment had increased risks of bilateral visual impairment (hazard rate [HR] 6.5; 95% CI 2.6-16.0) and blindness (HR 5.9; 95% CI 1.5-23.2) than patients without HIV-NRD, as well as a greater mortality risk (HR 1.7; 95% CI 1.3-2.1)) during follow-up.

The incidence of HIV-NRD was 1.9/100 person-years (95% CI 1.7-2.2/100 PY); risk factors for incident HIV-NRD included- in addition to being female or African-American- a higher age at AIDS diagnosis (HR 1.6; 95% CI 1.2-2.1)), current CD4 counts <100 cells/µl (HR 1.9; 95% CI 1.4-2.8), a detectable (>2.6 log10 copies/ml) HIV viral load (HR 2.2; 95% CI 1.6-3.0) and not being on cART (HR cART-use 0.6; 95% CI 0.4-0.9). The estimated cumulative incidence for HIV-NRD by 20 years after AIDS diagnosis was 51% (95% CI 46-55); among patients with immune recovery (HIV VL<2,6 $\log_{10}$ copies/ml and current CD4 >100 cells/µl), cumulative incidence at 15 years was 30% (95% CI, 21-39).

STRUCTURAL STUDIES

Retinal nerve fiber layer (RNFL) thickness

Since subtle visual abnormalities have been demonstrated in HIV patients, it could be expected that subtle structural changes of the neuroretina are also present, such as a

thinner retinal nerve fiber layer (RNFL) thickness and/or decreased retinal thickness. Several studies have addressed this question, using different imaging techniques, including optical coherence tomography (OCT; see also section *"Structure-Function Relationships"*).

In the last years, OCT (**Figure 2**) has proven to be a highly valuable and commonly used retinal imaging modality. It is a non-invasive technique, similar to ultrasound. With OCT, reflected light is used to produce cross-sectional and 3D images of the retina, making it possible to evaluate retinal layers and the optic disc in great detail.

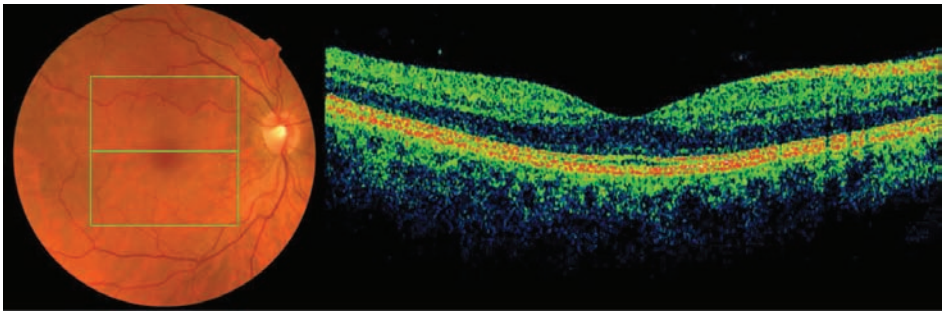

FIGURE 2. Example of a fundus photo (left) and corresponding Spectral-Domain (SD)- OCT scan (right) of the right fovea of a healthy individual, both taken simultaneously with a Topcon 3D OCT-2000 device. In OCT, reflected (near infrared) light is used to form a cross-sectional (B-scan) image of the retina by automatic analysis of the reflective properties of retinal tissue. OCT technology is continually evolving and the introduction of SD-OCT provided greater scanning resolution, higher scan density and a significant increase in scanning speed, allowing for greater data acquisition than the original Time Domain (TD)-OCT (such as the Stratus OCT).

Kozak et al.[14] measured the peripapillary RNFL thickness (Stratus OCT 3000) in HIV patients (n=18) with nadir CD4 counts > 100 cells/µl, HIV patients (n=25) with a history of CD4 counts < 100 cells/µl for at least 6 months, and compared the results with a healthy control group, consisting of 22 individuals. All patients were on cART and most patients were Hispanic. The low nadir CD4 group had a significant lower average RNFL thickness than the other two groups in all quadrants, except the nasal quadrant. No significant differences were found in thickness between the CD4 group with nadir CD4 counts >100 cells/µl and the HIV-negative controls.

Confocal laser scanning ophthalmoscopy (Heidelberg Retinal Tomograph; HRT) and scanning laser polarimetry (GDx-variable corneal compensator [VCC]) were used in a few studies investigating peripapillary RNFL thickness and optic disc parameters in HIV patients without retinitis. Besada et al.[13] compared HRT values between 13 HIV patients, all on antiretroviral therapy, with 12 patients having current CD4 counts >100 cells/µl,

and 13 HIV-negative control subjects. A subgroup of 6 patients and 5 controls were also examined with GDx-VCC. HRT and GDx-VCC indicators of peripapillary RNFL thickness were significantly reduced in HIV-positive patients, while there was a lack of correlation between CD4 counts, viral load, number of ART medications, years since diagnosis of HIV and RNFL thinning, possibly due to the small sample size.

Plummer et al.[17] used the HRT in a cross-sectional study between 17 HIV patients without CMV retinitis or cotton wool spots and 24 age-matched controls. Significant differences were found between the two groups in a number of measures of the peripapillary retinal nerve fiber layer, with worse outcomes in HIV patients without retinitis. Plummer et al. did not indicate whether the patients in his study were using cART nor did he provide information regarding the subjects' CD4 counts or viral load levels.

In a study by Kozak et al.,[15] GDx-VCC was used to measure the peripapillary RNFL in 26 HIV patients with CD4 counts always > 100 cells/μl, 35 HIV patients with nadir CD4 counts <100 cells/μl for at least six months and 25 HIV-negative controls. All patients were on cART. The low nadir CD4 group had significantly lower RNFL values (superior average, inferior average, ellipse average) and a higher nerve fiber indicator value (NFI; a global index of RNFL integrity; higher values increase the likelihood of having glaucoma) than the controls. No significant differences were detected between the high nadir CD4 group and the controls.

It is difficult to correctly interpret these studies, since detailed information on HIV- and cART-related parameters was not given, such as duration of HIV and cART use, current/nadir CD4 counts (and their distribution) and peak/current viral load (and their distribution); however the results of these studies suggest that HIV patients with nadir CD4 counts< 100 cells/μl are more at risk for having a thinner peripapillary RNFL.

STRUCTURE-FUNCTION RELATIONSHIPS

In addition to the aforementioned studies addressing only functional or structural retinal changes in HIV, in recent years there has been an increasing interest in examining possible associations between functional and structural abnormalities in HIV patients.

RNFL thickness and contrast sensitivity/ color vision

In 2012, Kalyani et al.[7] evaluated relationships between contrast sensitivity (Pelli -Robson chart; logCS score), color vision (Lanthony D-15 test; color-confusion index) and peripapillary RNFL thickness (SD-OCT; RTvue) among 57, predominantly male, HIV

patients (89% diagnosed with AIDS; these patients were also enrolled in the LSOCA Study). Median time since HIV diagnosis was 194 (range; 3-359) months, median current CD4 count was 420 (range; 80-1037) cells/µl, median nadir CD4 count was 66 (range; 0-602) cells/µl and median current HIV viral load was 0 (range; 0-188.393) copies/µl. Duration and proportion of patients on cART was not given. The results were compared with published values for normal populations. Mean CS was 1.85 ± 0.14 logCS and mean color-confusion index was 1.74 ± 0.74. Only 2,9% of the eyes had abnormal CS (<1,5 log CS; as described earlier[42]) in contrast to 40,2% of examined eyes with abnormal color vision (color confusion index >1.78, as described by Vingrys and King-Smith[43]). Temporal RNFL thickness was significantly positively correlated with logCS and inversely correlated with color-confusion index. A surprising finding was the presence of a subgroup with average RNFL thickness greater than normal (n=10 eyes; > 1 SD of mean value of average peripapillary RNFL thickness described by Rao et al.[44]). There was a trend for shorter duration of HIV disease for this subgroup than for those with a thin RNFL thickness (13.3 versus 18 years), although this was not statistically significant.

Pathai et al.[10] performed a similar study on peripapillary RNFL thickness (SD-OCT: Opko/OTI) and CS (Pelli-Robson chart) in a South-African (± 70% female) population, consisting of 225 HIV patients without retinal opportunistic infections and 203 healthy controls. Eighty-eight percent of the HIV patients were on cART for a medianduration of 56.5 (IQR 34-74) months. Current and nadir median CD4 counts in this group were 468 (IQR 327-607) cells/µl and 136 (IQR 77-175) cells/µl, respectively. Peak viral load was 4.47(IQR 3.74-4.97) $\log_{10}$ copies/ml, while at present 85% had an undetectable plasma viral load (<50 copies/ml).

Contrast sensitivity was significantly lower in the patient group compared to the controls, although the difference was only one letter (1,76 vs 1,82 logCS). A higher percentage of HIV patients had 'poor' CS (<1.65 logCS; defined using the cut-off value of the 25th percentile in the control group) compared to the control group (43.5% vs 31.8%). Among the HIV patients on cART, 'poor' CS was significantly associated with a positive frailty status and HIV viral load > 2 log copies/ml.

The peripapillary RNFL thickness (average and per quadrants) was not significantly different between the two groups, in contrast to other studies reporting a thinner RNFL, especially in HIV patients with low nadir CD4 counts.[5,14] Associations between RNFL thickness and nadir/current CD4 counts were not detected. An unexpected and new finding was a trend for increased superior quadrant RNFL thickness with higher values of viremia, with ART-naïve HIV patients and a detectable viral load having an increased

RNFL thickness (140 µm) in comparison with HIV negative controls (132.2 µm) and HIV patients on cART with undetectable VL (133.8 µm).This is the second study reporting an increased RNFL thickness in a subgroup of HIV patients. Longer ART duration was significantly associated with thinning of inferior and nasal RNFL quadrants. A lower CS was associated with a thin temporal RNFL, in agreement with the previous study by Kalyani et al.[11]

RNFL, macular thickness and visual fields

Arantes et al. conducted two studies comparing OCT findings (Stratus OCT) with frequency-doubling technology (FDT) perimetry (FDT Humphrey Matrix; Carl Zeiss Meditac, Dublin, California; and Welch-Allyn, Skaneateles, New York, USA) outcomes. It is thought that FDT reflects the function of ganglion cells involved in the magnocellular pathway. Like the Humphrey Field Analyzer, the main FDT outcome measures are mean deviation (MD), pattern standard deviation (PSD) and glaucoma hemifield test (GHT). The first study[5] was published in 2010 and compared macular retinal thickness and peripapillary RNFL thickness with visual field outcomes between 26 HIV patients with a CD4 count < 100 cells/mm^3 for minimal 6 months in their medical history (Group A), 25 HIV patients with CD4 counts always >100 cells/mm^3 since diagnosis (Group B) and 22 HIV negative controls (Group C). Nadir and current mean (± standard error [SE]) CD4 counts were 28.31 ± 4.67 cells/mm^3 and 219.96 ± 49.18 cells/mm^3 in group A and 301.08 ± 31.11 cells/mm^3 and 502.29 ± 41.36 cells/mm^3 in group B. All HIV patients were on cART and mean (±SE) time since HIV lab diagnosis (group A: 100.73 ± 15.45 months; group B: 85.88 ± 10.03 months) and cART use (group A: 70.96 ± 13.81 months; group B: 76.96 ± 10.34 months) was not significantly different between the two groups.

Average peripapillary RNFL thickness as well as RNFL thickness in quadrants (with the exception of the temporal quadrant) was significantly reduced in the low nadir CD4 group compared to the other groups. The temporal and inferior outer macula were also significantly thinner in the low nadir CD4 group. Thickness measurements were not significantly different between the high nadir CD4 group and the controls. The FDT mean deviation (MD) values were significantly worse in the low nadir CD4 group versus the controls; the pattern standard deviation (PSD) values were significantly worse in the low nadir CD4 group compared to both the high nadir CD4 group and controls. In addition, abnormal Glaucoma Hemi-field Test (GHT) results were found more frequently in patients with low nadir CD4 counts. Eyes of HIV patients with GHT and PSD results outside normal confidence limits of the normative database of the perimeter had a significant thinner average peripapillary RNFL than eyes with results within normal limits in the same group of patients. These results are in accordance with previous studies

demonstrating that patients with low nadir CD4 counts are more at risk of developing structural and/or functional retinal abnormalities.

The next study by Arantes et al.[2] also compared peripapillary RNFL thickness (Stratus OCT) with FDT results (Humphrey Matrix) in a group of 51 HIV patients, all on cART, versus 22 HIV negative controls. These patients presumably represent the same cohort as reported in the previous study, but without a distinction being made between patients with a low and high nadir CD4 count. Duration since HIV diagnosis and cART were 93.45 ± 66.06 months and 73.90 ± 60.21 months, respectively. Mean current and nadir CD4 counts were 355.48 ± 267.69 cells/µl and 162.02 ± 175.69 cells/µl, respectively. Associations between RNFL thickness and VF sensitivity were evaluated in 12 clock-hour OCT sectors and in 21 VF zones. The HIV-group was significant thinner in sectors 2, 7 and 11. Other sectors as well as the average RNFL thickness were not different between the groups. Statistically significant differences in VF zones were observed in (nasal) zones 14 and 15 only. In HIV-patients, there was no association between the FDT Matrix MD and the OCT average RNFL thickness, although the association between the FDT Matrix PSD and average RNFL thickness was significant. When comparing regional RNFL thinning with locally measured VF zones, the strongest correlations were found between the superior RNFL measurements and inferior VF zones and between the nasal RNFL measurements and temporal VF zones. There were no significant associations between average RNFL thickness and current CD4 count, nadir CD4+ T-cell count, duration of lab diagnosis of HIV-infection or duration of cART. Associations between these HIV-related parameters and VF results were not mentioned.

RNFL thickness & computer-based simulators

Two studies examined the relationship between peripapillary RNFL thickness and specific computer-based simulations. The first study [37] included 22 HIV patients (45% with a nadir CD4 count<100; exact values of nadir and current CD4 counts were not described) and 16 HIV negative controls, who completed a 10.2-mile computer-based, wide field-of-view driving simulation (STISIM driving simulator) in which they had to obey traffic rules and participate in emergency situations as well as more routine settings. A ''weighted error score'' was calculated in order to summarize the participants' driving performance and give greater weight to more dangerous situations. The mean peripapillary RNFL thickness (Stratus OCT3) was significantly thinner in the low nadir CD4 group than the high CD4 group, while a comparison with the HIV negative control group was not made. The HIV group in general had a significantly higher weighted error score than the controls, which was not associated with nadir CD4 counts. Within the HIV group, RNFL thickness was significantly correlated with driving errors. The highest num-

ber of driving errors occurred in individuals with both a low CD4 count and significantly reduced RNFL thickness (<80 µm).

The second study[38] used an interactive computer program (Central Vision Analyzer) to assess vision performance in a time-dependent manner (900 msec. per test) under a variety of light/contrast conditions that simulate stressful and real-world environments. In addition, peripapillary RNFL thickness was measured (Heidelberg Spectralis OCT) and associations between thickness and visual performance were investigated. The patient group included 37 eyes of 19 HIV patients with a nadir CD4 count >200 cells/µl and 52 eyes of 28 HIV patients with a nadir CD4 count <200 cells/µl for a minimum period of 6 months; the exact values and distribution of the nadir CD4 counts were, again, not reported. All patients were on cART for at least 6 months (total duration unknown), mean CD4 count was 672 ± 281 cells/µl (range 264-1305 cells/µl), mean HIV plasma viral load was 24.9 ± 19.8 copies/ml (range 0-50 copies/ml) and the mean estimated duration of HIV was 17.7 years. The control group consisted of 105 eyes of 57 HIV negative controls. The HIV group –in particular the low nadir CD4 group, and also, but to a lesser extent the high nadir CD4 group- performed significantly worse in various mesopic and backlight-glare conditions than the control group. There was no difference in visual performance between the two HIV subgroups. The average peripapillary RNFL thickness was similar between the 3 groups, but after changing the definition of low nadir CD4 from 200 to 100 cells/µl, the thickness turned out to be significantly different between the groups, more specifically in the low nadir CD4 group versus the controls. There was no significant correlation between estimated duration of HIV and visual scores in any CVA module or RNFL thickness, respectively. RNFL thickness, and more specifically the temporal-inferior sector, was significantly associated with visual scores under various mesopic conditions. Like in previous studies mentioned earlier, this study shows that patients with low nadir CD4 counts are at a higher risk for developing thinning of the RNFL and visual abnormalities.

RETINAL VASCULAR CALIBERS AND HEMORHEOLOGY

Despite a substantial decrease in incidence of non-infectious HIV retinopathy, subclinical retinal microvascular changes and abnormalities in blood flow have been reported in HIV patients, even in the cART era. It is thought that these abnormalities play a role in developing HIV-NRD (see also section ''*Pathophysiology*'').

Hemorheological abnormalities

Blue field entoptoscopy uses the 'blue field entoptic phenomenon', allowing patients to view their own circulating macular leukocytes. The retina is exposed to a diffuse blue light with a wavelength of 430 nm, enabling perception of tiny bright dots moving quickly along curved lines in the visual field, corresponding to the patient's leukocytes moving in the macular retinal capillaries within a 20 degree region centered around the foveola. The patient compares the velocity and density of these particles to that of similar particles in a computer-generated simulation that is intermittently shown to the patients. Macular leukocyte velocity and perceived leukocyte density are measured.

Lim et al.[21] determined whether HIV patients have decreased macular capillary blood flow in vivo, by using the blue field simulation technique (BFS-2000, Oculix). Forty-one HIV patients without CMV retinitis or any signs of retinopathy, and 31 HIV negative controls were examined. Current CD4 counts ranged between 0-800 cells/µl in the HIV positive group, with counts <50 cells/µl in 10 patients, between 50 – 200 cells/µl in 9 patients and > 200 cells/ul in 22 patients. Among the last group, nadir CD4 count had been <50 cells/µl in 7 individuals and >200 cells/µl in 9 individuals.

Mean current HIV viral load was 65 ± 125 x 10^3 copies/ml. Both mean macular leukocyte velocity and mean perceived leukocyte density were found to be significantly lower in the patient group. No correlations were observed between velocity measurements and current or nadir CD4, HIV VL, duration of medication use or duration of elevated CD4 counts (determined in 6 patients on ART with current CD4 count >200 and nadir CD4 count <50).

Blue field entoptic technique (BFS-2000, Oculix) was also used in a study by Dejaco-Ruhswurm et al.,[24] to measure macular leukocyte flow. In addition, fundus pulsation amplitude and blood flow velocities in the retrobulbar vessels were determined by laser interferometry and Doppler sonography, respectively. The fundus pulsation amplitude (FPA), representing the maximum distance change between the cornea and the fundus during a cardiac cycle, gives an estimate pulsatile blood flow on a selected fundus location. Doppler sonography of the retrobulbar vessels yields information about blood velocity due to the Doppler effect. Peak systolic and minimal diastolic flow velocities of the ophthalmic artery (OA), the central retinal artery (CRA) and the posterior ciliary arteries (PCAs) are assessed and from these parameters the mean flow velocity and the resistive index (= peak systolic flow velocity- minimal diastolic flow velocity) are calculated.

The eyes of 37 HIV patients and 25 HIV-negative controls were evaluated; current CD4 counts were not above 500 cells/µl, with 22 patients having CD4 counts <200 cells/µl. Mean current and nadir CD4 counts were 206.8 ± 145.6 cells/µl and 119.2 ± 109.4 cells/µl, respectively. Mean HIV viral load was 5.9×10^4 (range; 0 – 4.5×10^5) copies/ml at time of examination. Eighty-nine % of the patients were on cART, of whom 81% took protease inhibitors. Mean duration since HIV diagnosis was 6 ± 3.8 years. Five patients had HIV retinopathy.

A significant reduction in leukocyte density was seen in HIV patients compared to the control group. The resistive index in the central retinal artery was higher in the HIV group, but other hemodynamic parameters were not significantly different between the groups. Like in the previous study, no correlations were found between flow parameters and current/nadir CD4 count, viral load or HIV retinopathy.

Other hemorheologic abnormalities (measured in vitro) reported in HIV patients are abnormal erythrocyte aggregation[20] and increased polymorphonuclear leukocyte rigidity.[25] Because these changes can alter microvascular blood flow and appear to be unrelated to immunodeficiency, HIV patients may remain at risk for retinal vascular damage, even in the cART era. It is suggested that some antiretroviral agents (in particular the nucleoside reverse transcriptase inhibitors [NRTI's], such as zidovudine) may make these changes even worse, by causing macrocytosis.[20]

Retinal vascular calibers

In recent years, advances in fundus photography and retinal image analysis techniques have enabled the objective and accurate assessment of quantitative retinal vascular caliber measurements **(Figure 3)**. Epidemiological studies have shown that changes in retinal arteriolar and venular caliber size are associated with several factors, including age. For example, both narrower retinal arteriolar and venular calibers are associated with an older age, with absolute differences in changes between individuals > 80 years compared to those who are 55-60 years in the order of magnitude of 10-15 µm.[45]

Retinal vascular calibers have also been measured in HIV patients. Gangaputra et al.[18] evaluated potential relationships between retinal vessel calibers and HIV-associated factors as well as mortality in the LSOCA study. Included were 1250 patients with AIDS without ocular opportunistic infections, with a median time of 4.2 (range; 1.6-7.1) years since AIDS diagnosis, of whom 85% were on cART at baseline. Median CD4 count at baseline was 192 (range; 81-350) cells/µl.

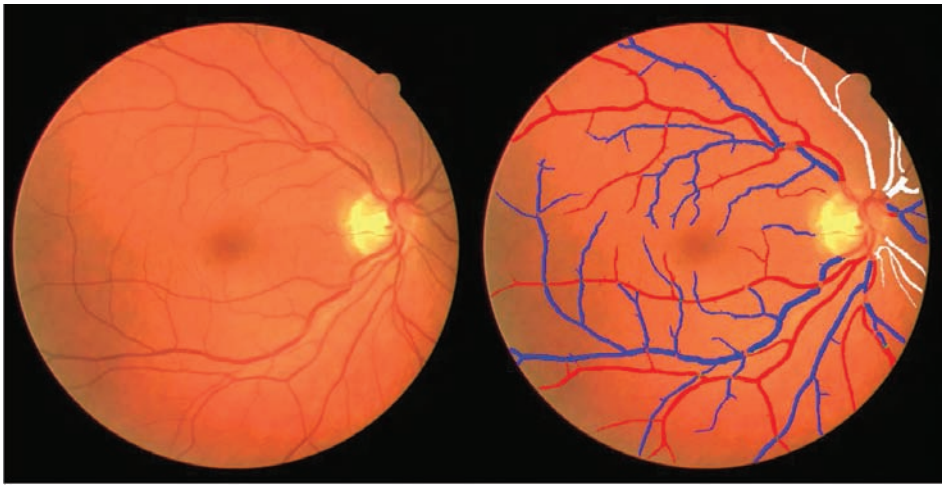

FIGURE 3. Example of a measurement of retinal arteriolar (red) and venular (blue) calibers using special algorithms[41-43] (white is undetermined). In general, 3 summary variables are determined in a semi-automated manner, using fundus photographs: the central retinal artery equivalent (CRAE; the projected caliber size of the central retinal artery), central retinal vein equivalent (CRVE; the projected caliber size of the central retinal vein) and arteriole-to-venule-ratio (AVR). Images used with permission of references.[41-43]

Mean follow-up time for determination of mortality was 6.1 years. A smaller CRAE and larger CRVE were significantly associated with (previous or current) cART, and larger CRAE was associated with lower baseline CD4 counts. No relationships were found between vessel calibers and HIV viral load, duration of AIDS, nadir CD4 count and CD8+ T-cell count. Worse Karnofsky scores were correlated with larger CRVE and smaller AVR. There was a 12% (95% CI, 2-21%) increase in mortality risk per quartile of decreasing AVR.

Data from the same group of patients was used in a separate analysis, comparing retinal vessel calibers with visual function outcomes, measured by Goldmann perimetry, Humphrey Field Analyzer and Pelli-Robson CS testing.[19] CRAE and CRVE were not associated with visual function parameters, but a smaller AVR was correlated with reduced visual field by Goldmann perimetry and worse MD and possibly worse PSD on automated perimetry. In addition, there was a weak association between smaller AVR and worse CS. These relationships were independent of ART use and level of immunodeficiency (CD4 counts and HIV viral load). Retinal vascular indices at baseline did not predict changes in visual function during follow-up. Since a control group was not available in both these studies, the hypothesis of accelerated aging in HIV patients, with more advanced retinal vessel caliber changes compared to an age matched healthy control group, could not be tested. Furthermore, in these studies, retinal vessel calibers were measured at baseline

only, leaving the question unanswered whether changes in vessel caliber indices predict changes in visual function and whether caliber sizes are influenced/reversible by changes in CD4 counts or viral load over time.

Pathai et al.[22] assessed associations between retinal vessel calibers and clinical and demographic characteristics in a population of 242 HIV patients and 249 HIV negative controls in South-Africa. Among HIV patients, 72,7% had a history of WHO stage 3 (moderately symptomatic stage) or stage 4 (severely symptomatic stage= AIDS) defining illness. Eighty-seven % of the patients were receiving cART, of whom 84% had an undetectable VL at examination. Among the patients on cART, current CD4 count was 468 (IQR, 325-607) cells/µl and nadir CD4 count was 127 (IQR, 76-171) cells/µl. Peak viral load in the cART group was 4.56 (3.84-4.98) $\log_{10}$ copies/ml. Median cART duration was 58 (IQR, 34-75) months.

Surprisingly, no significant differences were found in CRAE and CRVE between patients and controls. Pathai does not further address this in her discussion. When analyzing the HIV patients (on cART) separately, narrower arterioles were associated with an increasing duration of cART, independently of age, and with a higher viral load (>10.000 copies/ml) while on cART.

Tan et al.[23] performed a similar study in Singapore, examining 85 HIV patients (98% was receiving cART at enrollment) without ocular opportunistic infections and 251, age-, sex- and race matched controls. Both median time since HIV diagnosis and duration of cART were 7 (range 1-94) months. Median (current?) CD4 count was 91 (range, 15-952) cells/µl.

In addition to the retinal vessel calibers (CRAE, CRVE and AVR), retinal branching angle, tortuosity and fractal dimension (a measure summarizing the branching pattern of the retinal vasculature) were determined. Like in the study by Pathai,[22] no significant differences in retinal vessel calibers were found between patients and controls, nor in vascular branching angle or fractal dimension. However, the patients had more tortuous arterioles and venules compared with the controls. Among HIV patients, increasing viral load (unclear whether viral load was measured pre-cART or at time of enrollment) was associated with decreased CRAE and AVR, again in line with Pathai's results.[22] In contrast to Pathai,[22] this study found no association between cART duration and retinal vascular abnormalities. Tan notes that the duration of cART use was much shorter in this population, compared to Pathai's population, where retinal arteriolar narrowing was found only after cART duration of 6 years. Both Pathai and Tan[22,23] found no correlations with CD4 counts and vascular calibers, contrary to the LSOCA Study.[18]

GENETICS

The LSOCA Study group conducted a few genetic studies, to evaluate the influence of several host genetic factors on HIV-NRD development. The authors hypothesized that HIV-NRD could be related to a worse AIDS prognosis[6] and that host genetic factors, known to influence HIV infection, AIDS progression, therapy response and antiviral drug metabolism,[46-50] might therefore also affect the development of HIV-NRD. Furthermore, associations between hepatitis C co-infection and HIV-NRD were assessed, as well as variations in mitochondrial DNA haplogroups and HIV-NRD development.

Mitochondrial haplogroup J

Loss of optic nerve axons has been described in AIDS patients, in histological studies in the pre-HAART era, suggestive of mitochondrial dysfunction.[51] Furthermore, among patients with HIV, mitochondrial dysfunction has been associated with mitochondrial DNA (mtDNA) depletion, disruption of energy production, antioxidant enzyme deficiency and increased oxidative damage.[52]

Hendrickson et al.[53] explored whether variation in mitochondrial DNA haplogroups influenced the development of HIV-NRD (from the time of AIDS diagnosis), defined as having a Pelli-Robson contrast sensitivity <1,5 log units, in 503 European-American AIDS patients (having mitochondrial macrohaplogroup ''N''), participating in the LSOCA Study.

In genetic studies, the definition of a haplogroup is a group of individuals with similar haplotypes who share a common ancestor and for that reason have the same single nucleotide polymorphism (SNP) mutation in all haplotypes. A human mitochondrial DNA haplogroup is a haplogroup defined by such similarities in human mitochondrial DNA.

The patients in this study had no infectious retinitis, mean duration of time since AIDS diagnosis was 5,1 years and 84% were on cART. Sixty-four (7.9%) patients had HIV-NRD at enrollment and among the 439 patients without HIV-NRD, 19.6% developed HIV-NRD during follow-up.

Within the macrohaplogroup N, haplogroup J was found to be protective in both a survivorship analysis of time-to-NRD in patients with no prior NRD diagnosis at enrollment (80% decrease in risk; HR 0.20; 95% CI 0,03-1.48) as well as in a cross-sectional analysis comparing the prevalence of HIV-NRD at enrollment between patients with and without haplogroup J (1.5% vs 8.9%; OR 0.39; 95% CI 0.15-1.00). Haplogroup J

is associated with accelerated AIDS progression in untreated patients.[54] In patients on cART however, J seemed to be protective against lipoatrophy, an ART side effect.[55] The results of this HIV-NRD study seem to confirm the protective role of haplogroup J in patients on cART.

IL-10 and RANTES gene polymorphisms

Another LSOCA study[56] found significant correlations between HIV-NRD and polymorphisms that have a crucial role in the IL-10 signaling pathway (in European Americans), and polymorphisms in the RANTES gene (in African Americans).

In 345 European Americans (55 with HIV-NRD, 290 without HIV-NRD), IL-10-5A variant and its promotor haplotype HG1 were found to be associated with HIV-NRD development (HR 2.72, CI 1.19-3.67).[46] The IL-10-5A variant (in the promotor region of IL-10) is a low producer of IL-10 and together

with its associated haplotype has been shown to influence HIV infection and accelerate progression to AIDS in European Americans.[57-59]

In a group of 234 African Americans (54 patients with HIV-NRD, 180 without HIV-NRD), RANTES-In1.1.C and the associated haplotypes H2 and H3 showed increased HIV-NRD susceptibility (HR 2.72, CI 1.48-5.00). RANTES (Regulated on Activation, Normal T cell Expressed and Secreted) is a CC chemokine receptor 5 (CCR5) ligand; a potent inhibitor of HIV entry and replication.[60] RANTES variants and haplotypes influence RANTES production and affect HIV infection, progression to AIDS and cART outcome.[46,48,61-64]

Hepatitis C virus co-infection

A third genetic LSOCA study examined the impact of hepatitis C virus (HCV) infection on the prevalence and incidence of HIV-NRD,[65] in view of the fact that HCV is pro-inflammatory[66] and penetrates the central nervous system,[67-71] thereby possibly increasing the susceptibility of developing HIV-NRD. Associations between HCV and single-nucleotide polymorphisms (SNPs) in the IL-10 receptor 1 gene, found to be associated with HIV-NRD in the previous genetic LSOCA Study,[56] were assessed as well. The group included 244 AIDS patients with NRD at baseline and 1332 AIDS patients without NRD. Median follow-up time was 4.9 (IQR 2.4-8.8) years. There were 263 incident cases of HIV-NRD. After adjustment for several factors, both incidence and prevalence of HIV-NRD were significantly higher in patients with chronic HCV infection (OR 1.54, 95% CI 1.03-2.31 and HR 1.62, 95% CI 1.13-2.34, respectively), compared to patients without HCV markers. Three of the 4 SNPs analyzed (in a subset of 902 patients), expected to reduce IL-10 signaling, were associated with chronic HCV infection, but none of these SNPs were

associated with HIV-NRD. These results indicate that HCV is a possible risk factor for HIV-NRD and that alterations in the IL-10 signaling pathway may increase susceptibility to HCV infection and HIV-NRD.

PATHOPHYSIOLOGY

The pathogenesis of HIV-NRD remains uncertain and speculative. Proposed hypotheses include 1) direct HIV infection of neuroretinal tissue, 2) damage caused by chronic immune activation and (para) inflammation, 3) cumulative damage to the neuroretina from a longstanding microvasculopathy and associated hemorheological abnormalities and 4) accelerated/premature aging, presumably induced by a combination of several factors, including HIV infection itself, ART side-effects and the accelerated aging of the immune system in the setting of a (cART-treated) HIV infection. In addition, recent studies indicate that specific host genetic factors might make an individual more susceptible for HIV-NRD.[53,56] Associated socio-demographic risk factors include (Black/Hispanic) race, a history of injection drug use, lower Karnofsky scores and lack of private health insurance.[6] Presumably HIV-NRD is not caused by just a single mechanism, but rather by an interplay between several processes **(Figure 4).**

Severity of immune-deficiency

Abovementioned studies illustrate that in particular HIV patients with a more advanced disease status (e.g. low (nadir) CD4 counts, high viral load, prior (non-ocular) AIDS diagnosis and a lower Karnofsky score) develop the visual symptoms and structural retinal changes related to HIV-NRD. Abnormalities in mf-ERG, visual field results, color vision, contrast sensitivity and worse performances with computer-based simulators were all found to be correlated with low (nadir) CD4 counts.[4-6,8,37,38] In addition, several studies reported a thinner peripapillary RNFL thickness in HIV patients with low (nadir) CD4 counts.[5,14,15,38]

Most of these studies categorized patients according to their nadir CD4 count, in particular below and above a threshold of 100 cells/μl, and did not detect any significant changes between HIV patients with nadir CD4 counts >100 cells/μl and HIV-negative controls. Moreover, studies that compared a more heterogeneous group of HIV patients (with varying levels of immune-deficiency), with a HIV negative control group, found similar outcomes of tests between the two groups.[2,10,22,23,38] These findings suggest that patients with higher (>100 cells/μl) nadir CD4 counts are less susceptible for developing HIV-NRD.

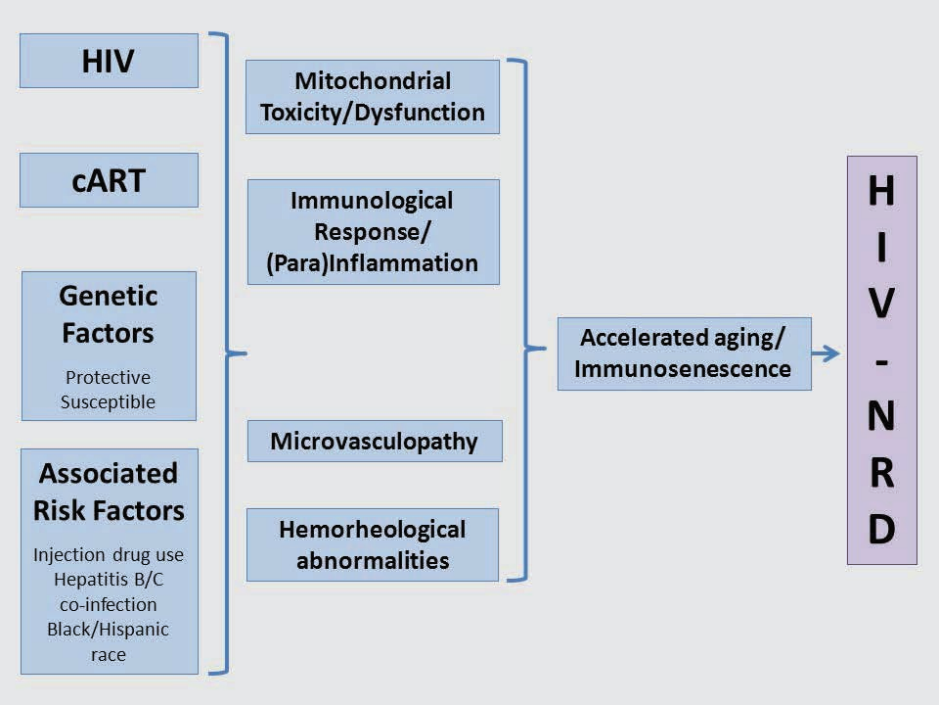

FIGURE 4. Simplified diagram of factors/mechanisms thought to be involved in the development of HIV-NRD.

Chronic (para)inflammation and aging

In contrast to a decreasing RNFL thickness, two studies described a subgroup of HIV patients with a *thicker* RNFL than normal. Kalyani et al.[7] found a trend for increasing peripapillary RNFL thickness with shorter HIV duration, while Pathai reports an association with detectable viremia.[10] Kalyani hypothesizes that it could be that the RNFL goes through an initial phase of swelling, as the axons are compromised by mitochondrial toxicity (mediated by HIV or ART (in particular the nucleoside analog reverse-transcriptase inhibitors)), before becoming atrophic. Mitochondrial dysfunction contributes to para-inflammation and aging.[72] Para-inflammation is a chronic, low-level inflammatory response to tissue stress or dysfunction and is shown to be associated with the aging process.[32,73] Pathai speculates that increased levels of HIV viremia may initiate a para-inflammatory process in the retina, which may initially manifest as increased thickness of the RNFL.

Pathai et al. demonstrated earlier that HIV infection is associated with frailty[74] and that frailty is an important predictor of poor CS in HIV patients, supporting the theory of accelerated/accentuated aging in HIV.[10] The finding that abnormal CS is also indepen-

dently associated with mortality in patients with AIDS corroborates this point of view.[75] Other –non-retinal- studies described changes in features of the corneal endothelium[76] and increased ocular lens density/ cataract formation[77] in HIV patients compared to HIV negative individuals, which are all known to be age-related changes.

Subclinical microvasculopathy

Microvascular changes, in combination with hemorheological abnormalities, are thought to mediate damage to the neuroretina, thereby playing a role in developing HIV-NRD.

It is proposed that activated leukocytes in HIV patients play a key role in the development of blood flow alterations. Activated leukocytes are capable of causing direct microvascular damage by adhering to endothelial cells followed by degranulation, in addition to altering blood flow directly, through increased persistent leukocyte rigidity[25] and increased aggregation and decreased deformability of erythrocytes.[20] Some antiretroviral agents have been associated with macrocytosis, thereby also influencing erythrocyte deformability.[20] These hemorheological abnormalities[20,21,24,25] could contribute to developing hypoxia, which might in turn contribute to subtle retinal vascular parametric changes of narrower arterioles and increased tortuosity, as observed in HIV patients.

Narrower retinal arterioles were found to be associated with a higher viral load, and not with nadir CD4 counts[22,23]; possibly reflecting a heightened inflammatory state associated with chronic HIV infection. In addition, cART use/duration[18,22] was also identified as a risk factor for narrower retinal arterioles; which is more difficult to explain. Although initially the increased (cardio)vascular risk in HIV patients was primarily attributed to metabolic alterations associated with the use of particular antiretroviral agents, findings from especially the Strategies for Management of Anti-Retroviral Therapy Study (SMART Study)[78] showed that patients on intermittent antiretroviral therapy had a significant higher risk for vascular events than patients who received continuous antiretroviral therapy. In recent years, there has been more focus on inflammation, immune activation and endothelial dysfunction, facilitated by HIV infection itself, as key factors for vascular risk in HIV.[79] As for the eye, detectable HIV RNA levels have been observed in ocular tissues,[80-82] even in the absence of a detectable plasma viral load[83] and it has been suggested that HIV impairs and penetrates the blood-retinal barrier, by inducing an inflammatory state in retinal pigment epithelium cells through exposure to HIV proteins.[84,85]

Genetic factors

Mitochondrial haplogroup 'J' (within the Western-European macrohaplogroup 'N') was found to have a protective effect against the development of HIV-NRD in cART-treated patients with AIDS.[53]

On the other hand, mutations in an IL-10 receptor gene (in European-Americans having AIDS[56]), as well as mutations in the RANTES gene (in African Americans with AIDS[56]), were associated with an increasing risk for HIV-NRD. These genes are known to affect HIV infection and AIDS progression[57-59] and considering that HIV-NRD is predominantly present in patients with a worse HIV outcome, it is possible that these host genetic variants may be affecting the severity of the AIDS progression rather than having a direct effect on the neuroretina and the development of HIV-NRD. Whether the observed associations are specific for NRD could be explored in a study with a population of HIV patients who develop HIV-NRD independent of AIDS.

Neural damage

IL-10 is a suppressor of TNF[86-88] (associated with myelin and membrane damage in optic nerves[89-92]), therefore, the correlation between a low IL-10 producing genetic variant in European Americans with an increased HIV-NRD risk, may be partly explained by increased immune activity (higher TNF production) leading to optic neuronal damage. Furthermore, the central nervous system (CNS) is considered to be a sanctuary for HIV, which crosses the blood-brain barrier early in the course of the disease and produces neurotoxic viral proteins, irrespective of HIV stage.[93] These proteins can be transported along the neural pathways, causing damage.[94]

In addition to hepatitis C virus, other frequent co- infections known to penetrate the central nervous system (CNS), such as hepatitis B virus[95] and syphilis,[96] may also indirectly affect the neuroretina, possibly through persistent or heightened immune activation and increased HIV replication.

Finally, there are some reports suggesting potential neurotoxicity of several antiretroviral agents penetrating the CNS, although the evidence from these (predominantly preclinical) studies is mixed and inconclusive.[97]

DISCUSSION

In summary, HIV-NRD comprises subtle vision abnormalities[2,3,5-7,9-11,37,38,75] (reduced contrast sensitivity, color vision, visual field loss), changes in peripapillary RNFL thickness[2,5,7,10,13-17,37] and subclinical microvascular alterations[18-25,98] (hemorheological abnormalities, changes in retinal vessel calibers) in HIV-patients without opportunistic ocular infections or visible non-infectious ischemic HIV retinopathy. The subtle abnormalities are not manifested as overt clinical symptoms and as the pathophysiology is complex and partly unknown, it is complicated to identify the individuals who are at risk, although the disorder is more common among patients with current or prior severe immune-deficiency. The prevalence of HIV-NRD (Pelli-Robson CS< 1.5 logCS) is reportedly between 3-16%,[6,7,10,11,75,99] and the LSOCA study estimated a cumulative incidence as high as 51%, 20 years after AIDS diagnosis.[99] Patients with higher nadir CD4 counts seem to have a lower risk of developing HIV-NRD. However, there is a lack of clinical data on the occurrence and risk factors of HIV-NRD in HIV patients with high nadir CD4 counts (> 350 cells/µl) and well-suppressed HIV-infection, who constitute a growing part of the (Western) HIV-infected population.

Although the alterations in visual function are subtle, they can lead to difficulties in activities, such as reading or driving, thereby affecting the quality of life of a patient. Since HIV has become a chronic disease, its long-term effects with respect to visual function loss become more important, especially in patients with severe-immune deficiency, as the LSOCA study demonstrated recently.[99] AIDS patients with HIV-NRD had considerably increased risks of bilateral visual impairment and even blindness versus those without HIV neuroretinal disorder.[99]

The studies in this review have several important limitations.

Although all studies were conducted in the cART era, most of them included HIV patients who became infected in the pre-cART era, thereby presumably having a different risk profile than HIV patients infected in the cART era, for example due to exposure to toxic and ineffective mono- and duo-nucleoside analogues. In addition, several studies examined patients with a more advanced disease status, like the LSOCA study, including only patients with an (prior) AIDS diagnosis and excluding patients in earlier stages of the disease. The patients examined in these studies showed no signs of opportunistic ocular infections or visible HIV retinopathy at the time of examination, but having low CD4 counts at some point during their disease implies they might have had some microvascular abnormalities, that were resolved at the time of testing, but led to permanent inner retinal damage.[100]

Another important issue is the lack of a gold standard for the diagnosis of HIV-NRD. Contrast sensitivity testing (Pelli Robson chart) was used by many studies as a marker for HIV-NRD. In addition to being a subjective method, this test does not purely measure retinal function, since the outcome is also influenced by alterations in the anterior segment, like (subtle) media opacities. As HIV patients have been reported to have increased lens densities and undergo cataract surgeries more frequently than their HIV-negative counterparts,[77,101] contrast sensitivity is a less sensitive method for assessing HIV-NRD. Furthermore, as cART has prolonged the life expectancy of HIV patients, they are at increased risk for other comorbidities affecting the eye, such as diabetes, hypertension and glaucoma. These conditions can also confound the results of the tests used in the studies investigating HIV-NRD.

The majority of the studies performed were cross-sectional with a small sample size and lacked relevant information regarding HIV-related factors (VL, CD4 counts, cART), making it difficult to interpret the results in terms of causality/pathophysiology.

The longitudinal studies that were conducted (LSOCA) did not report whether adequate immune recovery had a protective effect on progression of the neuroretinal damage observed earlier on in patients with severe immune-deficiency. In addition, an overview of causes of visual impairment and blindness observed in patients with HIV-NRD in the long term was not provided.

Finally, a major limitation of some of the studies, like the LSOCA, was the lack of a control group to compare with the patient group.

To investigate the long term effects of HIV infection on the neuroretina, prospective longitudinal studies with HIV patients at varying disease stages (with a follow-up of at least 2 to 5 years) are warranted. Some major questions remain unanswered to date. Among HIV-patients with immune-deficiency, is the neuroretinal damage stationary or progressive after adequate immune recovery? Are patients with high nadir CD4 counts- who will likely never develop AIDS- still at risk for HIV-NRD? A highly similar control group is essential to delineate the specific effects of the HIV infection itself.

In addition to structural (SD-OCT measurements, retinal vessel calibers) and functional (mf-ERG, VF, etc.) examinations, genetic and immunological tests (cytokines) can help elucidate the underlying cascade of reactions leading to neural damage. Fluorescence angiography/OCT angiography could be used to determine the extent of the involvement of the vascular component in HIV-NRD. Studies so far have purely investigated the peripapillary RNFL or total macular thickness, but the question is whether there

are also changes in individual retinal layer thicknesses in HIV-NRD. Since HIV-NRD is a subtle disorder, the peripapillary RNFL thickness and total macular thickness can appear normal, while there could be changes in individual retinal layers.

Lastly, it is possible that neuroretinal dysfunction in HIV is part of central nervous system dysfunction in general. A comparison of ocular examinations with CNS assessment (MRI techniques, neuropsychological assessment) can give more information on this matter.

ACKNOWLEDGEMENTS

This publication was made possible by a research grant from the Aids Fonds (Project Number 2012023).

AUTHOR DISCLOSURE STATEMENT

No competing financial interests exist.

AUTHORS' CONTRIBUTIONS

ND researched data, has written all drafts and was responsible for submitting the final version of the manuscript. FDV supervised the writing of this review. All authors discussed the content of the article, reviewed and edited the manuscript before submission.

REFERENCES

1. Miller C, Short WR, Perez-Povis L, et al. The spectrum of eye disease in hospitalized adults living with HIV, 1995-2010. *AIDS Patient Care STDS*. 2014;28:47-55.
2. Arantes TE, Garcia CR, Tavares IM, Mello PA, Muccioli C. Relationship between retinal nerve fiber layer and visual field function in human immunodeficiency virus-infected patients without retinitis. *Retina*. 2012;32:152-159.
3. Falkenstein I, Kozak I, Kayikcioglu O, et al. Assessment of retinal function in patients with HIV without infectious retinitis by multifocal electroretinogram and automated perimetry. *Retina*. 2006;26:928-934.
4. Falkenstein IA, Bartsch DU, Azen SP, Dustin L, Sadun AA, Freeman WR. Multifocal electroretinography in HIV-positive patients without infectious retinitis. *Am J Ophthalmol*. 2008;146:579-588.
5. Faria E Arantes TE, Garcia CR, Mello PA, Muccioli C. Structural and functional assessment in HIV-infected patients using optical coherence tomography and frequency-doubling technology perimetry. *Am J Ophthalmol*. 2010;149:571-576.
6. Freeman WR, Van Natta ML, Jabs D, et al. Vision function in HIV-infected individuals without retinitis: report of the Studies of Ocular Complications of AIDS Research Group. *Am J Ophthalmol*. 2008;145:453-462.
7. Kalyani PS, Holland GN, Fawzi AA, Arantes TE, Yu F, Sadun AA. Association between retinal nerve fiber layer thickness and abnormalities of vision in people with human immunodeficiency virus infection. *Am J Ophthalmol*. 2012;153:734-42, 742.
8. Kozak I, Sample PA, Hao J, et al. Machine learning classifiers detect subtle field defects in eyes of HIV individuals. *Trans Am Ophthalmol Soc*. 2007;105:111-118.
9. Moschos MM, Margetis I, Markopoulos I, Moschos MN. Optical coherence tomography and multifocal electroretinogram study in human immunodeficiency virus-positive children without infectious retinitis. *Clin Exp Optom*. 2011;94:291-295.
10. Pathai S, Lawn SD, Weiss HA, Cook C, Bekker LG, Gilbert CE. Retinal Nerve Fibre Layer Thickness and Contrast Sensitivity in HIV-Infected Individuals in South Africa: A Case-Control Study. *PLoS One*. 2013;8:e73694.
11. Shah KH, Holland GN, Yu F, Van NM, Nusinowitz S. Contrast sensitivity and color vision in HIV-infected individuals without infectious retinopathy. *Am J Ophthalmol*. 2006;142:284-292.
12. Goldbaum MH, Falkenstein I, Kozak I, et al. Analysis with support vector machine shows HIV-positive subjects without infectious retinitis have mfERG deficiencies compared to normal eyes. *Trans Am Ophthalmol Soc*. 2008;106:196-204.
13. Besada E, Shechtman D, Black G, Hardigan PC. Laser scanning confocal ophthalmoscopy and polarimetry of human immunodeficiency virus patients without retinopathy, under antiretroviral therapy. *Optom Vis Sci*. 2007;84:189-196.
14. Kozak I, Bartsch DU, Cheng L, Kosobucki BR, Freeman WR. Objective analysis of retinal damage in HIV-positive patients in the HAART era using OCT. *Am J Ophthalmol*. 2005;139:295-301.
15. Kozak I, Bartsch DU, Cheng L, McCutchan A, Weinreb RN, Freeman WR. Scanning laser polarimetry demonstration of retinal nerve fiber layer damage in human immunodeficiency virus-positive patients without infectious retinitis. *Retina*. 2007;27:1267-1273.

16. Moschos MM, Mostrou G, Psimenidou E, Spoulou V, Theodoridou M. Objective analysis of retinal function in HIV-positive children without retinitis using optical coherence tomography. *Ocul Immunol Inflamm*. 2007;15:319-323.
17. Plummer DJ, Bartsch DU, Azen SP, Max S, Sadun AA, Freeman WR. Retinal nerve fiber layer evaluation in human immunodeficiency virus-positive patients. *Am J Ophthalmol*. 2001;131:216-222.
18. Gangaputra S, Kalyani PS, Fawzi AA, et al. Retinal vessel caliber among people with acquired immunodeficiency syndrome: relationships with disease-associated factors and mortality. *Am J Ophthalmol*. 2012;153:434-444.
19. Kalyani PS, Fawzi AA, Gangaputra S, et al. Retinal vessel caliber among people with acquired immunodeficiency syndrome: relationships with visual function. *Am J Ophthalmol*. 2012;153:428-433.
20. Kim A, Dadgostar H, Holland GN, et al. Hemorheologic abnormalities associated with HIV infection: altered erythrocyte aggregation and deformability. *Invest Ophthalmol Vis Sci*. 2006;47:3927-3932.
21. Lim MC, Cumberland WG, Minassian SL, et al. Decreased macular leukocyte velocity in human immunodeficiency virus-infected individuals. *Am J Ophthalmol*. 2001;132:711-719.
22. Pathai S, Weiss HA, Lawn SD, et al. Retinal arterioles narrow with increasing duration of anti-retroviral therapy in HIV infection: a novel estimator of vascular risk in HIV? *PLoS One*. 2012;7:e51405.
23. Tan PB, Hee OK, Cheung C, et al. Retinal vascular parameter variations in patients with human immunodeficiency virus. *Invest Ophthalmol Vis Sci*. 2013;54:7962-7967.
24. Dejaco-Ruhswurm I, Kiss B, Rainer G, et al. Ocular blood flow in patients infected with human immunodeficiency virus. *Am J Ophthalmol*. 2001;132:720-726.
25. Goldenberg DT, Holland GN, Cumberland WG, et al. An assessment of polymorphonuclear leukocyte rigidity in HIV-infected individuals after immune recovery. *Invest Ophthalmol Vis Sci*. 2002;43:1857-1861.
26. Su T, Schouten J, Geurtsen GJ, et al. Multivariate normative comparison, a novel method for more reliably detecting cognitive impairment in HIV infection. *AIDS*. 2015;29:547-557.
27. Haddow LJ, Dudau C, Chandrashekar H, et al. Cross-sectional study of unexplained white matter lesions in HIV positive individuals undergoing brain magnetic resonance imaging. *AIDS Patient Care STDS*. 2014;28:341-349.
28. Leite SC, Correa DG, Doring TM, et al. Diffusion tensor MRI evaluation of the corona radiata, cingulate gyri, and corpus callosum in HIV patients. *J Magn Reson Imaging*. 2013;38:1488-1493.
29. Robinson-Papp J, Sharma SK. Autonomic neuropathy in HIV is unrecognized and associated with medical morbidity. *AIDS Patient Care STDS*. 2013;27:539-543.
30. Dadgostar H, Holland GN, Huang X, et al. Hemorheologic abnormalities associated with HIV infection: in vivo assessment of retinal microvascular blood flow. *Invest Ophthalmol Vis Sci*. 2006;47:3933-3938.
31. Tenhula WN, Xu SZ, Madigan MC, Heller K, Freeman WR, Sadun AA. Morphometric comparisons of optic nerve axon loss in acquired immunodeficiency syndrome. *Am J Ophthalmol*. 1992;113:14-20.
32. Xu H, Chen M, Forrester JV. Para-inflammation in the aging retina. *Prog Retin Eye Res*. 2009;28:348-368.

33. Hong S, Banks WA. Role of the immune system in HIV-associated neuroinflammation and neurocognitive implications. *Brain Behav Immun.* 2015;45:1-12.
34. Pathai S, Bajillan H, Landay AL, High KP. Is HIV a Model of Accelerated or Accentuated Aging? *J Gerontol A Biol Sci Med Sci.* 2013.
35. Deeks SG, Verdin E, McCune JM. Immunosenescence and HIV. *Curr Opin Immunol.* 2012;24:501-506.
36. West SK, Rubin GS, Broman AT, Munoz B, Bandeen-Roche K, Turano K. How does visual impairment affect performance on tasks of everyday life? The SEE Project. Salisbury Eye Evaluation. *Arch Ophthalmol.* 2002;120:774-780.
37. Cheng S, Klein H, Bartsch DU, Kozak I, Marcotte TD, Freeman WR. Relationship between retinal nerve fiber layer thickness and driving ability in patients with human immunodeficiency virus infection. *Graefes Arch Clin Exp Ophthalmol.* 2011;249:1643-1647.
38. Barteselli G, Chhablani J, Gomez ML, et al. Visual function assessment in simulated real-life situations in HIV-infected subjects. *PLoS One.* 2014;9:e97023.
39. Myers VS, Gidlewski N, Quinn GE, Miller D, Dobson V. Distance and near visual acuity, contrast sensitivity, and visual fields of 10-year-old children. *Arch Ophthalmol.* 1999;117:94-99.
40. Verriest G, Van LJ, Uvijls A. A new assessment of the normal ranges of the Farnsworth-Munsell 100-hue test scores. *Am J Ophthalmol.* 1982;93:635-642.
41. Jabs DA, Drye L, Van Natta ML, Thorne JE, Holland GN. Incidence and Long-term Outcomes of the Human Immunodeficiency Virus Neuroretinal Disorder in Patients with AIDS. *Ophthalmology.* 2015;122:760-768.
42. Myers VS, Gidlewski N, Quinn GE, Miller D, Dobson V. Distance and near visual acuity, contrast sensitivity, and visual fields of 10-year-old children. *Arch Ophthalmol.* 1999;117:94-99.
43. Vingrys AJ, King-Smith PE. A quantitative scoring technique for panel tests of color vision. *Invest Ophthalmol Vis Sci.* 1988;29:50-63.
44. Rao HL, Kumar AU, Babu JG, Kumar A, Senthil S, Garudadri CS. Predictors of normal optic nerve head, retinal nerve fiber layer, and macular parameters measured by spectral domain optical coherence tomography. *Invest Ophthalmol Vis Sci.* 2011;52:1103-1110.
45. Ikram MK, Ong YT, Cheung CY, Wong TY. Retinal vascular caliber measurements: clinical significance, current knowledge and future perspectives. *Ophthalmologica.* 2013;229:125-136.
46. An P, Nelson GW, Wang L, et al. Modulating influence on HIV/AIDS by interacting RANTES gene variants. *Proc Natl Acad Sci U S A.* 2002;99:10002-10007.
47. Carrington M, O'Brien SJ. The influence of HLA genotype on AIDS. *Annu Rev Med.* 2003;54:535-551.
48. Hendrickson SL, Jacobson LP, Nelson GW, et al. Host genetic influences on highly active antiretroviral therapy efficacy and AIDS-free survival. *J Acquir Immune Defic Syndr.* 2008;48:263-271.
49. O'Brien SJ, Nelson GW. Human genes that limit AIDS. *Nat Genet.* 2004;36:565-574.
50. O'Brien TR, McDermott DH, Ioannidis JP, et al. Effect of chemokine receptor gene polymorphisms on the response to potent antiretroviral therapy. *AIDS.* 2000;14:821-826.
51. Tenhula WN, Xu SZ, Madigan MC, Heller K, Freeman WR, Sadun AA. Morphometric comparisons of optic nerve axon loss in acquired immunodeficiency syndrome. *Am J Ophthalmol.* 1992;113:14-20.

52. Hart AB, Samuels DC, Hulgan T. The other genome: a systematic review of studies of mitochondrial DNA haplogroups and outcomes of HIV infection and antiretroviral therapy. *AIDS Rev*. 2013;15:213-220.
53. Hendrickson SL, Jabs DA, Van NM, Lewis RA, Wallace DC, O'Brien SJ. Mitochondrial haplogroups are associated with risk of neuroretinal disorder in HIV-positive patients. *J Acquir Immune Defic Syndr*. 2010;53:451-455.
54. Hendrickson SL, Hutcheson HB, Ruiz-Pesini E, et al. Mitochondrial DNA haplogroups influence AIDS progression. *AIDS*. 2008;22:2429-2439.
55. Hulgan T, Tebas P, Canter JA, et al. Hemochromatosis gene polymorphisms, mitochondrial haplogroups, and peripheral lipoatrophy during antiretroviral therapy. *J Infect Dis*. 2008;197:858-866.
56. Sezgin E, Hendrickson SL, Jabs DA, et al. Effect of host genetics on incidence of HIV neuroretinal disorder in patients with AIDS. *J Acquir Immune Defic Syndr*. 2010;54:343-351.
57. Oleksyk TK, Shrestha S, Truelove AL, et al. Extended IL10 haplotypes and their association with HIV progression to AIDS. *Genes Immun*. 2009;10:309-322.
58. Shin HD, Winkler C, Stephens JC, et al. Genetic restriction of HIV-1 pathogenesis to AIDS by promoter alleles of IL10. *Proc Natl Acad Sci U S A*. 2000;97:14467-14472.
59. Vasilescu A, Heath SC, Ivanova R, et al. Genomic analysis of Th1-Th2 cytokine genes in an AIDS cohort: identification of IL4 and IL10 haplotypes associated with the disease progression. *Genes Immun*. 2003;4:441-449.
60. Berger EA, Murphy PM, Farber JM. Chemokine receptors as HIV-1 coreceptors: roles in viral entry, tropism, and disease. *Annu Rev Immunol*. 1999;17:657-700.
61. Cocchi F, DeVico AL, Garzino-Demo A, Arya SK, Gallo RC, Lusso P. Identification of RANTES, MIP-1 alpha, and MIP-1 beta as the major HIV-suppressive factors produced by CD8+ T cells. *Science*. 1995;270:1811-1815.
62. Gonzalez E, Dhanda R, Bamshad M, et al. Global survey of genetic variation in CCR5, RANTES, and MIP-1alpha: impact on the epidemiology of the HIV-1 pandemic. *Proc Natl Acad Sci U S A*. 2001;98:5199-5204.
63. McDermott DH, Beecroft MJ, Kleeberger CA, et al. Chemokine RANTES promoter polymorphism affects risk of both HIV infection and disease progression in the Multicenter AIDS Cohort Study. *AIDS*. 2000;14:2671-2678.
64. Trkola A, Gordon C, Matthews J, et al. The CC-chemokine RANTES increases the attachment of human immunodeficiency virus type 1 to target cells via glycosaminoglycans and also activates a signal transduction pathway that enhances viral infectivity. *J Virol*. 1999;73:6370-6379.
65. Branch AD, Drye LT, Van Natta ML, et al. Evaluation of Hepatitis C Virus as a Risk Factor for HIV-Associated Neuroretinal Disorder. *Clin Infect Dis*. 2013.
66. Matsuzaki K, Murata M, Yoshida K, et al. Chronic inflammation associated with hepatitis C virus infection perturbs hepatic transforming growth factor beta signaling, promoting cirrhosis and hepatocellular carcinoma. *Hepatology*. 2007;46:48-57.
67. Fishman SL, Murray JM, Eng FJ, Walewski JL, Morgello S, Branch AD. Molecular and bioinformatic evidence of hepatitis C virus evolution in brain. *J Infect Dis*. 2008;197:597-607.
68. Forton DM, Karayiannis P, Mahmud N, Taylor-Robinson SD, Thomas HC. Identification of unique hepatitis C virus quasispecies in the central nervous system and comparative analysis of internal translational efficiency of brain, liver, and serum variants. *J Virol*. 2004;78:5170-5183.

69. Radkowski M, Wilkinson J, Nowicki M, et al. Search for hepatitis C virus negative-strand RNA sequences and analysis of viral sequences in the central nervous system: evidence of replication. *J Virol.* 2002;76:600-608.
70. Vargas HE, Laskus T, Radkowski M, et al. Detection of hepatitis C virus sequences in brain tissue obtained in recurrent hepatitis C after liver transplantation. *Liver Transpl.* 2002;8:1014-1019.
71. Wilkinson J, Radkowski M, Laskus T. Hepatitis C virus neuroinvasion: identification of infected cells. *J Virol.* 2009;83:1312-1319.
72. Lauri A, Pompilio G, Capogrossi MC. The Mitochondrial Genome in Aging and Senescence. *Ageing Res Rev.* 2014.
73. Medzhitov R. Origin and physiological roles of inflammation. *Nature.* 2008;454:428-435.
74. Pathai S, Gilbert C, Weiss HA, et al. Frailty in HIV-infected adults in South Africa. *J Acquir Immune Defic Syndr.* 2013;62:43-51.
75. Holland GN, Kappel PJ, Van Natta ML, et al. Association between abnormal contrast sensitivity and mortality among people with acquired immunodeficiency syndrome. *Am J Ophthalmol.* 2010;149:807-816.
76. Pathai S, Lawn SD, Shiels PG, et al. Corneal endothelial cells provide evidence of accelerated cellular senescence associated with HIV infection: a case-control study. *PLoS One.* 2013;8:e57422.
77. Pathai S, Lawn SD, Weiss HA, Cook C, Bekker LG, Gilbert CE. Increased ocular lens density in HIV-infected individuals with low nadir CD4 counts in South Africa: evidence of accelerated aging. *J Acquir Immune Defic Syndr.* 2013;63:307-314.
78. El-Sadr WM, Lundgren J, Neaton JD, et al. CD4+ count-guided interruption of antiretroviral treatment. *N Engl J Med.* 2006;355:2283-2296.
79. Beltran LM, Rubio-Navarro A, Amaro-Villalobos JM, Egido J, Garcia-Puig J, Moreno JA. Influence of immune activation and inflammatory response on cardiovascular risk associated with the human immunodeficiency virus. *Vasc Health Risk Manag.* 2015;11:35-48.
80. Ablashi DV, Sturzenegger S, Hunter EA, et al. Presence of HTLV-III in tears and cells from the eyes of AIDS patients. *J Exp Pathol.* 1987;3:693-703.
81. Fujikawa LS, Salahuddin SZ, Palestine AG, Masur H, Nussenblatt RB, Gallo RC. Isolation of human T-lymphotropic virus type III from the tears of a patient with the acquired immunodeficiency syndrome. *Lancet.* 1985;2:529-530.
82. Pathanapitoon K, Riemens A, Kongyai N, et al. Intraocular and plasma HIV-1 RNA loads and HIV uveitis. *AIDS.* 2011;25:81-86.
83. Han Y, Wu N, Zhu W, et al. Detection of HIV-1 viruses in tears of patients even under long-term HAART. *AIDS.* 2011;25:1925-1927.
84. Che X, Fan XQ, Wang ZL. Mechanism of blood-retinal barrier breakdown induced by HIV-1 (Review). *Exp Ther Med.* 2014;7:768-772.
85. Tan S, Duan H, Xun T, et al. HIV-1 impairs human retinal pigment epithelial barrier function: possible association with the pathogenesis of HIV-associated retinopathy. *Lab Invest.* 2014;94:777-787.
86. Gasche C, Grundtner P, Zwirn P, et al. Novel variants of the IL-10 receptor 1 affect inhibition of monocyte TNF-alpha production. *J Immunol.* 2003;170:5578-5582.
87. Ho AS, Moore KW. Interleukin-10 and its receptor. *Ther Immunol.* 1994;1:173-185.
88. Moore KW, de Waal MR, Coffman RL, O'Garra A. Interleukin-10 and the interleukin-10 receptor. *Annu Rev Immunol.* 2001;19:683-765.

89. Lin XH, Kashima Y, Khan M, Heller KB, Gu XZ, Sadun AA. An immunohistochemical study of TNF-alpha in optic nerves from AIDS patients. *Curr Eye Res.* 1997;16:1064-1068.
90. Madigan MC, Sadun AA, Rao NS, Dugel PU, Tenhula WN, Gill PS. Tumor necrosis factor-alpha (TNF-alpha)-induced optic neuropathy in rabbits. *Neurol Res.* 1996;18:176-184.
91. Petrovich MS, Hsu HY, Gu X, Dugal P, Heller KB, Sadun AA. Pentoxifylline suppression of TNF-alpha mediated axonal degeneration in the rabbit optic nerve. *Neurol Res.* 1997;19:551-554.
92. Saadati HG, Khan IA, Lin XH, Kadakia AB, Heller KB, Sadun AA. Immunolocalization of IL-1beta and IL-6 in optic nerves of patients with AIDS. *Curr Eye Res.* 1999;19:264-268.
93. Kaul M, Garden GA, Lipton SA. Pathways to neuronal injury and apoptosis in HIV-associated dementia. *Nature.* 2001;410:988-994.
94. Bruce-Keller AJ, Chauhan A, Dimayuga FO, Gee J, Keller JN, Nath A. Synaptic transport of human immunodeficiency virus-Tat protein causes neurotoxicity and gliosis in rat brain. *J Neurosci.* 2003;23:8417-8422.
95. Ene L, Duiculescu D, Tardei G, et al. Hepatitis B virus compartmentalization in the cerebrospinal fluid of HIV-infected patients. *Clin Microbiol Infect.* 2015;21:387-388.
96. de Almeida SM, Bhatt A, Riggs PK, et al. Cerebrospinal fluid human immunodeficiency virus viral load in patients with neurosyphilis. *J Neurovirol.* 2010;16:6-12.
97. Underwood J, Robertson KR, Winston A. Could antiretroviral neurotoxicity play a role in the pathogenesis of cognitive impairment in treated HIV disease? *AIDS.* 2015;29:253-261.
98. Tan PB, Li LJ, Hee OK, et al. Retinal vascular changes and immune restoration in a cohort of HIV patients on highly active antiretroviral therapy. In: 2014.
99. Jabs DA, Drye L, Van Natta ML, Thorne JE, Holland GN. Incidence and Long-term Outcomes of the Human Immunodeficiency Virus Neuroretinal Disorder in Patients with AIDS. *Ophthalmology.* 2015;122:760-768.
100. Gomez ML, Mojana F, Bartsch DU, Freeman WR. Imaging of long-term retinal damage after resolved cotton wool spots. *Ophthalmology.* 2009;116:2407-2414.
101. Rasmussen LD, Kessel L, Molander LD, et al. Risk of cataract surgery in HIV-infected individuals: a Danish Nationwide Population-based cohort study. *Clin Infect Dis.* 2011;53:1156-1163.

CHAPTER 3

Effect of age on individual retinal layer thickness in normal eyes as measured with spectral-domain optical coherence tomography

Nazli Demirkaya
Hille W. van Dijk
Sanne M. van Schuppen
Michael D.Abràmoff
Mona K. Garvin
Milan Sonka
Reinier O. Schlingemann
Frank D. Verbraak

Published in: IOVS, 2013 Jul 22; 54(7):4934-40.

ABSTRACT

Purpose

To determine the effect of age on the thickness of individual retinal layers, measured with spectral-domain optical coherence tomography (SD-OCT), in a population of healthy Caucasians.

Methods

One hundred and twenty subjects with an age ranging between 18 and 81 years were examined with SD-OCT (Topcon, Mark II). Mean layer thickness was calculated for 7 retinal layers, in the fovea (region 1 of the 9 ETDRS regions), in the pericentral ring (ETDRS regions 2 to 5), and the peripheral ring (ETDRS region 6 to 9) following automated segmentation using the Iowa Reference Algorithm. In addition, mean peripapillary retinal nerve fiber layer (RNFL) thickness was measured. The partial correlation test was performed on each layer to determine the effect of age on layer thickness, while correcting for spherical equivalent, gender and Topcon image quality factor as confounders, followed by Bonferroni corrections to adjust for multiple testing.

Results

The thickness of the peripapillary RNFL (R-0,332, P<0,001), pericentral GCL (R-0,354, P <0,001), peripheral IPL (R-0,328, P<0,001) and foveal OSL (R-0,381, P<0,001) decreased significantly with increasing age. Foveal RPE thickness (R0,467, P<0,001) increased significantly with increasing age; other layers showed no significant differences with age.

Conclusions

Several macular layers and the peripapillary RNFL thickness showed significant changes correlated with age. This should be taken into consideration when analyzing macular layers and the RNFL in SD-OCT studies of retinal diseases and glaucoma.

INTRODUCTION

The introduction of optical coherence tomography (OCT) has made it possible to visualize the human retina non-invasively in vivo with high resolution and to quantify retinal structures, such as total retinal thickness (RT) with high accuracy. Measurement of RT is important in the diagnosis and monitoring of retinal and optic nerve diseases, but to distinguish disease processes from normal age-related changes it is important to know the effect of aging on OCT measurements of the retina. Multiple OCT studies measuring the total RT in healthy subjects have shown a significant decrease in RT with age, in the pericentral and peripheral ETDRS macular regions.[1-10]

In recent years, several algorithms have been developed for Spectral Domain OCT (SD-OCT) that allow for automatic measurement of the thickness of individual retinal layers in the macula,[11-18] in addition to the segmentation of the retinal nerve fiber layer (RNFL), a tool provided by all commercially available devices.

Employing one of these techniques, *the Iowa Reference Algorithm*, a thinning of the ganglion cell layer (GCL) has been demonstrated in the pericentral macula and a corresponding loss of retinal nerve fiber layer (RNFL) thickness in the peripheral macula in patients with type 1 or type 2 diabetes and no or minimal diabetic retinopathy compared with control subjects.[19,20] For studies of changes in retinal layer thickness due to diseases like diabetes mellitus, Alzheimer's disease, glaucoma or multiple sclerosis, it is essential to include the influence of age as a confounder of individual retinal layer thickness in the analysis. In support of this notion, in a recent study, Ooto et al. have shown changes in individual retinal layer thickness with increasing age in the eyes of a Japanese population, using an automated layer segmentation algorithm.[15]

There is an increasing interest in the effects of aging in general and parameters of the aging process that can be objectively measured. The eye is of interest in that respect, and several ocular parameters have been defined in a review by Pathai et al.,[21] such as the RNFL, but changes in the macular area could be of interest as well.

To collect reference data on the effect of aging on individual retinal layers, in the present pilot study we used 3D volume scans of the macula and the optic disc made with a SD-OCT (Topcon, Mark II) in combination with the *Iowa Reference Algorithm*[12,13] to determine the effect of aging on the thickness of 7 individual retinal layers in 120 eyes of 120 healthy Caucasian men and women between 18 and 81 years of age.

SUBJECTS AND METHODS

Subjects

In this prospective cross-sectional observational study, the subjects were randomly recruited from accompanying persons of patients visiting the ophthalmology outpatient clinic of the Academic Medical Center, Amsterdam, the Netherlands, between January 2012 and January 2013 who fulfilled all in- and exclusion criteria. The study adhered to the tenets of the Declaration of Helsinki. Investigative Review Board approval was obtained at the AMC and all participants gave written informed consent.

Inclusion criteria were a history without any ocular disease, diabetes, systemic hypertension or any other (chronic) autoimmune or infectious disease, such as HIV, multiple sclerosis and rheumatoid arthritis, that could affect the retina.

Exclusion criteria were refractive errors over S+5.5 or under S-8.5 diopters, visual acuity below 0,1 logMAR, intra-ocular pressure (IOP) higher than 21 mm Hg, significant media opacities, previous ocular surgery and a previous diagnosis or any present sign of glaucoma, uveitis or retinal disease. Visual acuity was measured using a modified Early Treatment Diabetic Retinopathy Study (ETDRS) chart with Sloan letters (Lighthouse, NY) at 4 meters. Best corrected visual acuity (BCVA) was recorded in logMAR units. IOP was measured by air-puff tonometry (Topcon, computerized tonometer, CT80). All subjects underwent pupil dilation (0,1% Tropicamide) and an ophthalmic examination, including slitlamp biomicroscopy with a handheld lens, as well as fundus photography to rule out any signs of retinopathy or glaucoma. Only one eye of each participant was randomly selected for OCT examination (3D OCT-1000, Topcon Corporation, Tokyo, Japan) and was scanned after pupil dilation.

Spectral Domain Optical Coherence Tomography and Layer Segmentation

OCT images of the subjects were obtained with SD-OCT (3D OCT-1000, Topcon Corporation, Tokyo, Japan) using the 3D macular and disc volume scan protocols (6 ×6 ×2.2 mm3), consisting of 128 (y) by 512 (x) by 650 (z) voxels. Only high-quality images with a Topcon Image Quality Factor (QF) > 60 were used.

From each 3D macular volume, 11 intraretinal surfaces defining 10 retinal layers were segmented automatically by *The Iowa Reference Algorithm* (Retinal Image Analysis Lab, Iowa Institute for Biomedical Imaging, Iowa City, IA. http://www.biomed-imaging.uiowa.edu/downloads/[12,13]), which uses an extensively validated, robust fully three-dimensional graph search approach. In this study, the highly reflective layer between inner and outer segments, and the outer segments up to the retinal pigment layer were

taken together as one layer, the outer segment layer (OSL), ignoring the line ascribed to the cone outer segments. The remaining 8 layers were interpreted as follows (from inner to outer surface): 1/ retinal nerve fiber layer (RNFL), 2/ ganglion cell layer (GCL), 3/ inner plexiform layer (IPL), 4/ inner nuclear layer (INL), 5/ outer plexiform layer (OPL), 6/ outer nuclear layer (ONL) + inner segments (photoreceptors) (IS), 7/ outer segment layer (from inner –outer segment transition up to retinal pigment epithelium), 8/ retinal pigment epithelium (RPE) (Figure 1).

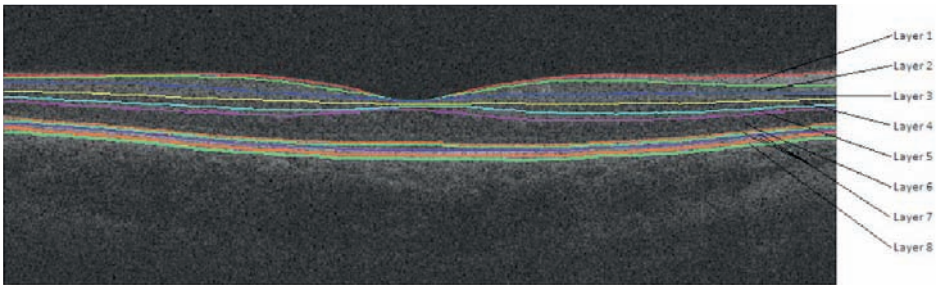

FIGURE 1. Macular B-scan with intraretinal surfaces as indicated by the colored lines and corresponding retinal layers. 1/ retinal nerve fiber layer, 2/ ganglion cell layer, 3/ inner plexiform layer, 4/ inner nuclear layer, 5/ outer plexiform layer, 6/ outer nuclear layer + inner segments (photoreceptors), 7/ outer segments (photoreceptors), 8/ retinal pigment epithelium.

The *Iowa Reference* Algorithm[12,13] allows analysis according to the ETDRS grid, which allows for the calculation of the thickness of all individual retinal layers for each of the 9 ETDRS-grid defined regions. In this study for each layer, three retinal areas were defined using this ETDRS grid: the fovea, the central circle with a diameter of 1 mm; the pericentral ring, a donut shaped ring centered on the fovea with an inner diameter of 1 mm and an outer diameter of 3 mm; and the peripheral ring, with an inner diameter of 3 mm and outer diameter of 6 mm (Figure 2). Because inner retinal layers are nearly absent in the fovea, only outer retinal layer thicknesses were analyzed in this 1-mm diameter area in the center of the fovea.

Thickness measurements of the pericentral and peripheral rings were estimated by averaging the thickness measurements of the four corresponding quadrant areas (segments 2 - 5 for the pericentral ring and segments 6 - 9 for the peripheral ring; Figure 2). In addition, thickness measurements of the entire area within the ETDRS grid were calculated automatically by the *Iowa Reference Algorithm*[12,13] and this area was defined as ''Whole macular region'' (Table 2).

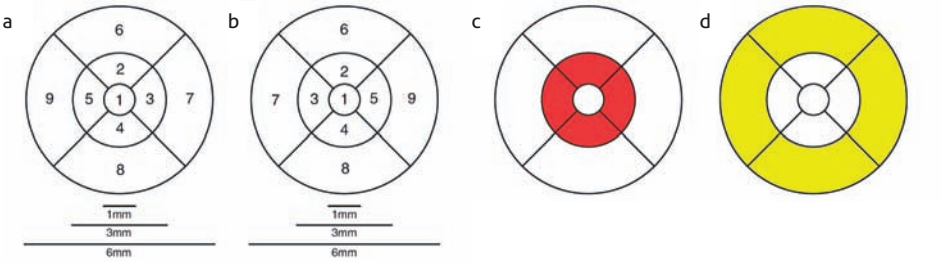

FIGURE 2. ETDRS grid. 9 subfields of the 9 ETDRS regions in each eye. (a) Right eye. (b) Left eye. (c) The four regions around the fovea constitute the pericentral ring (red coloured ring). Thickness measurement of the pericentral ring is estimated by averaging the thickness measurements of the four quadrant areas. (d) The four yellow-coloured regions constitute the peripheral ring. Thickness measurement of this area is estimated by averaging the thickness measurements of the four quadrant areas.

Finally, peripapillary RNFL thickness measurements were acquired from the 3D optic nerve head OCT's using the same *Iowa Reference Algorithm.*[12,13] The peripapillary ring was centered manually if needed, with the center of the ring coinciding with the center of the optic disc.

Statistical Analysis

Statistical analyses were performed with IBM SPSS Statistics version 19 for Windows (SPSS Inc., Chicago, IL). The Partial correlation test was used to determine the effect of age on individual layer thickness with spherical equivalent (SE),[8,22] (Topcon) image quality factor (QF)[8,23,24] and gender[2,4,5,9,15,25-29] as confounders, since these parameters are known to influence OCT thickness measurements. Bonferroni corrections were applied to counteract the effect of multiple testing with statistical significance set at $p < 0.001$. Finally, linear regression analysis was performed for the layers that correlated significantly with age.

TABLE 1. Demographic and ocular features of included subjects

	Mean ± SD	Range
OD:OS (ratio)	73:47	--
Men: women (ratio)	63:57	--
Age, Y	46,9 ± 16,5	18 - 81
Topcon image quality factor, disc scan	85,0 ± 7,5	60 – 98,9
Topcon image quality factor, macula scan	84,5 ± 7,0	63,5 – 100
Spherical equivalent refraction, D	-1,6 ± 2,8	- 8,5 – 5,25
Intra-ocular pressure, mm Hg	14,6 ± 3,2	7 – 20
Best-corrected visual acuity, LogMar	0,0 ± 0,1	-0,3 – 0,1

TABLE 2. Correlations of age with thickness of macular layers after adjusting for spherical equivalent, Topcon image quality factor and gender.

Macular layer	Mean thickness (n=120)	R	P*
RNFL			
Whole	31,8 ± 3,1	0,109	0,241
Pericentral ring	23,1 ± 1,8	0,216	0,019
Peripheral ring	35,4 ± 3,8	0,082	0,382
GCL			
Whole	33,1 ± 3,3	-0,270	0,003
Pericentral ring	**50,6 ± 5,6**	**-0,354**	**<0,001 §**
Peripheral ring	28,5 ± 3,0	-0,193	0,037
IPL			
Whole	37,5 ± 2,6	-0,273	0,003
Pericentral ring	40,7 ± 3,3	-0,030	0,747
Peripheral ring	**37,0 ± 2,9**	**-0,328**	**<0,001 §**
INL			
Whole	32,6 ± 2,4	-0,193	0,037
Pericentral ring	39,6 ± 3,2	-0,055	0,556
Peripheral ring	30,9 ± 2,5	-0,259	0,005
OPL			
Whole	26,1 ± 2,0	0,180	0,053
Fovea	24,4 ± 5,1	-0,097	0,299
Pericentral ring	29,0 ± 3,5	0,156	0,093
Peripheral ring	25,2 ± 1,8	0,188	0,042
ONL + IS			
Whole	84,5 ± 7,6	-0,177	0,056
Fovea	117,0 ± 11,7	0,138	0,138
Pericentral ring	95,9 ± 9,3	-0,063	0,499
Peripheral ring	79,9 ± 7,3	-0,230	0,013
OSL			
Whole	39,7 ± 2,8	-0,047	0,613
Fovea	**48,6 ± 3,9**	**-0,381**	**<0,001 §**
Pericentral ring	42,6 ± 3,6	-0,105	0,258
Peripheral ring	38,4 ± 2,9	-0,006	0,945
RPE			
Whole	19,2 ± 1,7	-0,032	0,730
Fovea	**18,3 ± 2,4**	**0,467**	**<0,001 §**
Pericentral ring	18,2 ± 1,9	0,177	0,056
Peripheral ring	19,6 ± 1,8	-0,124	0,183

Values are mean ± SD (μm). Whole, entire ETDRS area; fovea, central fovea (1 mm); pericentral ring, 1-3 mm from the fovea; peripheral ring, 3-6 mm from the fovea. RNFL: retinal nerve fiber layer, GCL: ganglion cell layer, IPL: inner plexiform layer, INL: inner nuclear layer, OPL: outer plexiform layer, ONL+IS: outer nuclear layer + inner segments (photoreceptors), OSL: outer segment layer (photoreceptors), RPE: retinal pigment epithelium.

* P using Partial Correlation Coefficient. § Statistically significant after Bonferroni correction.

In bold the layers with significant correlation with age are shown.

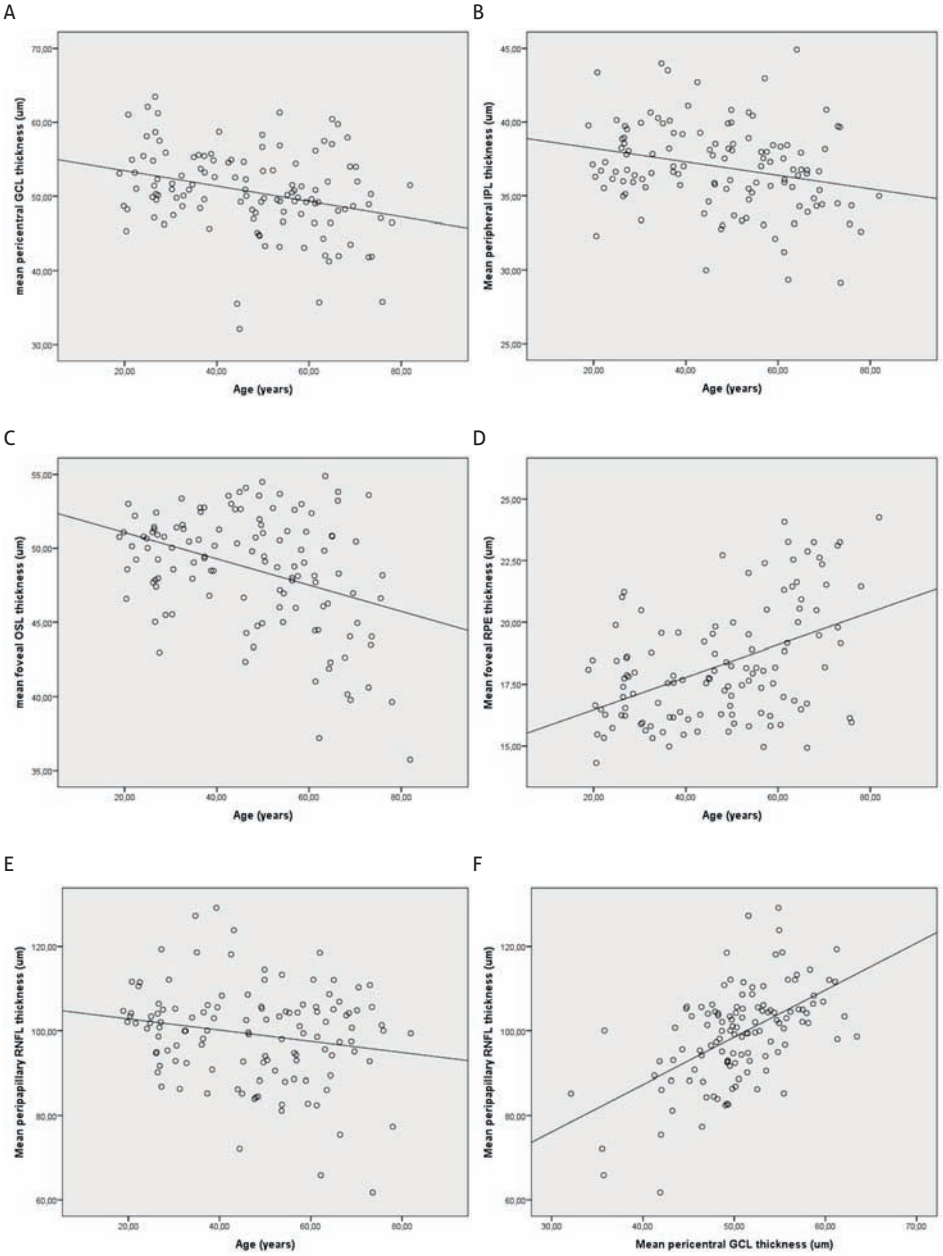

FIGURE 3. Scatterplots of simple linear regression between: age and mean pericentral GCL thickness (A), mean peripheral IPL thickness (B), mean foveal OSL thickness (C), mean foveal RPE thickness (D), and mean peripapillary RNFL thickness (E); and 2) between mean pericentral GCL thickness and mean peripapillary RNFL thickness (F). PCR: pericentral, GCL: ganglion cell layer, PR: peripheral, IPL: inner plexiform layer, OSL: outer segment layer, RPE: retinal pigment epithelium, PP: peripapillary, RNFL: retinal nerve fiber layer.

RESULTS

Demographic and ocular features of the study population are presented in Table 1. There were no significant differences in any of the parameters between men and women.

Table 2 shows the mean layer thickness measurements (µm) of the individual retinal layers of the subjects in the central fovea (only outer retinal layer thicknesses), pericentral and peripheral rings (all retinal layers) and the correlation between these layers with age, adjusted for Topcon image quality factor (QF), spherical equivalent and gender. The thickness of the pericentral GCL, peripheral IPL and foveal OSL decreased significantly with increasing age (Table 2; Figure 3A-C). Foveal RPE thickness increased significantly with increasing age (Table 2; Figure 3D); other layers showed no significant differences with age.

Mean peripapillary RNFL thickness decreased significantly with age (R-0,332, P<0,001; Partial Correlation Test; adjusted for spherical equivalent, gender and Topcon image quality factor; Figure 3E). There was a significant positive correlation between mean peripapillary RNFL thickness and mean pericentral GCL thickness (R0,553 P<0,001; Pearson correlation coefficient; Figure 3F).

DISCUSSION

The purpose of this study was to evaluate the effect of age on individual retinal layer thickness and peripapillary RNFL thickness, calculated from 3D-volume scans made with a SD-OCT (Topcon, Mark II), using the *Iowa Reference Algorithm*.[12, 13] The data were adjusted for confounders spherical equivalent (SE),[8,22] (Topcon) Image Quality Factor (QF)[8,23,24] and gender,[2,4,5,9,15,25-29] since these factors are known to influence OCT thickness measurements.

The present study demonstrated a significant decrease in peripapillary RNFL thickness, pericentral GCL thickness, peripheral IPL thickness and foveal OSL thickness with increasing age, while foveal RPE thickness correlated positively with age. Regarding the topographic distribution of the changes in retinal layer thickness over time, we postulated that the effect of age on the neuroretina would be most probably a diffuse loss of neural tissue over time, and would include all cells of the retina. A minute percentage loss of cells/ tissue would be best measured in those areas where a certain cell type in a certain retinal layer is thickest. For that reason changes in RNFL can be best measured in a ring around the optic nerve and changes in the ganglion cell layer in the pericentral

area. The same could be true for the changes in RPE thickness and outer segment layer in the fovea, but another explanation for these central changes can be the excessive metabolic strain that accumulates over the years in this most central part of the retina. The inner plexiform layer in the peripheral area reflects perhaps the loss of the pericentral GCL and the connections with the bipolar cells.

Using the findings of this study (Figure 3) one can estimate that, over a period of 20 years, an individual will lose approximately 2,66 µm of peripapillary RNFL, 2,06 µm of pericentral GCL, 0,92 µm of peripheral IPL and 1,76 µm of foveal OSL, while the foveal RPE will increase with 3,08 µm. However, these numbers are just an impression of the theoretical speed of age related changes based on the found linear relationship between thickness measurements and age (Figure 3). These figures are hypothetical, and can only be demonstrated with a longitudinal study (perhaps changes do not occur early in life, but only from a certain age, and this would be obscured in our analysis).

The mean OCT based thickness data of the layers acquired in this study (Table 2 and Table 3) are similar to those reported in other SD-OCT studies,[8,11,14,15,30] with some small differences that can be attributed to differences in study populations, the OCT devices used, and the algorithms to calculate the thickness of the individual layers.

The differences of the thickness of the individual retinal layers with age observed in the present study are mostly in concordance with previous studies,[6,10,15,31] although Ooto et al[15] report a thickening of the OSL while we describe a thinning with aging and while the RPE was not included in other segmentation algorithms. Ooto et al.[15] used a different definition of the OSL, compared to the present study, and mention in their discussion that RPE and OS tip lines were difficult to identify independently in some subjects, which may have led to an underestimation of OSL thickness in their study. Because of this ambiguity in the definition of the OS tips, we defined the layer between the IS/OS transition and RPE as representing the OSL.

Histological studies support our results : the GCL and their axons (the RNFL) are vulnerable to loss during aging[32,33] and there is a decrease in cone pigment (contained within several hundreds of infolded plasma membrane discs of the outer segments) with age,[33,34] which indicates a loss and displacement of photoreceptors with age.[35] Several structural changes occur as the RPE ages, including loss of melanin granules, increase in the density of residual bodies and accumulation of lipofuscin, accumulation of basal deposits on or within Bruch's membrane, formation of drusen and thickening of Bruch's membrane.[36] This can all lead to a thickening of the RPE with older age on OCT

measurements, either real or due to increased reflectivity leading to optical 'pseudo-thickening'.

In the present study there is a significant positive correlation between pericentral GCL thickness and peripapillary RNFL thickness (Figure 3F). Since the RNFL consists of axons of the GCL, it is feasible that a thinner GCL would indeed lead to a thinner RNFL.

This is also described in other studies where the GCL(-IPL) thickness correlated with peripapillary RNFL thickness.[26,27,37]

Limitations of the present study are the relatively small sample size (n=120 compared to larger numbers in other studies) and the fact that it was based on cross sectional data rather than longitudinal data. Another pitfall is that the subjects were not objectively checked for systemic diseases such as diabetes or hypertension, but that rather self-reported health information was used.

In conclusion, this study indicates that changes in the thickness of several retinal layers occur with increasing age and this should be taken into consideration while interpreting retinal layer and RNFL thickness data in studies concerned with the effects of disease on the retina. The age related changes of the retina may also be of use as a simple method to provide an objective parameter for aging in general, or aging in the course of systemic diseases.[21]

ACKNOWLEDGEMENTS

Disclosure: **N. Demirkaya**, None; **H.W. van Dijk**, None; **S.M. van Schuppen**, None; **M.D. Abràmoff**, None; **M.K. Garvin**, None; **M. Sonka**, None; **R.O. Schlingemann**, None; **F.D. Verbraak**, None

AUTHORS' CONTRIBUTIONS

ND contributed to the study design, data collection, data analysis and interpretation, writing of the manuscript and producing and submitting the final manuscript.

HWvD contributed to the study design and provided preliminary data.

SMvS contributed to the study design, data collection and data analysis.

MDA, MKG and MS invented and provided the Iowa Reference Algorithms. MDA revised the manuscript. ROS revised the manuscript.

FDV contributed to study design, data interpretation and writing of the manuscript.

REFERENCES

1. Alamouti B, Funk J. Retinal thickness decreases with age: an OCT study. *Br J Ophthalmol.* 2003;87:899-901.
2. Duan XR, Liang YB, Friedman DS, et al. Normal macular thickness measurements using optical coherence tomography in healthy eyes of adult Chinese persons: the Handan Eye Study. *Ophthalmology.* 2010;117:1585-1594.
3. Eriksson U, Alm A. Macular thickness decreases with age in normal eyes: a study on the macular thickness map protocol in the Stratus OCT. *Br J Ophthalmol.* 2009;93:1448-1452.
4. Kim NR, Kim JH, Lee J, Lee ES, Seong GJ, Kim CY. Determinants of perimacular inner retinal layer thickness in normal eyes measured by Fourier-domain optical coherence tomography. *Invest Ophthalmol Vis Sci.* 2011;52:3413-3418.
5. Liu T, Hu AY, Kaines A, Yu F, Schwartz SD, Hubschman JP. A pilot study of normative data for macular thickness and volume measurements using Cirrus high-definition optical coherence tomography. *Retina.* 2011.
6. Manassakorn A, Chaidaroon W, Ausayakhun S, Aupapong S, Wattananikorn S. Normative database of retinal nerve fiber layer and macular retinal thickness in a Thai population. *Jpn J Ophthalmol.* 2008;52:450-456.
7. Neuville JM, Bronson-Castain K, Bearse MA, Jr., et al. OCT reveals regional differences in macular thickness with age. *Optom Vis Sci.* 2009;86:E810-E816.
8. Rao HL, Kumar AU, Babu JG, Kumar A, Senthil S, Garudadri CS. Predictors of normal optic nerve head, retinal nerve fiber layer, and macular parameters measured by spectral domain optical coherence tomography. *Invest Ophthalmol Vis Sci.* 2011;52:1103-1110.
9. Song WK, Lee SC, Lee ES, Kim CY, Kim SS. Macular thickness variations with sex, age, and axial length in healthy subjects: a spectral domain-optical coherence tomography study. *Invest Ophthalmol Vis Sci.* 2010;51:3913-3918.
10. Sung KR, Wollstein G, Bilonick RA, et al. Effects of age on optical coherence tomography measurements of healthy retinal nerve fiber layer, macula, and optic nerve head. *Ophthalmology.* 2009;116:1119-1124.
11. Bagci AM, Shahidi M, Ansari R, Blair M, Blair NP, Zelkha R. Thickness profiles of retinal layers by optical coherence tomography image segmentation. *Am J Ophthalmol.* 2008;146:679-687.
12. Garvin MK, Abramoff MD, Kardon R, Russell SR, Wu X, Sonka M. Intraretinal layer segmentation of macular optical coherence tomography images using optimal 3-D graph search. *IEEE Trans Med Imaging.* 2008;27:1495-1505.
13. Garvin MK, Abramoff MD, Wu X, Russell SR, Burns TL, Sonka M. Automated 3-D intraretinal layer segmentation of macular spectral-domain optical coherence tomography images. *IEEE Trans Med Imaging.* 2009;28:1436-1447.
14. Loduca AL, Zhang C, Zelkha R, Shahidi M. Thickness mapping of retinal layers by spectral-domain optical coherence tomography. *Am J Ophthalmol.* 2010;150:849-855.
15. Ooto S, Hangai M, Tomidokoro A, et al. Effects of age, sex, and axial length on the three-dimensional profile of normal macular layer structures. *Invest Ophthalmol Vis Sci.* 2011;52:8769-8779.
16. Chiu SJ, Li XT, Nicholas P, Toth CA, Izatt JA, Farsiu S. Automatic segmentation of seven retinal layers in SDOCT images congruent with expert manual segmentation. *Opt Express.* 2010;18:19413-19428.

17. Kajic V, Povazay B, Hermann B, et al. Robust segmentation of intraretinal layers in the normal human fovea using a novel statistical model based on texture and shape analysis. *Opt Express*. 2010;18:14730-14744.
18. Yang Q, Reisman CA, Wang Z, et al. Automated layer segmentation of macular OCT images using dual-scale gradient information. *Opt Express*. 2010;18:21293-21307.
19. van Dijk HW, Verbraak FD, Kok PH, et al. Decreased retinal ganglion cell layer thickness in patients with type 1 diabetes. *Invest Ophthalmol Vis Sci*. 2010;51:3660-3665.
20. van Dijk HW, Verbraak FD, Kok PH, et al. Early neurodegeneration in the retina of type 2 diabetic patients. *Invest Ophthalmol Vis Sci*. 2012;53:2715-2719.
21. Pathai S, Shiels PG, Lawn SD, Cook C, Gilbert C. The eye as a model of ageing in translational research - Molecular, epigenetic and clinical aspects. *Ageing Res Rev*. 2012;12:490-508.
22. Lim MC, Hoh ST, Foster PJ, et al. Use of optical coherence tomography to assess variations in macular retinal thickness in myopia. *Invest Ophthalmol Vis Sci*. 2005;46:974-978.

Neuroretinal changes in HIV-infected adults: The AGE$_h$IV Study

CHAPTER 4

HIV-associated neuroretinal disorder in patients with well-suppressed HIV-infection: a comparative cohort study

Nazli Demirkaya
Ferdinand W.N.M. Wit
Thomas J. T. P. van Den Berg
Katherine W. Kooij
Maria Prins
Reinier O. Schlingemann
Michael D. Abramoff
Peter Reiss
Frank D. Verbraak

on behalf of the AGE$_h$IV Study Group
Published in: IOVS, 2016 Mar 1;57(3):1388-97.

ABSTRACT

Purpose

Loss of neuroretinal structure and function, ascribed to a '*HIV-associated Neuroretinal Disorder*' (HIV-NRD), in the absence of ocular opportunistic infections, has been reported in HIV-infected individuals treated with combination antiretroviral therapy (cART). Whether HIV-infected individuals with prolonged well-suppressed infection remain at risk for HIV-NRD, is unknown.

Methods

Ninety-two HIV-infected men with suppressed viremia on cART for at least 12 months (HIV+) and 63 HIV-uninfected, highly comparable, male controls (HIV-), aged at least 45 years, underwent functional measurements of spatial (Pelli Robson contrast sensitivity [PR CS]) and temporal contrast sensitivity (TCS) and straylight, as well as Spectral-Domain Optical Coherence Tomography analysis measured total and individual retinal layer thickness. Mixed linear regression models were used to assess possible associations between HIV-related and ocular parameters, while accounting for several confounders.

Results

Pelli Robson CS was significantly lower in HIV+ (1.89 vs 1.93 logCS, *P*-value=0.001), while TCS values did not differ (2.17 vs 2.17 logCS; *P*-value=0.888). Straylight values were higher in HIV+ (1.15 vs 1.09 log units; *P*-value=0.026). Peripheral total retinal thickness in the HIV+ group was increased compared to HIV- (+4.6 µm, *P*-value=0.029), predominantly due to an increase in inner nuclear layer (+1.04 µm, *P*-value=0.006) and outer plexiform layer (+0.95 µm, *P*-value=0.006) thickness.

Conclusions

Pelli Robson CS was significantly reduced in HIV-infected individuals, although the loss was one letter and likely not clinically relevant. Instead of an expected neuroretinal thinning, an *increase* of retinal thickness was detected in the HIV-infected group. These findings should be confirmed and further explored in longitudinal studies.

Keywords: HIV-NRD, Pelli Robson contrast sensitivity, temporal contrast sensitivity, straylight, optical coherence tomography, retinal layer thickness

INTRODUCTION

The spectrum of HIV-related retinal disease has changed drastically since the introduction of combination antiretroviral therapy (cART), with a major decline in incidence of both opportunistic infections, such as cytomegalovirus (CMV) retinitis, and non-infectious ischemic HIV retinopathy. However, even in cART-treated individuals without ocular opportunistic infections or visible fundus abnormalities, functional and structural retinal changes have been reported, such as a subtle loss of color vision and/or contrast sensitivity,[1-3] visual field deficits[4-6] and a thinner peripapillary retinal nerve fiber layer (RNFL) thickness.[7-9] These changes are ascribed to a '*HIV-associated Neuroretinal Disorder*' (HIV-NRD), and may be mediated by several processes, such as a long-standing microvasculopathy,[10-14] direct damage of neural tissue by HIV and/or cART,[15-17] or chronic inflammation.[18] HIV-NRD is part of a spectrum of abnormalities in HIV patients considered by some to potentially represent accelerated biological aging associated with HIV infection.[19,20]

The disorder (defined by many studies as having a Pelli Robson contrast sensitivity <1.5 logCS[21]) is more common among HIV patients with (prior) severe immune-deficiency, with a prevalence reportedly between 3-16% and an estimated cumulative incidence at 20 years after AIDS diagnosis as high as 51%.[22] A recent study found that AIDS patients with HIV-NRD have considerably increased risks of bilateral visual impairment and even blindness in the long term versus those without HIV-NRD.[22]

At present however, with the widespread availability of cART, an increasing number of HIV patients will likely never develop AIDS and fewer patients are likely to remain severely immune-deficient for prolonged periods of time. Against this background, whether patients in the current era of cART still remain at risk for HIV-associated neuroretinal degeneration is an outstanding question.

The purpose of the present study is to assess the prevalence and risk factors of retinal structural and functional loss by means of spatial and temporal contrast sensitivity and total and individual retinal layer thickness measurements using Spectral Domain-Optical Coherence Tomography (SD-OCT) analysis, comparing HIV-infected men with prolonged suppressed viremia on cART with highly comparable HIV-uninfected men, all aged ≥ 45 years.

SUBJECTS AND METHODS

Study design and participants: the AGE$_h$IV cohort study and neuroretinal substudy

The AGE$_h$IV Cohort Study is a prospective comparative cohort study investigating prevalence, incidence and risk factors of aging-associated comorbidities and organ dysfunction among HIV-1 infected individuals and highly comparable HIV-uninfected controls. Inclusion criteria are age ≥45 years and laboratory-confirmed presence - in HIV infected individuals - or absence of HIV-1 infection - in the HIV uninfected controls.

HIV-1-infected participants were recruited at the HIV outpatient clinic of the Academic Medical Center in Amsterdam, The Netherlands, and HIV-uninfected controls from the ongoing Amsterdam Cohort Studies on HIV/AIDS and among persons attending the sexual health clinic of the Public Health Service of Amsterdam (details concerning AGE$_h$IV Cohort Study have been described in a previous publication).[23]

All eligible participants from the AGE$_h$IV Cohort were consecutively invited to participate in a nested neuroretinal substudy,[24] assessing the presence of HIV-associated cognitive impairment and subtle brain and eye alterations in patients with well-suppressed HIV infection. Enrollment began in December 2011. Additional eligibility criteria for the substudy were male gender (as the availability of Dutch-speaking women in the main AGE$_h$IV Cohort was very limited), and for the HIV-infected group: sustained suppression of HIV viremia on antiretroviral treatment (plasma HIV-RNA <40 copies/mL) for ≥12 months; the presence of so-called viral 'blips' (transient low-level viremia) was not an exclusion-criterion.

Exclusion criteria for the substudy were a history of severe neurological disorder (e.g. stroke, seizure disorders, multiple sclerosis, dementia (including previous or current diagnosis of HIV-associated dementia (HAD)), history of traumatic brain injury with loss of consciousness >30 minutes, current/past (HIV-1-associated) central nervous system infection or tumour, current severe psychiatric disorder (e.g. psychosis, major depression), current injecting drug use, daily use of non-injecting recreational drugs (with the exception of daily cannabis use), current excessive alcohol consumption (>48 units of alcohol/week), insufficient command of the Dutch language or mental retardation.

Additional ophthalmic exclusion criteria were high refractive errors (SE> +5.5 or > −8.5 D), visual acuity below 0.2 logMAR, intraocular pressure (IOP) higher than 22 mm Hg, significant media opacities, and (a history of) ocular opportunistic infections, uveitis or other retinal disease. Amblyopic eyes were excluded, and we did not use straylight

and Pelli Robson data of eyes that did previously have refractive or cataract surgery.[25,26] A total of 103 HIV-infected and 74 HIV-uninfected participants were enrolled into the AGE_hIV neuroretinal substudy; of those individuals, 92 patients and 63 controls were included in the ophthalmic part of the study. The other participants were excluded for varying reasons, including having glaucoma, staphyloma, cataract preventing a reliable OCT examination, toxoplasmosis scars, retinal detachment and pseudovitelliform macular degeneration.

Standard protocol approval, registration, and patient consent

The protocol of the AGE_hIV Cohort Study and the protocol of the substudy were approved by the local ethics committee and have been registered at www.clinicaltrials.gov (identifier: NCT01466582). Written informed consent was obtained from all participants, separately for the main study and substudy.

Demographic, clinical and laboratory data collection

Participants were asked to complete a questionnaire evaluating demographics, (family) medical history, use of medication, substance use and sexual (risk) behavior. Blood samples were collected for extensive laboratory testing. Markers of inflammation (high-sensitivity C-reactive protein [hsCRP], coagulation [D-dimer), microbial translocation (soluble CD14 [sCD14]) and monocyte activation (soluble CD163 [sCD163]) were determined for all study participants. Plasma HIV-1 RNA levels were determined in the HIV-infected participants. Detailed information concerning HIV infection and antiretroviral therapy (ART) history was extracted from the Dutch HIV Monitoring Foundation database.[27]

Frailty assessment

Frailty is increasingly been recognized as a common and important HIV-associated non-AIDS condition.[28] A previous study reported a significant association between positive frailty status and abnormal Pelli Robson CS^2. We estimated the prevalence of (pre)frailty in our study population and examined possible associations with ocular parameters, indicative of neuroretinal degeneration.

The Fried frailty phenotype, as modified by Önen, was assessed in all participants in a standardized manner.[29,30] Presence of at least 3 out of the following 5 criteria was defined as frailty, presence of 1 or 2 was defined as pre-frailty and absence of all 5 factors was considered robust: self-reported unintentional weight loss [1], low physical activity [2], exhaustion [3], weak grip strength [4] and slow walking time [5].

AGE reader

Enhanced accumulation of Advanced Glycation Endproducts (AGE) is associated with a number of (age-related) chronic diseases, and has also been implicated in retinal aging and disease.[31] In our study, we assessed whether higher skin AGE levels were associated with retinal parameters of aging/neurodegeneration. AGE levels were non-invasively measured by autofluorescence using the AGE Reader (Diagnoptics Technologies B.V., Groningen, The Netherlands). This device uses characteristic fluorescent properties of certain AGE to estimate skin AGE-accumulation. This method has been validated and strongly correlates with AGE-accumulation measured in skin biopsies.[32,33]

Ophthalmic examination

Visual acuity was measured using a modified ETDRS chart with Sloan letters (Lighthouse, NY) at 4 meters. Visual acuity (VA) was recorded in LogMAR units. Intraocular pressure (IOP) was measured by air-puff tonometry (computerized tonometer, CT80; Topcon Medical Systems, Inc.). All subjects underwent pupil dilation (0.5% Tropicamide and 5% Phenylephrine) and a standard ophthalmic examination, including slit-lamp biomicroscopy with a handheld lens, as well as fundus photography.

Straylight measurement (C-Quant)

Intraocular straylight was measured with the C-Quant straylight meter (Oculus GmbH, Germany), according to the manufacturer's instructions.[34] The measurement is based on the compensation comparison method and has proven to give reliable and objective measurements of intraocular straylight. Briefly, the test field consisted of a dark circle divided into two halves (left and right), surrounded by a ring-shaped flickering light, which served as the glare source (**Figure 1**). Light emitted from the ring was scattered in the eye, resulting in the perception that the test field was flickering. A counter phase compensation light was then presented in one of the semicircles. The participants had to choose the side that flickered more intensely.

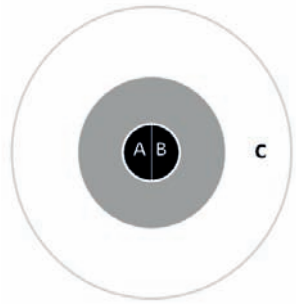

FIGURE 1. Stimulus layout for straylight and temporal contrast sensitivity measurements with the C-Quant device. The stimulus consists of a circular test area, radius 1.6°, divided in two halves (A en B), surrounded by a ring shaped light (C), that flickers as the glare source, during the straylight measurement and illuminates constantly during the temporal contrast sensitivity test.

Temporal contrast (flicker) sensitivity (C-Quant)

Temporal contrast sensitivity (TCS) was measured with the same C-Quant device, using custom written software (Matlab). Testing procedures were similar to those for straylight measurement, but with a ring of constant luminance- instead of a flickering ring- surrounding the semicircles **(Figure 1**). Randomly in one half, flicker was presented and the subject had to decide which half was flickering. The method is described more in detail in a previous report.[35]

Both straylight and TCS were measured twice per eye and the mean of the two measurements per eye was used for statistical analysis.

Pelli Robson contrast sensitivity

Spatial contrast sensitivity was determined using Pelli Robson contrast sensitivity charts (Haag-Streit, Essex, UK) at a distance of 1 m with chart background luminance within the range recommended by the manufacturer (60-120 cd/m^2). The logCS score was calculated as the total number of letters read correctly minus 3, then multiplied by 0.05.[36] Our protocol does not permit confusion between "C" and "O," which is consistent with the technique described by Myers and associates.[36] A different chart was used per eye.

SD-OCT and Retinal Layer Segmentation

OCT images of the subjects were obtained with SD-OCT (Topcon 3D OCT-1000; Topcon Inc., Paramus, NJ) using the 3D macular and disc volume scan protocols. From each 3D macular volume, individual retinal layers were segmented automatically by the publicly available and extensively validated *Iowa Reference Algorithm*.[37,38] The *Iowa Reference Algorithm*[37,38] allows for the calculation of the thickness of all individual retinal layers (**Figure 2A**) for each of the nine ETDRS-grid defined regions. We selected on the foveal, pericentral and peripheral ETDRS rings (**Figure 2B-E**), as we have done in previous studies.[39-42]

In addition, peripapillary RNFL thickness measurements (average and quadrantal) were acquired from the 3D optic nerve head OCT's using the same *Iowa Reference Algorithm*.[37,38] The peripapillary ring was centered manually with the center of the ring coinciding with the center of the optic disc.

Statistical Analysis

Statistical analysis was performed using IBM SPSS Statistics software version 21 and SAS software version 9.3 (Cary, NC, USA). Demographic/clinical characteristics were compared between the two groups using the Student's t-test, the Mann-Whitney *U*

test or the χ^2 test, as appropriate. Mixed linear regression models with a compound symmetry covariance structure were used to explore associations between HIV-status and ocular variables in all study participants, while taking the correlation between both eyes of an individual into account. All models were adjusted for age (as well as spherical equivalent and OCT Quality Factor in the OCT analyses).

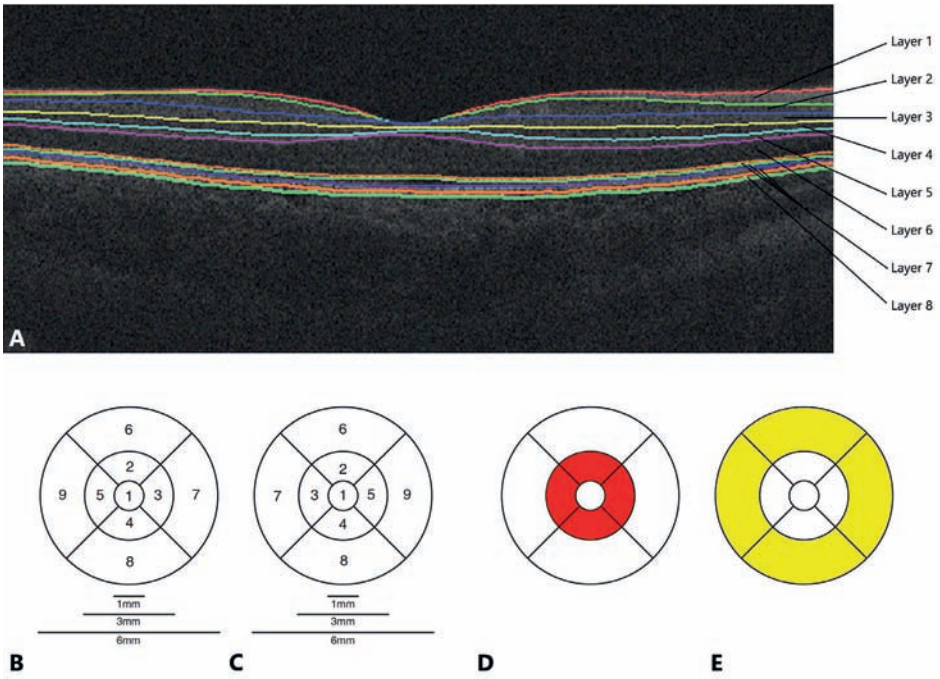

FIGURE 2. A) Macular SD-OCT B-scan with intraretinal surfaces as indicated by the colored lines and segmented using the *Iowa Reference Algorithm.*[37,38] In this study, the highly reflective layer between inner and outer segments, and the outer segments up to the retinal pigment layer were taken together as one layer, the outer segment layer (OSL), ignoring the line ascribed to the cone outer segments.[48] Corresponding retinal layers: 1/ retinal nerve fiber layer, 2/ ganglion cell layer, 3/ inner plexiform layer, 4/ inner nuclear layer, 5/ outer plexiform layer, 6/ outer nuclear layer + inner segments (photoreceptors), 7/ outer segments (photoreceptors), 8/ retinal pigment epithelium.
B-E) ETDRS grid. Nine subfields of the 9 ETDRS regions in each eye. (**B**) Right eye. (**C**) Left eye. For each retinal layer, three areas were defined using this ETDRS grid: the fovea, the central circle with a diameter of 1 mm (depicted as 1 in Figures 1B-C); the pericentral ring, a donut-shaped ring centered on the fovea with an inner diameter of 1 mm and an outer diameter of 3 mm (Figure 1**D**); and the peripheral ring, with an inner diameter of 3 mm and outer diameter of 6 mm (Figure 1**E**). Thickness measurements of the pericentral and peripheral rings were estimated by averaging the thickness measurements of the four corresponding quadrant areas (segments 2 to 5 for the pericentral ring and segments 6 to 9 for the peripheral ring).

Subsequently, within the HIV-positive group, we investigated potential associations between visual function/OCT parameters and 1) HIV/cART-related factors (prior AIDS diagnosis, nadir CD4 counts [≤ and ≥ 100 cells/μl], mean CD4 and CD8 counts during year prior to study enrollment, mean log^{10} plasma HIV-1 RNA load in 12 months prior to enrollment and before start of ART, years since start first ART) and 2) other (risk) factors possibly involved in the pathophysiology of HIV-NRD (including markers of inflammation and innate immune activation, frailty status and AGE-reader measurement). With respect to OCT parameters, we focused in particular on the retinal layers known to change with increasing age[40] (to test the hypothesis of accelerated/accentuated aging in HIV) as well as the inner retinal layers (to assess possible neuroretinal degeneration[42]) instead of exploring all individual layers, to reduce the chance of type I errors. Because of the exploratory nature of this study and established a priori hypotheses, adjustment for multiple comparisons was not performed. Statistical significance was set at a two-sided *P*-value of 0.05.

RESULTS

Subject characteristics

Table 1 shows the baseline characteristics of all study participants; the two groups were comparable in terms of age, nationality, sexual orientation, comorbidities and frailty status. However, HIV-infected individuals had higher plasma levels of inflammation markers as well as a higher AGE-reader measurement and were more likely to be ever-smokers, whereas ecstasy use was more prevalent among controls. On average, HIV-infected individuals were known to be infected for a prolonged period of time and approximately 32% had previously been diagnosed with AIDS. Most men used cART for many years, 99% had an undetectable viral load and the majority had experienced immune recovery on treatment, with a median nadir CD4 count of 180 cells/μl and current median CD4 count of 595 cells/μl.

TABLE 1. Participant characteristics.

Socio-demographic characteristics	HIV-infected participants (n=92)	HIV-uninfected participants (n=63)	*P*-value
Age, years	53.5 (45-76)	52 (45-80)	0.940[a]
Male sex	100%	100%	-
Nationality, Dutch	88%	85%	0.587[b]
MSM	94.5%	88%	0.164[b]
Smoking			
Current	28.2%	16.7%	0.100[b]

TABLE 1. Participant characteristics.

Socio-demographic characteristics	HIV-infected participants (n=92)	HIV-uninfected participants (n=63)	*P*-value
Ever smoked	76.1%	56.7%	**0.012**[b]
Pack-years of smoking	20.3 (0.2-90)	9 (0-74.3)	**0.013**[a]
Heavy daily drinker	5.4%	8.3%	0.517[c]
Recreational drug use, daily to monthly			
Cannabis	15.2%	15.0%	1.000[c]
Cocaine	3.3%	5%	0.681[c]
XTC	2.2%	13.3%	**0.014**[c]
Comorbidities			
DM type II; (using medication)	2.2% (0)	0 (0)	0.517[c]
Hypertension; (using medication)	29.3% (63.0%)	29.5% (44.4%)	0.983[b]
HIV- and cART related characteristics			
Years known to be HIV positive	14.5 (1-27)	-	-
Prior clinical AIDS	32.6%	-	-
CD4 cell count, cells/µl			
Current	595 (320-1110)	-	-
In year prior to enrollment	620.8 (216-1130)	-	-
Nadir	180 (0-620)	-	-
Cumulative duration of CD4 cell count			-
<200 cells/µl ; months	0.78 (0-96.8)	-	-
<100 cells/µl; months	0 (0-66.5)	-	-
CD8 cell count, cells/µl			
Current	860 (190-1620)	-	-
In year prior to enrollment	890 (162-1992)	-	-
CD4/8 ratio	0.75 (0.29-4.13)	-	-
Plasma viral load			
Prior start ART	4.9 (3.4-6.7)		
Current	1.6 (1.6-1.94)	-	-
In year prior to enrollment	1.6 (1.6-2.73)	-	-
Undetectable during year before enrollment	98.9%	-	-
Cumulative duration of undetectability; y	10.2 (0-15.1)	-	-
Years since start of first ART	12 (1-21)	-	-
Naïve at start of first cART	81.5%	-	-
ART naïve at enrollment	0%	-	-
Markers of systemic inflammation			
High sensitivity C-reactive protein (CRP), mg/L	1.5 (0-60.4)	0.9 (0.3-8.3)	**0.011**[a]
D-dimer, mg/L	0.2 (0.2-1.59)	0.27 (0.2-2.3)	0.061[a]
Soluble CD14, ng/mL	1565 (726-3886)	1200 (569-3316)	**<0.001**[a]
Soluble CD163, ng/mL	268 (81-1146)	250 (111-783)	0.307[a]

TABLE 1. Participant characteristics.

Socio-demographic characteristics	HIV-infected participants (n=92)	HIV-uninfected participants (n=63)	*P*-value
Frailty status (presence of 0-5 criteria)			
Not frail (0)	68.5%	70%	0.203[b]
Pre-frail (1-2)	29.3%	30%	
Frail (≥3)	2.2%	0%	
AGE-reader measurement, arbitrary units	2.3 (0-4.7)	2 (1.5-2.7)	**<0.001**[a]
AGE-reader measurement higher compared to reference value (>+1SD)	20%	1.7%	0.001[c]

Data are presented as median (range) or percentage. [a]Mann Whitney *U* Test. [b] Chi-square Test. [c] Fisher's Exact Test. n=number of patients.

Contrast sensitivity and straylight measurements

Pelli Robson contrast sensitivity was significantly lower in the HIV-infected group, although the difference was only 1 letter (1.89 vs 1.93 logCS, *P*-value=0.001), while temporal contrast sensitivity values did not differ significantly among the two groups (2.17 vs 2.17 logCS; *P*-value=0.888). Straylight values were slightly higher among the HIV-infected individuals (1.15 vs 1.09 log units; *P*-value=0.026; **Table 2**). Of the HIV-infected patients, only 1 patient (1.3%) had a PR contrast sensitivity below 1.5 and 6 patients (7.7%) had a PR contrast sensitivity below 1.65 logCS (these cut-off values were used by previous studies to denote 'poor CS'[1-3]), respectively, while none of the HIV-uninfected participants had PR scores below 1.7 logCS.

TABLE 2. Visual function test results in HIV patients and controls.

Ocular parameters/ Visual function	HIV-infected participants (n=92)				HIV-uninfected participants (n=63)				Coef-ficient	*P*-value
	eyes	mean	SD	range	eyes	mean	SD	range		
Spherical equivalent refraction, D	161	-0.6	2.2	-7.5-4.8	111	-1.4	2.2	-8.0-3.5	0.721	**0.046**
Intra-ocular pressure, mm Hg	161	14.4	2.7	7-21	111	13.8	3.2	7-22	0.546	0.250
Visual acuity, LogMar	161	-0.01	0.08	-0.2-0.2	111	-0.03	0.07	-0.2-0.18	0.016	0.160
Pelli Robson CS; logCS	155	1.89	0.10	1.45-2.05	113	1.93	0.04	1.70-2.05	-0.040	**0.001**
Temporal CS; logCS	172	2.17	0.17	1.55-2.50	121	2.17	0.17	1.73-2.52	-0.004	0.888
Straylight; log units	161	1.15	0.19	0.75-1.79	113	1.09	0.16	0.79-1.64	0.060	**0.026**

P-values derived from linear mixed models; adjusted for age at assessment. n=number of patients; CS= contrast sensitivity. *P*-values in bold are P <0.05.

Thickness of retinal layers

Mean layer thickness measurements (individual retinal layers, peripapillary RNFL and total retinal thickness) -adjusted for age, OCT quality factor and spherical equivalent- for patients and controls are shown in **Table 3.** The two groups had comparable retinal thicknesses regarding most layers; the most notable difference was a significantly increased total peripheral retinal thickness in the HIV-infected group (+4.6 μm, *P*-value=0.029), predominantly due to an increase in inner nuclear layer (+1.04 μm, *P*-value=0.006) and outer plexiform layer (+0.95 μm, *P*-value=0.006) thickness. Peripapillary RNFL thickness was not significantly different among the two groups.

TABLE 3. OCT retinal layer thicknesses in HIV patients and controls.

Macular layer thickness (μm)	HIV-infected participants (n=92)				HIV-uninfected participants (n=63)				Coefficient	*P*-value
	eyes	mean	SD	range	eyes	mean	SD	range		
RNFL										
Fovea	167	8.08	3.2	1.6-19.6	120	7.8	3.1	2.3-18.5	0.646	0.215
Pericentral ring	167	24.4	2.3	18.3-32.2	120	24.4	2.1	19.7-28.9	0.310	0.374
Peripheral ring	167	36.6	4.7	26.3-53.6	120	36.1	3.9	26.8-48.1	1.045	0.135
GCL										
Fovea	167	12.8	5.4	1.9-29.9	120	12.4	5.6	3.7-35.2	0.615	0.503
Pericentral ring	167	48.3	6.7	27.9-65.3	120	47.3	7.4	24.2-63.2	1.222	0.301
Peripheral ring	167	28.0	3.3	19.2-36.7	120	26.9	4.0	17.6-34.8	0.792	0.193
IPL										
Fovea	167	30.6	5.3	16.2-46.2	120	30.9	5.2	10.6-44.4	0.095	0.915
Pericentral ring	167	42.6	3.8	34.2-59.4	120	42.5	3.7	33.3-55.0	0.303	0.634
Peripheral ring	167	38.6	2.2	33.2-48.8	120	38.3	2.7	31.9-47.9	0.401	0.329
INL										
Fovea	167	18.2	5.4	5.8-34.8	120	17.2	6.1	3.2-37.8	1.054	0.285
Pericentral ring	167	37.8	3.3	29.2-47.0	120	36.4	3.6	24.9-46.7	1.433	**0.019**
Peripheral ring	167	28.9	2.1	23.8-33.8	120	27.7	2.5	20.8-32.8	1.035	**0.006**
OPL										
Fovea	167	23.2	4.3	14.2-35.6	120	23.5	4.2	13.0-36.2	0.251	0.694
Pericentral ring	167	31.5	3.6	25.2-43.3	120	31.0	4.0	26.1-43.6	0.718	0.214
Peripheral ring	167	28.3	1.9	24.1-33.3	120	27.5	2.5	23.2-34.7	0.950	**0.006**
ONL + IS										
Fovea	167	123.8	9.9	90.1-151.6	120	120.7	9.5	100.1-151.4	2.026	0.222
Pericentral ring	167	97.2	7.8	75.9-114.9	120	94.8	7.9	75.1-111.3	1.604	0.224
Peripheral ring	167	78.9	6.8	59.5-95.7	120	77.6	6.1	63.6-91.4	0.658	0.542
OSL										
Fovea	167	48.5	3.7	36.7-58.2	120	49.0	3.8	27.6-55.2	-1.040	0.086

TABLE 3. OCT retinal layer thicknesses in HIV patients and controls. (continued)

Macular layer thickness (µm)	HIV-infected participants (n=92)				HIV-uninfected participants (n=63)				Coef-ficient	*P*-value
	eyes	mean	SD	range	eyes	mean	SD	range		
Pericentral ring	167	43.3	2.4	36.5-48.7	120	43.3	2.3	35.6-48.7	-0.276	0.465
Peripheral ring	167	40.5	2.9	30.4-47.8	120	40.3	2.5	34.5-45.5	-0.014	0.977
RPE										
Fovea	167	18.5	1.9	13.1-22.4	120	17.9	2.0	13.8-22.1	0.664	**0.029**
Pericentral ring	167	17.9	1.8	12.9-21.3	120	17.5	1.9	13.5-21.4	0.333	0.259
Peripheral ring	167	18.1	1.5	14.4-21.4	120	18.2	1.8	14.1-21.2	-0.086	0.758
Total foveal RT	167	265.2	22.6	214.2-317.6	120	261.6	21.7	208.4-326.0	3.556	0.367
Total pericentral RT	167	325.0	15.2	293.7-365.7	120	319.6	15.1	285.0-354.1	4.872	0.065
Total peripheral RT	167	279.8	12.5	249.2-310.4	120	274.4	12.0	249.5-308.1	4.575	**0.029**
Peripapillary RNFL (µm)										
Average	168	102.0	11.3	73.3-132.7	120	100.0	10.1	74.3-124.8	1.170	0.520
Superior	168	125.5	20.2	35.8-178.4	120	125.4	17.3	82.8-160.4	-0.345	0.916
Inferior	168	131.1	16.8	78.9-172.8	120	128.1	15.8	86.5-161.1	2.138	0.413
Temporal	168	72.9	13.5	43.2-115.9	120	72.4	12.5	50.5-127.5	0.729	0.732
Nasal	168	78.5	15.3	31.3-132.1	120	74.2	16.0	38.5-123.5	2.190	0.370

SD=standard deviation. n= number of patients. RNFL=retinal nerve fibre layer. GCL=ganglion cell layer. IPL= inner plexiform layer. INL=inner nuclear layer. OPL=outer plexiform layer. ONL-IS=outer nuclear layer- inner segments. OSL=outer segment layer. RPE=retinal pigment epithelium. RT=retinal thickness. *P*-values derived from linear mixed models and adjusted for age at assessment, OCT quality factor and spherical equivalent. *P*-values in bold are $P<0.05$.

Multivariable analyses within the HIV-infected group

Exploring potential risk factors of retinal structural and functional changes within the HIV-infected group, we did not detect significant associations between indicators of (past) HIV disease severity (nadir or current CD4 counts, CD8 counts, prior AIDS diagnosis and pre-ART plasma VL) and any of the visual function/OCT parameters tested.

We did observe significant associations between other explanatory variables and retinal measures: central outer segment layer thickness was negatively associated with ART duration (-0.141 microns/year; *P*-value: 0.048) and positively associated with soluble CD163 levels (+0.63 microns per 100 ng/mL, *P*-value:0.009). Central retinal pigment epithelium thickness was positively associated with pre-frailty (+1.075 microns; *P*-value 0.012) and peripheral ganglion cell layer thickness was negatively associated with a higher AGE-reader measurement (-1.28 microns/arbitrary unit, P-value 0.012).

DISCUSSION

In this study assessing HIV-related neuroretinal degeneration, we found only minimal changes in contrast sensitivity and no decrease in (neuro)retinal and peripapillary RNFL thickness when comparing HIV-infected men with prolonged suppressed viraemia on cART to a highly similar group of HIV-negative men, all aged 45 years or above.

HIV-infected patients scored only one letter less on the Pelli Robson (PR) contrast sensitivity chart, while having comparable temporal contrast sensitivity outcomes. Two recent comparable studies on contrast sensitivity and RNFL thickness in cART-treated HIV-infected patients without opportunistic ocular infections, reported similar subtle differences in PR contrast sensitivity between HIV-infected individuals and HIV-negative controls: Kalyani et al.[1] measured a median PR score of 1.90 logCS in a group of 57 HIV-infected individuals (89% with a prior diagnosis of AIDS), with only 2.9% of eyes having abnormal contrast sensitivity (<1.5 logCS; based on CS values of a control group described by Myers et al.). Pathai et al.[2] reported a mean difference of 0.06 logCS (approximately 1 letter) between a group of 225 HIV-infected subjects (72% with WHO stage III/IV HIV) and 203 HIV-negative controls, while the percentage of subjects with 'poor' CS (<1.65 logCS) was 43.5% in the HIV-infected group and 31.8% in the control group. Pathai also detected an association between poor CS and positive frailty status and HIV viral load >2 log copies/ml.

In our study, only 1 (1.3%) and 6 patients (7.7%) had a PR contrast sensitivity of 1.5 and 1.65 logCS, respectively. We couldn't confirm the findings of Pathai[2] and did not find an association between PR contrast sensitivity and either frailty status nor HIV viral load. However, compared to the previous two studies, our HIV-infected cohort has a better immunological and clinical status, with only 33% having been previously diagnosed with AIDS and 99% having had undetectable viraemia, and were treated for many years. These differences could explain the better contrast sensitivity outcomes of our patients and the lack of correlation detected between frailty status and contrast sensitivity.

In addition to measuring spatial contrast sensitivity, we also assessed temporal contrast sensitivity (TCS), using an adaptation of the C-Quant, and we found no significant differences between patients and controls. Since we are the first group evaluating TCS in HIV-infected patients in the cART era, we cannot compare our results to other studies. The discrepancy in PR CS scores and TCS values in the present study might be ascribed to the fact that PR outcome is influenced by both optical and retinal components, while TCS assesses purely retinal function,[35] although PR CS remained significantly lower in the patient group, after adjusting for straylight in the statistical analysis (data not shown).

However, straylight is known to influence spatial CS only very weakly[43] and while we did not test PR CS of participants with a history of refractive/cataract surgery, other optical factors, such as higher order aberrations, might have affected the PR outcomes.

We did not find any significant differences in peripapillary retinal nerve fiber layer (RNFL) thickness between HIV-infected individuals and HIV-negative controls. This is largely in accordance with the findings of Pathai[2] and Kalyani[1]. Pathai[2] reported a similar average RNFL thickness between patients and controls, while only 8.8% of the HIV-infected group examined by Kalyani[1] had a thinner RNFL than average. Other studies assessing peripapillary RNFL thickness in HIV-infected patients, reported a decrease in RNFL thickness particularly in patients with low (<100 cells/µl) nadir CD4 counts for at least 6 months, compared to patients with nadir CD4 counts higher than 100 cells/µl and HIV-uninfected controls.[5,7,8] In our HIV-infected group, 30% had nadir CD4 counts <100 cells/µl, for a short mean cumulative duration of 0.2 years, and no associations between (duration of) nadir CD4 counts and peripapillary RNFL thickness were detected.

Subsequently, we segmented and analysed total and individual retinal layer thickness in the central, pericentral and peripheral ETDRS areas, using the extensively validated Iowa Reference Algorithm. As it is hypothesized that damage (caused by HIV and/or other factors) to the optic nerve leads to thinning of the peripapillary RNFL in HIV, a decrease in ganglion cell layer thickness (and possibly other inner retinal layers) would also be expected, considering that the axons of the ganglion cell layer make up the optic nerve for a large part. Parallel to the peripapillary RNFL thickness in our study population however, we did not detect thinner inner retinal layers in the HIV-infected group versus the controls. In addition, the retinal layers known to change with increasing age,[40] were not significantly thinner in the HIV-infected individuals, providing no support for the hypothesis of accelerated retinal aging in HIV. We also did not find an association of retinal thickness with monocyte activation markers sCD14/sCD163 in the HIV-infected group, which are considered to be implicated in HIV-related neurodegeneration and –neurocognitive deficits.[44]

In contrast, we observed a significant *increase* in retinal thickness in HIV-infected individuals compared to the control group. At present, only one other study - by Arcinue et al.[45]- has measured individual retinal layer thickness in HIV-infected patients and they described an increase in retinal thickness as well - in particular the inner retinal layers- in a group of 10 HIV-positive patients compared to 10 HIV-negative controls. In our study, the increase in total retinal thickness was predominantly due to thicker inner nuclear and outer plexiform layers. A good comparison of our results with those of Arcinue et al.[45] is difficult, considering the very small sample size of their study,

different segmentation algorithm used (applied on only 3 B-scans), lack of correction for important confounders in the analyses and inclusion of patients with a history of more severe immune-deficiency. An increased volume of inner nuclear (and outer plexiform[46]) layer[46,47] has also been reported by recent studies assessing retinal layer thickness in multiple sclerosis, a disease characterized by neuro-inflammation and –degeneration, processes both regarded important in HIV-associated neurocognitive and –retinal changes as well. The authors speculated that these changes might reflect low grade inflammatory activity, which could also be relevant in the HIV-infected population. Furthermore in these studies, correlations were detected between INL thickening and inflammatory MRI activity and cerebrospinal fluid findings.[46,47]

Similar (longitudinal) research combining OCT, MRI and laboratory parameters would provide more insight in the potential role of (neuro-)inflammation in HIV-associated neuroretinal changes. Multivariable analyses within the HIV-infected group showed no consistent (e.g. the significant associations were not found in multiple retinal layers or regions) associations between predictive variables and retinal parameters. Considering the high number of *P*-values generated, it is likely that the significant associations we detected were due to type I errors.

Strengths of our study are the inclusion of a highly similar control group, and the adjustment for relevant confounding factors (e.g. age, OCT quality factor, spherical equivalent) in our statistical analyses. Furthermore, we introduced a novel, more accurate method[35] for assessing retinal function, instead of the standard Pelli Robson chart used by most studies, which is also confounded by the optics of the eye.

Nonetheless, there are a number of limitations to this study. The relatively small sample size may have hampered the detection of some potential associations. Secondly, a cross-sectional study of parameters known to have a high inter-individual variability is less able to detect small changes in retinal structure and function than a longitudinal study.

In summary, this is the first study in a group of patients with prolonged well-suppressed HIV-infection on cART, assessing the neuroretina by means of both spatial and temporal contrast sensitivity as well as individual retinal layer thickness measurements. Our results provide little evidence for neuroretinal loss in individuals with well-suppressed HIV-infection, compared to HIV-uninfected controls, with no clinically relevant reduction in PR CS and absence of neuroretinal atrophy.

The significantly *increased* retinal thickness we detected in the HIV-infected group was unexpected and should be confirmed and further explored by larger longitudinal studies. The long-term effects of HIV-infection on the retina are still unknown, and as life-expectancy of HIV-infected patients is increasing with the global roll-out of cART, vision loss might become more prevalent and symptomatic with time.

ACKNOWLEDGEMENTS

We thank Judith Schouten, Tanja Su and Rosan van Zoest for their excellent co-organization of the main AGE$_h$IV cohort study and neuroretinal substudy. We thank our colleagues at the Department of Experimental Immunology at the Academic Medical Center for the excellent collaboration both logistically and scientifically. We thank Barbara Elsenga, Aafien Henderiks, Jane Berkel, Sandra Moll, and Marjolein Martens for running the AGE$_h$IV study program with such care and passion. We thank Yolanda Ruijs-Tiggelman, Lia Veenenberg-Benschop, Tieme Woudstra, Sima Zaheri, and Mariska Hillebregt at the HIV Monitoring Foundation for their contributions to data-management. We thank all HIV-physicians and HIV-nurses at the Academic Medical Center for their efforts to include the HIV-infected participants into the AGE$_h$IV Cohort Study/neuroretinal substudy. We thank all Municipal Health Service Amsterdam personnel for their efforts to include the HIV-uninfected participants into the AGE$_h$IV Cohort Study/neuroretinal substudy. We thank all study participants without whom this research would not be possible.

AUTHORS' CONTRIBUTIONS

ND contributed to study design, data collection, data analysis and interpretation, writing of the manuscript and was responsible for producing and submitting the final manuscript.

FWNMW contributed to study design, supervised statistical analysis, contributed to data interpretation and revised the manuscript.

TJTPvdB invented and provided the C-Quant device, contributed to data interpretation and revised the manuscript. KWK contributed to data collection and revised the manuscript.

MP contributed to the study design and revised the manuscript.

ROS contributed to data interpretation and revised the manuscript.

MDA designed and provided the Iowa Reference Algorithms, contributed to data interpretation and revised the manuscript.

PR conceived the main AGEhIV cohort and the substudy, contributed to the study design, to data interpretation and revised the manuscript.

FDV contributed to study design, contributed to datainterpretation and supervised and revised all drafts of the manuscript.

REFERENCES

1. Kalyani PS, Holland GN, Fawzi AA, Arantes TE, Yu F, Sadun AA. Association between retinal nerve fiber layer thickness and abnormalities of vision in people with human immunodeficiency virus infection. *Am J Ophthalmol.* 2012;153:734-42, 742.
2. Pathai S, Lawn SD, Weiss HA, Cook C, Bekker LG, Gilbert CE. Retinal Nerve Fibre Layer Thickness and Contrast Sensitivity in HIV-Infected Individuals in South Africa: A Case-Control Study. *PLoS One.* 2013;8:e73694.
3. Shah KH, Holland GN, Yu F, Van NM, Nusinowitz S. Contrast sensitivity and color vision in HIV-infected individuals without infectious retinopathy. *Am J Ophthalmol.* 2006;142:284-292.
4. Arantes TE, Garcia CR, Tavares IM, Mello PA, Muccioli C. Relationship between retinal nerve fiber layer and visual field function in human immunodeficiency virus-infected patients without retinitis. *Retina.* 2012;32:152-159.
5. Faria E Arantes TE, Garcia CR, Mello PA, Muccioli C. Structural and functional assessment in HIV-infected patients using optical coherence tomography and frequency-doubling technology perimetry. *Am J Ophthalmol.* 2010;149:571-576.
6. Kozak I, Sample PA, Hao J, et al. Machine learning classifiers detect subtle field defects in eyes of HIV individuals. *Trans Am Ophthalmol Soc.* 2007;105:111-118.
7. Kozak I, Bartsch DU, Cheng L, Kosobucki BR, Freeman WR. Objective analysis of retinal damage in HIV-positive patients in the HAART era using OCT. *Am J Ophthalmol.* 2005;139:295-301.
8. Kozak I, Bartsch DU, Cheng L, McCutchan A, Weinreb RN, Freeman WR. Scanning laser polarimetry demonstration of retinal nerve fiber layer damage in human immunodeficiency virus-positive patients without infectious retinitis. *Retina.* 2007;27:1267-1273.
9. Plummer DJ, Bartsch DU, Azen SP, Max S, Sadun AA, Freeman WR. Retinal nerve fiber layer evaluation in human immunodeficiency virus-positive patients. *Am J Ophthalmol.* 2001;131:216-222.
10. Dadgostar H, Holland GN, Huang X, et al. Hemorheologic abnormalities associated with HIV infection: in vivo assessment of retinal microvascular blood flow. *Invest Ophthalmol Vis Sci.* 2006;47:3933-3938.
11. Gangaputra S, Kalyani PS, Fawzi AA, et al. Retinal vessel caliber among people with acquired immunodeficiency syndrome: relationships with disease-associated factors and mortality. *Am J Ophthalmol.* 2012;153:434-444.
12. Kalyani PS, Fawzi AA, Gangaputra S, et al. Retinal vessel caliber among people with acquired immunodeficiency syndrome: relationships with visual function. *Am J Ophthalmol.* 2012;153:428-433.
13. Kim A, Dadgostar H, Holland GN, et al. Hemorheologic abnormalities associated with HIV infection: altered erythrocyte aggregation and deformability. *Invest Ophthalmol Vis Sci.* 2006;47:3927-3932.
14. Lim MC, Cumberland WG, Minassian SL, et al. Decreased macular leukocyte velocity in human immunodeficiency virus-infected individuals. *Am J Ophthalmol.* 2001;132:711-719.
15. Kaul M, Garden GA, Lipton SA. Pathways to neuronal injury and apoptosis in HIV-associated dementia. *Nature.* 2001;410:988-994.
16. Kaul M, Lipton SA. Mechanisms of neuroimmunity and neurodegeneration associated with HIV-1 infection and AIDS. *J Neuroimmune Pharmacol.* 2006;1:138-151.

17. Tenhula WN, Xu SZ, Madigan MC, Heller K, Freeman WR, Sadun AA. Morphometric comparisons of optic nerve axon loss in acquired immunodeficiency syndrome. *Am J Ophthalmol*. 1992;113:14-20.
18. Xu H, Chen M, Forrester JV. Para-inflammation in the aging retina. *Prog Retin Eye Res*. 2009;28:348-368.
19. Pathai S, Bajillan H, Landay AL, High KP. Is HIV a Model of Accelerated or Accentuated Aging? *J Gerontol A Biol Sci Med Sci*. 2013.
20. Demirkaya N, Wit F, Schlingemann R, Verbraak F. Neuroretinal Degeneration in HIV Patients Without Opportunistic Ocular Infections in the cART Era. *AIDS Patient Care STDS*. 2015;29:519-532.
21. Freeman WR, Van Natta ML, Jabs D, et al. Vision function in HIV-infected individuals without retinitis: report of the Studies of Ocular Complications of AIDS Research Group. *Am J Ophthalmol*. 2008;145:453-462.
22. Jabs DA, Drye L, Van Natta ML, Thorne JE, Holland GN. Incidence and Long-term Outcomes of the Human Immunodeficiency Virus Neuroretinal Disorder in Patients with AIDS. *Ophthalmology*. 2015;122:760-768.
23. Schouten J, Wit FW, Stolte IG, et al. Cross-sectional comparison of the prevalence of age-associated comorbidities and their risk factors between HIV-infected and uninfected individuals: the AGEhIV cohort study. *Clin Infect Dis*. 2014;59:1787-1797.
24. Su T, Schouten J, Geurtsen GJ, et al. Multivariate normative comparison, a novel method for more reliably detecting cognitive impairment in HIV infection. *AIDS*. 2015;29:547-557.
25. Chan JW, Edwards MH, Woo GC, Woo VC. Contrast sensitivity after laser in situ keratomileusis. one-year follow-up. *J Cataract Refract Surg*. 2002;28:1774-1779.
26. van Bree MC, van Verre HP, Devreese MT, Larminier F, van den Berg TJ. Straylight values after refractive surgery: screening for ocular fitness in demanding professions. *Ophthalmology*. 2011;118:945-953.
27. . Stichting HIV monitoring. In: 2015.
28. Onen NF, Overton ET. A review of premature frailty in HIV-infected persons; another manifestation of HIV-related accelerated aging. *Curr Aging Sci*. 2011;4:33-41.
29. Fried LP, Tangen CM, Walston J, et al. Frailty in older adults: evidence for a phenotype. *J Gerontol A Biol Sci Med Sci*. 2001;56:M146-M156.
30. Onen NF, Agbebi A, Shacham E, Stamm KE, Onen AR, Overton ET. Frailty among HIV-infected persons in an urban outpatient care setting. *J Infect*. 2009;59:346-352.
31. Glenn JV, Stitt AW. The role of advanced glycation end products in retinal ageing and disease. *Biochim Biophys Acta*. 2009;1790:1109-1116.
32. Meerwaldt R, Graaff R, Oomen PH, et al. Simple non-invasive assessment of advanced glycation endproduct accumulation. *Diabetologia*. 2004;47:1324-1330.
33. Mulder DJ, Water TV, Lutgers HL, et al. Skin autofluorescence, a novel marker for glycemic and oxidative stress-derived advanced glycation endproducts: an overview of current clinical studies, evidence, and limitations. *Diabetes Technol Ther*. 2006;8:523-535.
34. Franssen L, Coppens JE, van den Berg TJ. Compensation comparison method for assessment of retinal straylight. *Invest Ophthalmol Vis Sci*. 2006;47:768-776.
35. van den Berg TJ, Franssen L, Kruijt B, Coppens JE. Psychophysics, reliability, and norm values for temporal contrast sensitivity implemented on the two alternative forced choice C-Quant device. *J Biomed Opt*. 2011;16:085004.

36. Myers VS, Gidlewski N, Quinn GE, Miller D, Dobson V. Distance and near visual acuity, contrast sensitivity, and visual fields of 10-year-old children. *Arch Ophthalmol.* 1999;117:94-99.
37. Garvin MK, Abramoff MD, Kardon R, Russell SR, Wu X, Sonka M. Intraretinal layer segmentation of macular optical coherence tomography images using optimal 3-D graph search. *IEEE Trans Med Imaging.* 2008;27:1495-1505.
38. Garvin MK, Abramoff MD, Wu X, Russell SR, Burns TL, Sonka M. Automated 3-D intraretinal layer segmentation of macular spectral-domain optical coherence tomography images. *IEEE Trans Med Imaging.* 2009;28:1436-1447.
39. Darma S, Kok PH, van den Berg TJ, et al. Optical density filters modeling media opacities cause decreased SD-OCT retinal layer thickness measurements with inter- and intra-individual variation. *Acta Ophthalmol.* 2015;93:355-361.
40. Demirkaya N, van Dijk HW, van Schuppen SM, et al. Effect of age on individual retinal layer thickness in normal eyes as measured with spectral-domain optical coherence tomography. *Invest Ophthalmol Vis Sci.* 2013;54:4934-4940.
41. Demirkaya N, Cohen S, Wit FW, et al. Retinal Structure and Function in Perinatally HIV-Infected and cART-Treated Children: A Matched Case-Control Study. *Invest Ophthalmol Vis Sci.* 2015;56:3945-3954.
42. van Dijk HW, Kok PH, Garvin M, et al. Selective loss of inner retinal layer thickness in type 1 diabetic patients with minimal diabetic retinopathy. *Invest Ophthalmol Vis Sci.* 2009;50:3404-3409.
43. van den Berg T, Franssen L, Coppens J. Ocular Media Clarity and Straylight. In: Dartt D., Besharse J, Dana R (eds), *Encyclopedia of the Eye*: Elsevier; 2010:173-183.
44. McGuire JL, Gill AJ, Douglas SD, Kolson DL. Central and peripheral markers of neurodegeneration and monocyte activation in HIV-associated neurocognitive disorders. *J Neurovirol.* 2015;21:439-448.
45. Arcinue CA, Bartsch DU, El-Emam SY, et al. Retinal Thickening and Photoreceptor Loss in HIV Eyes without Retinitis. *PLoS One.* 2015;10:e0132996.
46. Saidha S, Sotirchos ES, Ibrahim MA, et al. Microcystic macular oedema, thickness of the inner nuclear layer of the retina, and disease characteristics in multiple sclerosis: a retrospective study. *Lancet Neurol.* 2012;11:963-972.
47. Knier B, Berthele A, Buck D, et al. Optical coherence tomography indicates disease activity prior to clinical onset of central nervous system demyelination. *Mult Scler.* 2015.
48. Jonnal RS, Kocaoglu OP, Zawadzki RJ, Lee SH, Werner JS, Miller DT. The cellular origins of the outer retinal bands in optical coherence tomography images. *Invest Ophthalmol Vis Sci.* 2014;55:7904-7918

APPENDIX

AGE$_h$IV Cohort Study Group

Scientific oversight and coordination: P. Reiss (principal investigator), F.W.N.M. Wit, M. van der Valk, J. Schouten, K.W. Kooij, R.A. van Zoest, B.C. Elsenga (Academic Medical Center (AMC), Department of Global Health and Amsterdam Institute for Global Health and Development (AIGHD)).

M. Prins (co-principal investigator), M. Martens, S. Moll, J. Berkel, M. Totté, G.R. Visser, S. Kovalev (Public Health Service Amsterdam, Infectious Diseases Research Cluster).

Datamanagement: S. Zaheri, M.M.J. Hillebregt, Y.M.C. Ruijs, D.P. Benschop, P. Reiss (HIV Monitoring Foundation).

Central laboratory support: N.A. Kootstra, A.M. Harskamp-Holwerda, I. Maurer, M.M. Mangas Ruiz, A.F. Girigorie, E. van Leeuwen (AMC, Laboratory for Viral Immune Pathogenesis and Department of Experimental Immunology).

Project management and administrative support: F.R. Janssen, M. Heidenrijk, W. Zikkenheiner, L. Boumans (AIGHD), M. Wezel, C.S.M. Jansen-Kok (AMC).

Participating HIV physicians and nurses: S.E. Geerlings, M.H. Godfried, A. Goorhuis, J.W.R. Hovius, J.T.M. van der Meer, F.J.B. Nellen, T. van der Poll, J.M. Prins, P. Reiss, M. van der Valk, W.J. Wiersinga, F.W.N.M. Wit; J. van Eden, A.M.H. van Hes, M. Mutschelknauss, H.E. Nobel, F.J.J. Pijnappel, A.M. Westerman (AMC, Division of Infectious Diseases).

Other collaborators: J. de Jong, P.G. Postema (AMC, Department of Cardiology); P.H.L.T. Bisschop, M.J.M. Serlie (AMC, Division of Endocrinology and Metabolism); P. Lips (Free University Medical Center Amsterdam); E. Dekker (AMC, Department of Gastroenterology); S.E.J.A. de Rooij (AMC, Division of Geriatric Medicine); J.M.R. Willemsen, L. Vogt (AMC, Division of Nephrology); J. Schouten, P. Portegies, B.A. Schmand, G.J. Geurtsen, J.A. ter Stege, M. Klein Twennaar (AMC, Department of Neurology); B.L.F. van Eck-Smit, M. de Jong (AMC, Department of Nuclear medicine); D.J. Richel (retired) (AMC, Division of Clinical Oncology); F.D. Verbraak, N. Demirkaya (AMC, Department of Ophthalmology); I. Visser, H.G. Ruhé (AMC, Department of Psychiatry); P.T. Nieuwkerk (AMC, Department of Medical Psychology); R.P. van Steenwijk, E. Dijkers (AMC, Department of Pulmonary medicine); C.B.L.M. Majoie, M.W.A. Caan, T. Su (AMC, Department of Radiology); H.W. van Lunsen, M.A.F. Nievaard (AMC, Department of Gynaecology); B.J.H. van den Born, E.S.G. Stroes, (AMC, Division of Vascular Medicine); W.M.C. Mulder (HIV Vereniging Nederland).

CHAPTER 5

Associations between retinal thickness and cerebral (micro)structure in HIV-infected patients on long term cART compared with controls

Nazli Demirkaya
Ferdinand W.N.M. Wit
Tanja Su
Matthan W.A. Caan
Maria Prins
Reinier O. Schlingemann
Michael D. Abramoff
Peter Reiss
Charles B. Majoie
Frank D. Verbraak

on behalf of the AGE$_h$IV Study Group

Manuscript in preparation

ABSTRACT

Purpose

HIV infection with adequate antiretroviral suppression has previously been associated with neurodegeneration in the brain and retina. Here, we assessed possible associations between neuroretinal thickness (RT) and both cerebral white matter (WM) integrity and cerebral volume in a group of middle-aged HIV-infected patients with sustained suppressed viral replication on combination antiretroviral therapy (cART), as compared to a group of HIV-uninfected, but otherwise highly comparable controls.

Methods

This cross-sectional observational study included 86 patients and 50 controls. All participants underwent 3.0 Tesla magnetic resonance imaging (MRI), determining gray and white matter volumes from T1-weighted sequences, and white matter diffusivity, using diffusion tensor imaging (DTI). Retinal layer thickness was quantified using spectral-domain optical coherence tomography. Multivariable linear regression was used to assess associations between OCT (independent) and MRI (dependent) parameters. All analyses were corrected for age, spherical equivalent, OCT quality factor, HIV-status, MRI scanner system and additionally for intracranial volume in case of volumetric measurements.

Results

Regression analysis of OCT and DTI parameters showed significant positive correlations between pericentral retinal thickness- in particular of inner layers- and fractional anisotropy (FA) [***Total RT**: B-coeff. 2,99x10^{-4}, P-value 0.006; **RNFL**: B-coeff. 3x 10^{-3}, P-value 0.00022; **GCL**: B-coeff. 1x10^{-3}, P-value 0.009, **IPL**: B-coeff. 1x10^{-3}, P-value 0.038*] and negative associations between (mostly) the same layers and mean diffusivity (MD*) [**Total RT**: B-coeff. -3.75x10^{-7}, P-value 0.016; **RNFL**: B-coeff. -2.496x10^{-6}, P-value 0.029; **GCL**: B-coeff -7.481x10^{-7}, P-value 0.034].*

Comparing RT and cerebral volume measurements, we detected significant positive correlations between thickness of inner retinal layers and total gray matter volume *[**Total RT**: B-coeff. 648.126; P-value 0.003; **RNFL**: B-coeff. 3713.5, P-value: 0.021; **GCL**: B-coeff.1352.658, P-value 0.006].* Foveal [*B-coeff. 1330, P-value 0.049]* and pericentral GCL thickness *[B-coeff. 1339.7, P-value 0.014],* as well as peripheral RNFL thickness *[B-coeff. 1905, P-value 0.03]* were positively associated with cortical white matter volume. The detected associations did not significantly differ between HIV-infected patients and controls.

Conclusions

Our findings confirm previous studies describing correlations between retinal thickness and cerebral parameters in healthy people, possibly reflecting physiological retina-brain relationships, which seem to be unaffected in patients with well-suppressed HIV-infection.

INTRODUCTION

With the introduction of combination antiretroviral therapy (cART), the incidence of HIV-associated dementia and other severe central nervous system abnormalities, as well as HIV-related retinal disease, such as cytomegalovirus retinitis, has decreased dramatically.[1,2] Nevertheless, even in cART-treated HIV-patients both brain and retinal (micro)structural alterations have been reported, in particular in patients with a history of severe immuno-deficiency or clinical AIDS diagnosis.[3,4] As neuroretinal tissue can be considered to be an extension of the brain, these abnormalities may have a shared pathophysiology, which could include direct HIV neurotoxicity, HIV-induced immune activation and neuro-inflammation.[3,5,6]

Unlike the brain, direct visualization of the retina is relatively simple and rapid with non-invasive high-resolution optical imaging techniques, in particular optical coherence tomography (OCT). In past years, several combined OCT/MRI studies have explored retinal thickness (RT) as a potential proxy for brain dysfunction in neurodegenerative conditions, such as Alzheimer's disease, as well as healthy aging.[7-9] Similar comparative imaging studies on HIV-related neuroretinal degeneration are scarce. Recently, our study group demonstrated associations between retinal thinning and white matter microstructural alterations in perinatally HIV-infected children.[10]

In the current study, we examined similar potential associations of RT, measured with spectral-domain optical coherence tomography (SD-OCT), with cerebral volume and white matter microstructural changes, using multimodal magnetic resonance imaging (MRI), in a group of HIV-infected patients receiving suppressive cART, as compared to a group of HIV-uninfected controls, all 45 years of age or older.

If brain alterations are indeed correlated with a thinner retina in HIV-infected patients, OCT could be used as a marker to provide information on HIV-related neurodegeneration.

METHODS

Study design and participants

Suitable participants from the main AGE$_h$IV cohort study were consecutively invited to participate in a nested neuro(retinal) imaging substudy. The AGE$_h$IV Cohort Study is an ongoing study on prevalence, incidence and risk factors of ageing-associated comorbidities and organ dysfunction among HIV-positive patients and highly comparable

HIV-uninfected controls at least 45 years of age (i.e. from the same geographic region with similar socio-demographic and behavioural (risk) factors).[11]

Inclusion criteria specific for this neuroretinal imaging substudy were as follows: male gender, and for the HIV-positive patients sustained suppression of HIV viremia (plasma HIV-RNA <40 copies/ml) for at least 12 months. The presence of viral 'blips' (transient low level viremia, below 100 copies/ml) was not an exclusion criterion. Exclusion criteria were HIV-unrelated neurological disease, (history of) intracerebral neoplasms, significant traumatic brain injury, current significant psychiatric disorders, weekly to daily recreational drug use (with the exception of cannabis), excessive alcohol consumption, insufficient command of the Dutch language, low premorbid IQ and MRI contra-indications.[5]

Ophthalmic exclusion criteria were high refractive errors (SE> +5.5 or > −8.5 D), visual acuity below 0.2 logMAR, glaucoma, significant media opacities, and (a history of) ocular opportunistic infections, uveitis or other retinal disease. Amblyopic eyes were excluded.

A total of 103 HIV-infected and 74 HIV-uninfected participants were enrolled into the AGE_hIV neuroretinal substudy; of those individuals, 92 patients and 63 controls were included in the ophthalmic part of the study. The other participants were excluded for varying reasons, including having glaucoma, staphyloma, cataract precluding a reliable OCT scan, ocular toxoplasmosis scars, retinal detachment and pseudovitelliform macular degeneration.[12]

Finally, combined MRI and OCT data of 86 patients and 50 controls were available for analysis in the current study.

Standard protocol approval, registration, and patient consent

The protocol of the AGE_hIV Cohort Study and the protocol of the substudy were approved by the local ethics committee and have been registered at www.clinicaltrials.gov (identifier: NCT01466582). Written informed consent was obtained from all participants, separately for the main study and substudy.

Demographic, clinical and laboratory data collection

Participants were asked to complete a questionnaire evaluating demographics, (family) medical history, use of medication, substance use and sexual (risk) behavior. Blood samples were collected for extensive laboratory testing. Plasma HIV-1 RNA levels were determined in the HIV-infected participants. Detailed information concerning HIV

infection and antiretroviral therapy (ART) history was extracted from the Dutch HIV Monitoring Foundation database.[13]

Spectral-Domain optical coherence tomography and retinal layer segmentation

OCT images of the subjects were obtained with SD-OCT (Topcon 3D OCT-2000; Topcon Inc., Paramus, NJ) using the 3D macular and disc volume scan protocols. From each 3D macular volume, individual retinal layers were segmented automatically by the publicly available and extensively validated *Iowa Reference Algorithm*.[14,15] The *Iowa Reference Algorithm* allows for the calculation of the thickness of all individual retinal layers for each of the nine ETDRS-grid defined regions. We selected on the foveal, pericentral and peripheral ETDRS rings, as we have done in previous studies.[10,12,16,17] In addition, peripapillary RNFL thickness measurements were acquired from the 3D optic nerve head OCT's using the same *Iowa Reference Algorithm*. The peripapillary ring was centered manually with the center of the ring coinciding with the center of the optic disc.

MRI data acquisition and data processing

All patients underwent a MRI examination at the AMC and scanning was performed on a 3T Intera and continued on a 3T Ingenia system (Philips Healthcare, Best, the Netherlands) due to a scanner upgrade. This upgrade was statistically accounted for in all MRI analyses. MRI data acquisition and scanning parameters are described in further detail in previous papers.[5,18] A nonlinear least squares estimation of diffusion tensors was used to compute fractional anisotropy (FA) and mean diffusivity (MD), which were averaged over the entire skeleton to obtain whole brain white matter (WM) DTI measures. Anatomical images were used for grey matter (GM), WM and cerebrospinal fluid (CSF) segmentation by SPM8.[19] The intracranial volume (ICV) was computed by summing the GM, WM and CSF volumes.

Statistical analysis

Statistical analysis was performed using IBM SPSS Statistics software version 24. Demographic/clinical characteristics were compared between the two groups using the Student's t-test, the Mann-Whitney *U* test or the ^{2} test, as appropriate.

Prior to analysis, retinal thickness values obtained from both eyes were averaged. Group differences in retinal thickness (RT) were assessed by age, spherical equivalent (SE) and OCT quality factor (QF) adjusted linear regression models. Group differences in MRI parameters were assessed using linear regression, adjusted for age, scanner system and intracranial volume (ICV).

Multivariable linear regression was used to assess associations between OCT (independent) and MRI (dependent) parameters. All analyses were corrected for age, SE, QF, MRI scanner system and ICV. We used a two-step analysis approach to evaluate the relationship between OCT and MRI parameters in our cohort. First, we evaluated possible associations between OCT and MRI parameters, including HIV-status as a covariable. Second, we assessed whether being HIV-infected exerted a significant influence on the potential associations between RT and MRI parameters (i.e. if the predictive value of RT on DTI and volumetric parameters differed between groups), by including a HIV-RT interaction term to the first model. In line with the exploratory nature of this study,

adjustment for multiple comparisons was not performed and statistical significance was set at a two-sided P-value<0.05.

RESULTS

Participant characteristics

An overview of the demographics, clinical characteristics and relevant OCT and MRI findings are displayed in **Table 1**. The two groups were comparable in terms of age, nationality and sexual orientation. On average, the HIV-infected men were known to be infected for a long period of time and approximately 32% had previously been diagnosed with AIDS. Most men used cART for many years and showed substantial immune recovery, with a median nadir CD4 count of 175 cells/µl and current median CD4 count of 595 cells/µl. Total foveal thickness did not differ between groups, however, as we previously reported,[12] total pericentral and peripheral retinal thickness were slightly increased in the patient group. Thickness of pericentral inner retinal layers was comparable between the two groups.

HIV-infected men had a significantly lower total gray matter volume, as well as poorer WM integrity, as indicated by higher MD and lower FA.

Retinal thickness and white matter diffusivity

Associations between OCT and DTI parameters are described in **Table 2**. Most noticeable are the significant positive correlations between pericentral retinal thickness, in particular of the inner layers, and FA, and the negative associations between (mostly) the same layers and MD **(Figure 1)**. HIV-RT interaction terms were not significant for any layer/macular region; i.e. differences in OCT-DTI associations were not detected between HIV-infected and –uninfected patients **(Supplemental Table S1)**

TABLE 1. Participant characteristics.

	HIV-infected men (n=86)	HIV-uninfected men (n=50)	P-value
Demographics			
Age (y)	52.6 (45.1-74.1)	52.0 (45.7-75.8)	0.897[a]
Nationality, Dutch	87.2%	84.3%	0.503[b]
MSM[e]	94.2%	90.2%	0.220[b]
HIV- and cART related characteristics			
Years known to be HIV positive	13.4 (1-27)	-	-
Prior clinical AIDS[f]	32.6%	-	-
CD4 cell count, cells/µl			
At enrollment	595 (320-1110)	-	-
Nadir	175 (0-620)	-	-
Known duration of $CD4^+$< 500 cells/µl, years	3.9 (0-21.5)	-	-
Duration of undetectable plasma viral load (years)	8.5 (0-15.1)	-	-
Years since start of first ART	11.7 (0.8-19.9)	-	-
Naïve at start of first cART[g]	81.4%	-	-
Optical coherence tomography			
Foveal RT	263.1 (215.5-316.8)	259.1 (230.9-321.6)	0.470[c]
Pericentral RT	323.9 (293.7-365.2)	318.7 (294.9-352.1)	**0.018**[c]
RNFL	24.2 (18.7-31.6)	24.2 (20.4-28.4)	0.702[c]
GCL	48.9 (28.2-64.7)	48.4 (30.2-59.8)	0.256[c]
IPL	42.1 (34.2-54.2)	41.4 (36.5-47.6)	0.178[c]
Peripheral RT	279.1 (251.7-308.7)	273.4 (251.6-305.7)	**0.002**
RNFL	36.6 (26.5-53.5)	35.7 (28.7-47.0)	0.108
GCL	28.1 (19.2-36.7)	27.6 (20.1-34.4)	0.072
IPL	38.5 (33.2-42.5)	38.0 (32.5-41.9)	**0.004**
Peripapillary RNFL thickness	101.9 (73.3-132.1)	98.4 (77.8-124.3)	0.155[c]
Magnetic resonance imaging			
Total gray matter volume (cm^3)	637.7 (418.1-756.2)	647.3 (524.2-726.9)	**0.009**[d]
Cortical white matter volume (cm^3)	521.0 (296.6-662.8)	524.9 (425.7-642.6)	0.054[d]
WM FA	0.425 (0.383-0.480)	0.434 (0.401-0.479)	**0.008**[d]
WM MD $*10^{-3}$ mm^2/s	0.77 (0.68-0.83)	0.75 (0.70-0.81)	**0.013**[d]

All data are presented as median (range) or percentage as appropriate. Test type used: [a]Mann-Whitney U test, [b]Chi-squared test, [c]Linear regression, adjusted for age, SE and QF, [d]linear regression adjusted for age, scanner system and intracranial volume. [e]The term 'MSM' applied to male patients who self-reported to feel mostly or exclusively sexually attracted to men. [f]The term 'prior clinical AIDS' was used in case of a previous AIDS-defining condition according to the United States Centers for Disease Control and Prevention (CDC) classification. [g]The term 'cART' was used for a combination of at least three antiretroviral drugs, other than ritonavir used as a pharmacological booster. RT: retinal thickness, RNFL: retinal nerve fiber layer, GCL: ganglion cell layer, IPL: inner plexiform layer. P-values in bold: P <0.05.

TABLE 2. Associations between retinal thickness and white matter diffusivity

	WM-FA		WM-MD	
	B-coefficient	P-value	B-coefficient	P-value
Foveal layers				
Total RT	6.65×10^{-5}	0.362	-1.15×10^{-7}	0.274
RNFL	3.70×10^{-4}	0.500	-4.07×10^{-7}	0.606
GCL	3.53×10^{-4}	0.250	-4.52×10^{-7}	0.307
IPL	2.04×10^{-4}	0.526	-3.87×10^{-7}	0.404
INL	1.74×10^{-4}	0.594	-6.96×10^{-8}	0.869
OPL	1.0×10^{-3}	0.126	-9.76×10^{-7}	0.136
ONL-IS	6.5×10^{-5}	0.710	-3.11×10^{-8}	0.902
OS	1.5×10^{-4}	0.781	-1.55×10^{-6}	0.051
Pericentral layers				
Total RT	2.99×10^{-4}	**0.006**	-3.75×10^{-7}	**0.016**
RNFL	3.0×10^{-3}	**0.00022**	-2.50×10^{-6}	**0.029**
GCL	1.0×10^{-3}	**0.009**	-7.48×10^{-7}	**0.034**
IPL	1.0×10^{-3}	**0.038**	-9.51×10^{-7}	0.194
INL	1.0×10^{-3}	0.177	-1.36×10^{-6}	**0.050**
OPL	2.18×10^{-4}	0.671	-1.29×10^{-7}	0.862
ONL-IS	1.31×10^{-4}	0.548	-1.76×10^{-7}	0.574
OS	3.68×10^{-4}	0.641	-8.61×10^{-7}	0.449
Peripheral layers				
Total RT	2.65×10^{-4}	0.053	-3.22×10^{-7}	0.103
RNFL	1.0×10^{-3}	**0.010**	-8.96×10^{-7}	0.118
GCL	1.0×10^{-3}	0.202	-5.93×10^{-7}	0.421
IPL	2.0×10^{-3}	**0.038**	-1.39×10^{-6}	0.273
INL	1.0×10^{-3}	0.258	-2.26×10^{-6}	**0.045**
OPL	-4.19×10^{-4}	0.639	1.38×10^{-6}	0.281
ONL-IS	2.45×10^{-4}	0.346	-4.19×10^{-7}	0.263
OS	-1.0×10^{-3}	0.282	2.9×10^{-7}	0.745
Peripapillary RNFL	3.99×10^{-4}	**0.010**	-3.82×10^{-7}	0.086

Results of the multivariable linear regression analysis evaluating the associations between retinal layer thickness and WM diffusivity. All analyses were corrected for HIV-status, age, spherical equivalent (SE) and OCT quality factor (QF).

Coefficients represent the change in WM diffusivity outcomes per micron increase in retinal thickness (RT). WM-FA: white matter fractional anisotropy, corrected for MRI scanner system and intracranial volume; WM-MD: white matter mean diffusivity, corrected for MRI scanner system and intracranial volume; RNFL: retinal nerve fiber layer, GCL: ganglion cell layer, IPL: inner plexiform layer, INL: inner nuclear layer, OPL: outer plexiform layer, ONL-IS: outer nuclear layer-inner segments, OS: outer segment layer. P-values in bold: $P < 0.05$.

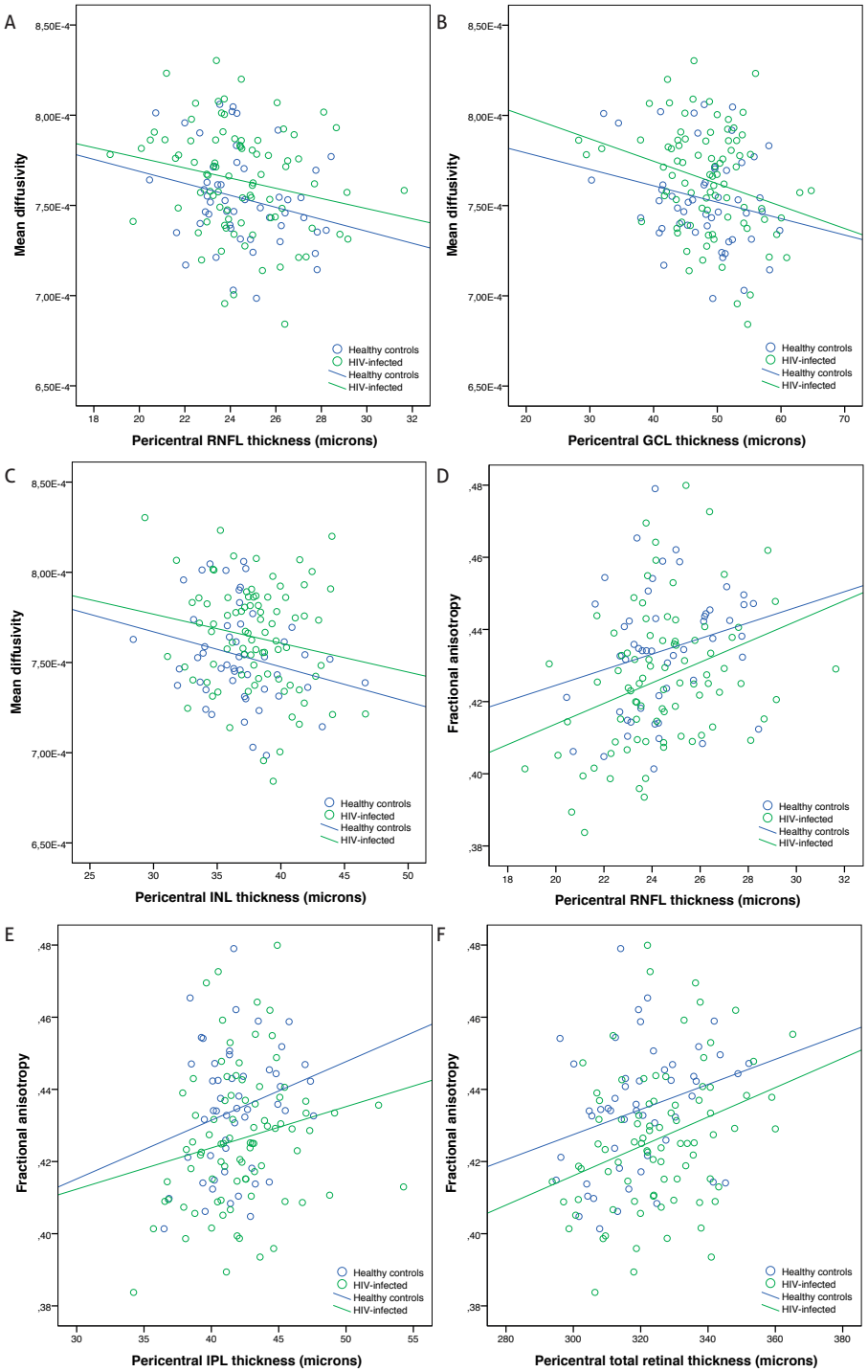

FIGURE 1. Associations between RT and WM microstructure in HIV-infected patients and healthy controls.

← Univariable scatter and linear fit plots illustrating associations between RT and MD **(a,b,c)**, and RT and FA **(d,e,f)**. No significant differences in RT-WM associations were detected between the two groups (i.e. the interaction between HIV-status and RT was not significantly associated with WM diffusivity outcomes (Supplementary Table S1). RNFL: retinal nerve fiber layer; GCL: ganglion cell layer; INL: inner nuclear layer.

Retinal thickness and cerebral volume

Results of the regression analysis of RT and cerebral volume measurements are summarized in **Table 3.** Positive correlations were detected between thickness of inner retinal layers in the pericentral **(Figure 2)** and peripheral macular regions and total gray matter volume. Foveal and pericentral GCL thickness, as well as peripheral RNFL thickness were positively associated with cortical white matter volume. The HIV-RT interaction term was significant for the association between peripheral RNFL thickness and cortical white matter volume only **(Supplemental Table S2).**

TABLE 3. Associations between retinal thickness and cerebral volume

	TGV		Cortical WMV	
	B-coefficient	P-value	B-coefficient	P-value
Foveal layers				
Total RT	251.71	0.083	107.94	0.504
RNFL	-429.06	0.697	-693.11	0.571
GCL	1383.64	**0.023**	1330.02	**0.049**
IPL	928.71	0.148	-21.42	0.976
INL	716.88	0.222	226.86	0.728
OPL	518.32	0.572	-858.16	0.398
ONL-IS	546.44	0.116	405.91	0.293
OS	-1036.81	0.336	-924.98	0.439
Pericentral layers				
Total RT	648.13	**0.003**	248.20	0.309
RNFL	3713.59	**0.021**	2332.99	0.194
GCL	1352.66	**0.006**	1339.75	**0.014**
IPL	1845.02	0.069	-249.24	0.826
INL	1080.08	0.268	-224.96	0.835
OPL	742.84	0.469	-755.65	0.506
ONL-IS	642.26	0.138	214.44	0.656
OS	-1344.72	0.399	-2788.99	0.113
Peripheral layers				
Total RT	828.32	**0.002**	393.07	0.202
RNFL	2079.33	**0.008**	1905	**0.030**
GCL	1358.14	0.187	2082.44	0.067
IPL	5255.87	**0.003**	2488	0.209
INL	2011.12	0.202	731.97	0.676
OPL	861.14	0.630	-2473.64	0.210

TABLE 3. Associations between retinal thickness and cerebral volume (continued)

	TGV		Cortical WMV	
	B-coefficient	P-value	B-coefficient	P-value
ONL-IS	998.48	0.054	199.58	0.730
OS	-391.37	0.754	-2788.99	0.113
Peripapillary RNFL	444.98	0.157	620.37	0.075

Results of the multivariable linear regression analysis evaluating the associations between retinal layer thickness and cerebral volume. All analyses were corrected for HIV-status, age, spherical equivalent (SE), OCT quality factor (QF), intracranial volume and MRI scanner system. Coefficients represent changes in volume (mm^3) per micron increase in retinal thickness (RT). TGV: total gray matter volume; WMV: white matter volume.;RNFL: retinal nerve fiber layer, GCL: ganglion cell layer, IPL: inner plexiform layer, INL: inner nuclear layer, OPL: outer plexiform layer, ONL-IS: outer nuclear layer-inner segments, OS: outer segment layer. P-values in bold: P <0.05.

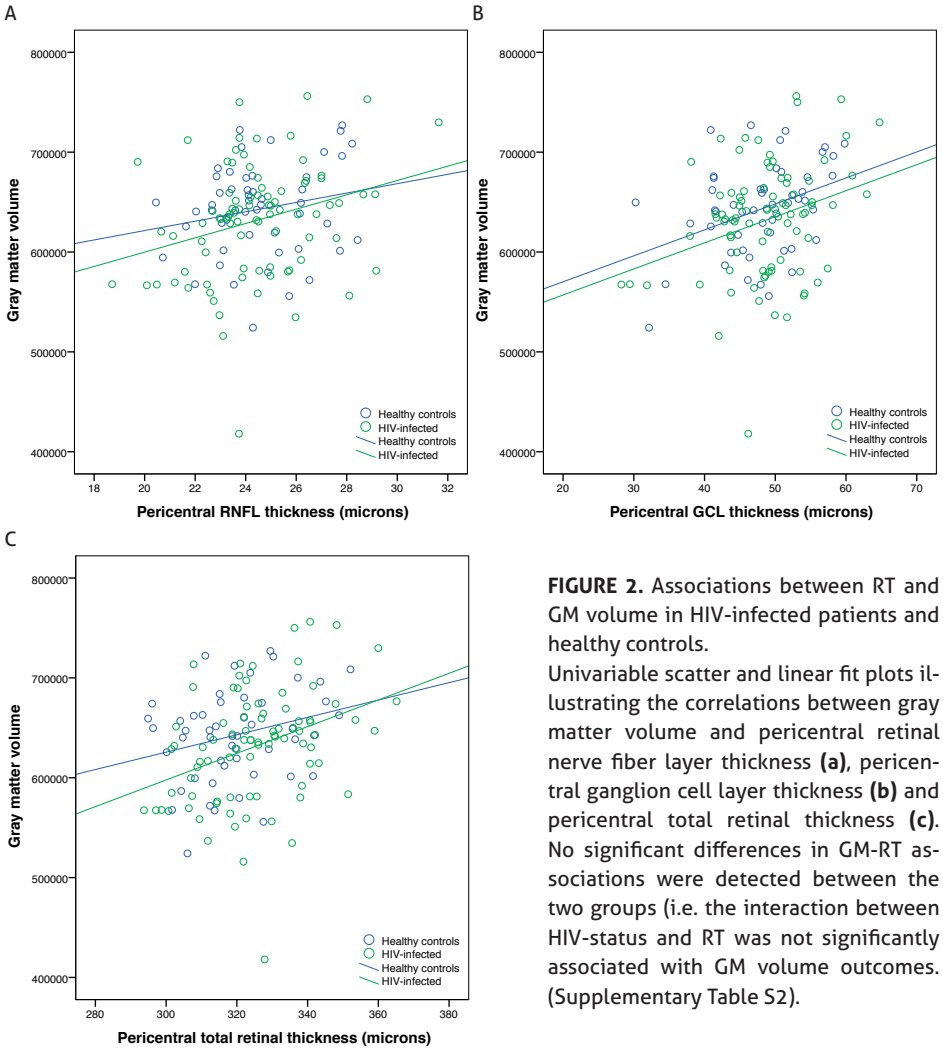

FIGURE 2. Associations between RT and GM volume in HIV-infected patients and healthy controls.
Univariable scatter and linear fit plots illustrating the correlations between gray matter volume and pericentral retinal nerve fiber layer thickness **(a)**, pericentral ganglion cell layer thickness **(b)** and pericentral total retinal thickness **(c)**. No significant differences in GM-RT associations were detected between the two groups (i.e. the interaction between HIV-status and RT was not significantly associated with GM volume outcomes. (Supplementary Table S2).

DISCUSSION

In the current study, we assessed associations between RT and both WM integrity and cerebral volume in a group of middle-aged HIV-infected men with well suppressed viral load on cART, as compared to a group of HIV-uninfected, but otherwise highly comparable controls.

Our findings indicate that RT, and in particular thickness of inner retinal layers, is associated with WM microstructure, as well as with cerebral volume in *both* groups.

As we described previously,[5] HIV-infected patients had lower fractional anisotropy and higher mean diffusivity than HIV-negative controls, indicative of disturbed WM integrity. Grey matter volume was also decreased in the patient group. Retinal thickness however was not reduced, but even slightly increased in HIV-infected patients.[12] These differences are reflected in the current OCT-MRI correlations as well, with HIV-infected patients having lower grey matter volume and worse DTI outcomes while having similar retinal (layer) thickness as the control group (**Table 1, Figures 1 and 2**), thus not supporting the hypothesis of a shared pathophysiology of retinal and cerebral alterations in HIV.

To our knowledge, our study group is the first in the HIV-related literature assessing correlations between retina and brain parameters, hampering comparison of our findings to other HIV-studies. However, our results are in line with the findings of several studies investigating associations between inner retinal layer thickness with volumetric and microstructural markers of brain tissue on MRI in the context of healthy aging. Ong et al.[20] reported associations between GC-IPL thinning and lower GMV in temporal and occipital lobes, and Liu et al.[8] found both WM microstructure and GMV to be associated with GC-IPL thickness in healthy older subjects over 60 years of age (n=164 and n=65 respectively). A recent report of the *Rotterdam Study* showed that thinner RNFL, GCL and IPL (assessed with a similar Topcon OCT device and the same *Iowa Reference Algorithms* as applied in our study) were associated with smaller gray- and white-matter volume, as well as disturbed white matter microstructure, in a population of 2124 elderly participants (mean age 67.0 years).[9]

Although our study population was much smaller, we detected similar positive correlations between thickness of the inner retinal layers (RNFL, GCL, IPL) (**Table 2**), and FA, and negative associations between (mostly) the same layers and MD. In addition, thinner inner layers were correlated with a decrease in gray matter volume (**Table 3**). The underlying pathophysiology of these correlations remains unclear, and several explanatory

mechanisms have been proposed by the formerly mentioned studies: inner retinal thinning might reflect degradation of brain structure in normal aging, simultaneous retinal and cerebral neuronal loss might be caused by a common neurodegenerative process, or on the other hand, damage to the retina might lead to cerebral damage or vice versa (e.g. retrograde versus anterograde neurodegeneration).[8,9,20]

Interestingly, in our study, the detected correlations were quite parallel between the HIV-infected and –uninfected group ; i.e. HIV-status did not influence the associations between MRI and OCT parameters (as reflected by non-significant HIV-RT interaction terms; **Supplemental Tables S1 and S2**), suggesting that potential physiological retina-brain relationships are not disrupted in patients with well-controlled HIV-infection.

Our results are not in concordance with the findings we published previously on patients with pediatric HIV infection.[10] In HIV-infected children we found lower pericentral neuroretinal thickness to be significantly associated with damaged white matter microstructure, in terms of lower FA and higher MD, while neuroretinal thickness was associated with grey and white matter volume in healthy children only.[10] This discrepancy in findings between HIV-infected children and –adults may be explained by several factors, such as time of infection. As children are still in development, (unsuppressed) HIV-infection in early years may disrupt or delay retinal and/or cerebral maturation. There may also be different contributions of underlying HIV-related pathogenic mechanisms, e.g. direct HIV neurotoxicity, chronic HIV-induced neuro-inflammation, cerebral perfusion changes or long-term cART toxicity. It is therefore difficult to extrapolate the findings in HIV-infected children to –adults and vice versa. A subsequent analysis of the *NOVICE* pediatric HIV cohort data revealed significant associations between neuroretinal thinning and inflammation-associated and neuronal injury biomarkers[21]; the presence/absence of similar potential associations in the *AGE$_h$IV* cohort will be explored in a future study.

Despite being the first combined OCT/MRI study of a cohort of middle-aged cART-treated HIV-infected subjects and a highly similar control group with regard to socio-demographic background, life style and risk factors, this study is subject to several limitations. First, the relatively modest sample size may have limited our power to detect potentially clinically relevant associations. Second, as this was an exploratory study, we did not adjust for multiple comparisons. Nevertheless, variations in the same (inner) retinal layers were consistently associated with the MRI parameters, making it unlikely that our findings are based on chance alone. Third, a more detailed assessment of region specific brain areas might reveal stronger associations with retinal thickness than the global MRI measures we currently used. Finally, this cross-sectional study does

not explain the mechanisms underlying the associations between retinal and cerebral measurements.

In conclusion, in this cross-sectional study we observed correlations between inner retinal thickness and both WM microstructural alterations and cerebral volume in healthy controls as well as in patients with well-suppressed HIV-infection, suggesting that physiological retina-brain relationships are not disrupted in the latter group. Our findings indicate and confirm that retinal OCT can indeed provide information on neurodegeneration in the brain, however it is not a useful biomarker for specific HIV-related neurodegeneration.

AUTHORS' CONTRIBUTIONS

ND contributed to study design, data collection, data analysis and interpretation and drafted the manuscript. FWNMW contributed to study design, data interpretation and critically reviewed and revised the manuscript.

TS contributed to study coordination and data collection. MWAC conceptualised the MRI imaging protocol, supervised MRI scanning, contributed to data interpretation and revised the manuscript. MP contributed to study design. ROS contributed to data interpretation and revised the manuscript. MDA invented and provided the Iowa Reference Algorithms. PR conceived the study and contributed to study design. CBM conceptualized the MRI imaging protocol and supervised MRI scanning. FDV contributed to study design, data interpretation and supervised and revised the manuscript.

Manuscript is in preparation for submission.

Supplementary Table S1. The influence of HIV status on associations between retinal thickness and white matter diffusivity.

	WM-FA		WM-MD	
	B-coefficient	**P-value**	**B-coefficient**	**P-value**
Foveal layers				
Total RT	1.4×10^{-4}	0.477	-2.5×10^{-7}	0.178
HIV status	2.1×10^{-2}	0.618	-4.0×10^{-5}	0.496
HIV-RT interaction	-1.1×10^{-4}	0.272	2.0×10^{-7}	0.374
RNFL	-1.8×10^{-4}	0.847	-7.0×10^{-7}	0.611
HIV status	-6.0×10^{-3}	0.529	8.6×10^{-6}	0.544
HIV-RT interaction	-2.7×10^{-4}	0.811	4.3×10^{-7}	0.795
GCL	1.0×10^{-3}	0.281	-7.3×10^{-7}	0.288
HIV status	-5.0×10^{-3}	0.563	5.7×10^{-6}	0.643
HIV-RT interaction	-2.7×10^{-4}	0.656	4.8×10^{-7}	0.594
IPL	$6.7x\ 10^{-5}$	0.904	-5.8×10^{-7}	0.471
HIV status	-1.5×10^{-2}	0.482	3.1×10^{-6}	0.917
HIV-RT interaction	2.0×10^{-4}	0.766	2.9×10^{-7}	0.766
INL	1.0×10^{-3}	0.258	-6.9×10^{-7}	0.275
HIV status	2.0×10^{-3}	0.867	-8.1×10^{-6}	0.610
HIV-RT interaction	-1.0×10^{-3}	0.323	1.1×10^{-6}	0.189
OPL	2.0×10^{-3} 2.1	**0.047**	-2.0×10^{-6}	0.079
HIV status	$\times 10^{-2}$	0.340	-2.3×10^{-5}	0.476
HIV-RT interaction	-1.0×10^{-3}	0.174	1.5×10^{-6}	0.270
ONL-IS	9.3×10^{-5}	0.769	-2.3×10^{-7}	0.614
HIV status	-3.7×10^{-3}	0.936	-2.2×10^{-5}	0.745
HIV-RT interaction	-4.1×10^{-5}	0.915	2.8×10^{-7}	0.614
OS	2.6×10^{-4}	0.826	-4.3×10^{-7}	0.795
HIV status	-2.0×10^{-3}	0.976	7.4×10^{-5}	0.399
HIV-RT interaction	-1.3×10^{-4}	0.918	-1.3×10^{-6}	0.459
Pericentral layers				
Total RT	3.3×10^{-4}	0.083	-4.6×10^{-7}	0.094
HIV status	2.0×10^{-3}	0.976	-2.3×10^{-5}	0.822
HIV-RT interaction	-4.0×10^{-5}	0.860	1.2×10^{-7}	0.717
RNFL	2.0×10^{-3}	0.098	-3.1×10^{-6}	0.114
HIV status	-3.4×10^{-2}	0.357	-8.5×10^{-6}	0.879
HIV-RT interaction	1.0×10^{-3}	0.494	8.5×10^{-7}	0.709
GCL	1.0×10^{-3}	0.150	-5.4×10^{-7}	0.362
HIV status	-1.3×10^{-2}	0.572	2.8×10^{-5}	0.410
HIV-RT interaction	8.3×10^{-5}	0.866	-3.2×10^{-7}	0.650
IPL	1.0×10^{-3}	0.442	-7.7×10^{-7}	0.614
HIV status	-2.3×10^{-2}	0.649	2.2×10^{-5}	0.758
HIV-RT interaction	3.0×10^{-4}	0.789	-2.3×10^{-7}	0.893
INL	1.0×10^{-3}	0.232	-1.6×10^{-6}	0.169
HIV status	8.0×10^{-3}	0.834	2.5×10^{-6}	0.962
HIV-RT interaction	-5.0×10^{-4}	0.641	3.0×10^{-7}	0.830
OPL	4.0×10^{-4}	0.663	-6.6×10^{-7}	0.619
HIV status	-6.0×10^{-4}	0.986	-1.2×10^{-5}	0.813
HIV-RT interaction	-3.0×10^{-4}	0.810	7.7×10^{-7}	0.629

Supplementary Table S1. The influence of HIV status on associations between retinal thickness and white matter diffusivity. (continued)

	WM-FA		WM-MD	
	B-coefficient	**P-value**	**B-coefficient**	**P-value**
ONL-IS	3.0×10^{-4}	0.430	-4.8×10^{-7}	0.345
HIV status	1.4×10^{-2}	0.743	-3.5×10^{-5}	0.575
HIV-RT interaction	-2.0×10^{-4}	0.593	4.9×10^{-7}	0.447
OS	-1.0×10^{-3}	0.451	-4.7×10^{-8}	0.983
HIV status	-5.3×10^{-2}	0.474	5.8×10^{-5}	0.585
HIV-RT interaction	1.0×10^{-3}	0.549	-1.1×10^{-6}	0.661
Peripheral layers				
Total RT	2.5×10^{-4}	0.289	-2.9×10^{-7}	0.397
HIV status	-1.7×10^{-2}	0.829	2.8×10^{-5}	0.803
HIV-RT interaction	2.3×10^{-5}	0.933	-5.1×10^{-8}	0.900
RNFL	1.0×10^{-3}	0.247	-9.0×10^{-7}	0.366
HIV status	-2.2×10^{-2}	0.460	1.3×10^{-5}	0.766
HIV-RT interaction	3.2×10^{-4}	0.684	7.1×10^{-9}	0.995
GCL	1.0×10^{-3}	0.432	1.3×10^{-7}	0.913
HIV status	-9.0×10^{-3}	0.739	4.4×10^{-5}	0.283
HIV-RT interaction	6.2×10^{-6}	0.995	-1.1×10^{-6}	0.438
IPL	1.0×10^{-3}	0.474	3.7×10^{-7}	0.849
HIV status	-6.4×10^{-2}	0.325	1.2×10^{-4}	0.190
HIV-RT interaction	1.0×10^{-3}	0.408	-2.9×10^{-6}	0.241
INL	1.0×10^{-3}	0.489	-1.0×10^{-6}	0.568
HIV status	-1.1×10^{-2}	0.806	7.3×10^{-5}	0.251
HIV-RT interaction	5.2×10^{-5}	0.974	-2.1×10^{-6}	0.356
OPL	-1.0×10^{-3}	0.557	1.2×10^{-6}	0.535
HIV status	-2.7×10^{-2}	0.595	2.6×10^{-6}	0.972
HIV-RT interaction	1.0×10^{-3}	0.709	2.8×10^{-7}	0.916
ONL-IS	3.8×10^{-4}	0.384	-7.2×10^{-7}	0.251
HIV status	8.0×10^{-3}	0.859	-2.4×10^{-5}	0.692
HIV-RT interaction	-2.1×10^{-4}	0.700	4.7×10^{-7}	0.549
OS	-1.0×10^{-3}	0.403	8.0×10^{-8}	0.963
HIV status	-2.7×10^{-2}	0.630	5.3×10^{-7}	0.995
HIV-RT interaction	4.5×10^{-4}	0.741	2.8×10^{-7}	0.888
Peripapillary RNFL	2.3×10^{-4}	0.387	-3.0×10^{-7}	0.432
HIV status	-3.5×10^{-2}	0.279	2.5×10^{-5}	0.585
HIV-RT interaction	2.5×10^{-4}	0.438	-1.1×10^{-7}	0.806

Results of the regression analysis evaluating the influence of HIV status on the relationship between retinal layer thickness and white matter diffusivity. The model included retinal thickness, HIV status, and the interaction between these two variables (as shown), and covariables age, OCT quality factor and spherical equivalent (not shown). Retinal thickness coefficients represent the change in white matter diffusivity outcome per micron increase in retinal thickness. The HIV status coefficient represents the intercept. The interaction term between HIV status and retinal thickness shows whether associations between retinal thickness and white matter diffusivity outcomes in HIV-infected adults are different from those in controls. Abbreviations: HIV: human immunodeficiency virus; WM-FA: white matter fractional anisotropy, corrected for MRI scanner system and intracranial volume; WM-MD: white matter mean diffusivity, corrected for MRI scanner system and intracranial volume; RNFL: retinal nerve fiber layer, GCL: ganglion cell layer, IPL: inner plexiform layer, INL: inner nuclear layer, OPL: outer plexiform layer, ONL-IS: outer nuclear layer-inner segments, OS: outer segment layer. P-values in bold: P <0.05.

Supplementary Table S2. The influence of HIV status on associations between retinal thickness and cerebral volume

	TGV		Cortical WMV	
	B-coefficient	**P-value**	**B-coefficient**	**P-value**
Foveal layers				
Total RT	171.2	0.509	-180.6	0.532
HIV status	-45023.5	0.586	-123245.1	0.182
HIV-RT interaction	117.3	0.708	420.4	0.230
RNFL	-1186.3	0.539	-406.6	0.849
HIV status	-22004.0	0.263	-8859.2	0.684
HIV-RT interaction	1117.2	0.480	-422.7	0.870
GCL	808.3	0.388	213.3	0.837
HIV status	-25844.3	0.127	-36713.4	0.051
HIV-RT interaction	978.6	0.422	1899.5	0.161
IPL	215.9	0.847	-1466.3	0.239
HIV status	-45879.6	0.272	-77387.1	0.096
HIV-RT interaction	1063.3	0.437	2155.1	0.157
INL	185.5	0.833	-863.8	0.375
HIV status	-30964.1	0.162	-47708.4	0.053
HIV-RT interaction	941.4	0.417	1932.2	0.134
OPL	429.1	0.790	-1889.8	0.290
HIV status	-16609.3	0.716	-47363.5	0.348
HIV-RT interaction	132.8	0.946	1536.1	0.481
ONL-IS	339.5	0.593	-41.0	0.954
HIV status	-51262.4	0.583	-91959.9	0.376
HIV-RT interaction	298.1	0.697	643.7	0.450
OS	2630.5	0.251	1649.6	0.519
HIV status	206125.2	0.094	141242.0	0.303
HIV-RT interaction	-4460.5	0.072	-3131.4	0.256
Pericentral layers				
Total RT	536.0	0.150	-115.2	0.785
HIV status	-70620.9	0.623	-186207.3	0.257
HIV-RT interaction	165.7	0.711	537.3	0.294
RNFL	2445.4	0.369	-1848.3	0.541
HIV status	-58399.0	0.451	-159492.5	0.066
HIV-RT interaction	1823.5	0.564	6012.1	0.090
GCL	1002.9	0.214	249.2	0.779
HIV status	-40334.4	0.391	-93070.3	0.075
HIV-RT interaction	530.9	0.586	1655.2	0.126
IPL	583.0	0.781	-2640.7	0.262
HIV status	-83201.8	0.405	-141773.0	0.206
HIV-RT interaction	1635.4	0.493	3099.0	0.247
INL	952.2	0.549	-1802.8	0.306
HIV status	-22608.2	0.761	-105365.7	0.202
HIV-RT interaction	203.272	0.919	2507.9	0.256
OPL	203.4	0.912	-1893.143	0.355
HIV status	-37960.4	0.577	-62118.5	0.411
HIV-RT interaction	780.9	0.725	1646.8	0.503

Supplementary Table S2. The influence of HIV status on associations between retinal thickness and cerebral volume (continued)

	TGV		Cortical WMV	
	B-coefficient	**P-value**	**B-coefficient**	**P-value**
ONL-IS	731.1	0.307	625.7	0.433
HIV status	-1283.0	0.988	49918.7	0.608
HIV-RT interaction	-142.4	0.876	-659.4	0.517
OS	-569.6	0.851	-1159.6	0.728
HIV status	30133.8	0.838	79017.5	0.625
HIV-RT interaction	-1017.7	0.763	-2139.2	0.565
Peripheral layers				
Total RT	561.7	0.219	-8.3	0.987
HIV status	-129088.6	0.398	-181166.8	0.299
HIV-RT interaction	401.0	0.469	603.7	0.341
RNFL	1172.2	0.386	-1283.9	0.384
HIV status	-63221.2	0.277	-181261.9	**0.005**
HIV-RT interaction	1309.9	0.412	4604.8	**0.009**
GCL	199.7	0.904	-297.7	0.869
HIV status	-64759.9	0.249	-117310.5	0.057
HIV-RT interaction	1819.0	0.370	3737.3	0.093
IPL	2898.2	0.278	-807.7	0.790
HIV status	-166373.0	0.194	-221806.6	0.129
HIV-RT interaction	3902.8	0.247	5455.6	0.156
INL	1482.1	0.551	-1620.8	0.557
HIV status	-40392.8	0.652	-122702.7	0.218
HIV-RT interaction	870.2	0.783	3869.7	0.271
OPL	543.0	0.844	-1591.1	0.600
HIV status	-29649.2	0.768	32605.2	0.768
HIV-RT interaction	553.0	0.879	-1534.1	0.702
ONL-IS	1075.5	0.215	1188.5	0.220
HIV status	-4787.0	0.955	108181.6	0.257
HIV-RT interaction	-120.9	0.912	-1553.2	0.204
OS	-1414.5	0.556	-1159.6	0.728
HIV status	-68201.6	0.536	79017.5	0.625
HIV-RT interaction	1364.3	0.618	-2139.2	0.565
Peripapillary RNFL	-103.0	0.849	-292.8	0.620
HIV status	-94487.1	0.146	-146973.7	**0.039**
HIV-RT interaction	796.2	0.215	1326.8	0.060

Results of the regression analysis evaluating the influence of HIV status on the relationship between retinal layer thickness and cerebral volume. The model included retinal thickness, HIV status, and the interaction between these two variables (as shown), and covariables age, spherical equivalent (SE), OCT quality factor (QF), intracranial volume and MRI scanner system (not shown). Retinal thickness coefficients represent changes in volume (mm^3) per micron increase in retinal thickness. The HIV status coefficient represents the intercept. The interaction term between HIV status and retinal thickness shows whether associations between retinal thickness and cerebral volume in HIV-infected adults are different from those in controls. Abbreviations: HIV: human immunodeficiency virus; TGV: total gray matter volume; WMV: white matter volume; RNFL: retinal nerve fiber layer, GCL: ganglion cell layer, IPL: inner plexiform layer, INL: inner nuclear layer, OPL: outer plexiform layer, ONL-IS: outer nuclear layer-inner segments, OS: outer segment layer. P-values in bold: P <0.05.

REFERENCES

1. Stewart MW. Ophthalmologic Disease in HIV Infection: Recent Changes in Pathophysiology and Treatment. *Curr Infect Dis Rep.* 2017;19(12):47.
2. d'Arminio Monforte A, Cinque P, Mocroft A, et al. Changing incidence of central nervous system diseases in the EuroSIDA cohort. *Ann Neurol.* 2004;55(3):320-328.
3. Demirkaya N, Wit F, Schlingemann R, Verbraak F. Neuroretinal Degeneration in HIV Patients Without Opportunistic Ocular Infections in the cART Era. *AIDS Patient Care STDS.* 2015;29(10):519-532.
4. van Zoest RA, Underwood J, De Francesco D, et al. Structural Brain Abnormalities in Successfully Treated HIV Infection: Associations With Disease and Cerebrospinal Fluid Biomarkers. *J Infect Dis.* 2017;217(1):69-81.
5. Su T, Caan MW, Wit FW, et al. White matter structure alterations in HIV-1-infected men with sustained suppression of viraemia on treatment. *AIDS.* 2016;30(2):311-322.
6. Xu H, Chen M, Forrester JV. Para-inflammation in the aging retina. *Prog Retin Eye Res.* 2009;28(5):348-368.
7. London A, Benhar I, Schwartz M. The retina as a window to the brain-from eye research to CNS disorders. *Nat Rev Neurol.* 2013;9(1):44-53.
8. Liu S, Ong YT, Hilal S, et al. The Association Between Retinal Neuronal Layer and Brain Structure is Disrupted in Patients with Cognitive Impairment and Alzheimer's Disease. *J Alzheimers Dis.* 2016;54(2):585-595.
9. Mutlu U, Bonnemaijer PWM, Ikram MA, et al. Retinal neurodegeneration and brain MRI markers: the Rotterdam Study. *Neurobiol Aging.* 2017;60:183-191.
10. Blokhuis C, Demirkaya N, Cohen S, et al. The Eye as a Window to the Brain: Neuroretinal Thickness Is Associated With Microstructural White Matter Injury in HIV-Infected Children. *Invest Ophthalmol Vis Sci.* 2016;57(8):3864-3871.
11. Schouten J, Wit FW, Stolte IG, et al. Cross-sectional comparison of the prevalence of age-associated comorbidities and their risk factors between HIV-infected and uninfected individuals: the AGEhIV cohort study. *Clin Infect Dis.* 2014;59(12):1787-1797.
12. Demirkaya N, Wit FW, van Den Berg TJ, et al. HIV-Associated Neuroretinal Disorder in Patients With Well-Suppressed HIV-Infection: A Comparative Cohort Study. *Invest Ophthalmol Vis Sci.* 2016;57(3):1388-1397.
13. Stichting HIV Monitoring. Available at: https://www.hiv-monitoring.nl/english/.
14. Garvin MK, Abramoff MD, Kardon R, Russell SR, Wu X, Sonka M. Intraretinal layer segmentation of macular optical coherence tomography images using optimal 3-D graph search. *IEEE Trans Med Imaging.* 2008;27(10):1495-1505.
15. Garvin MK, Abramoff MD, Wu X, Russell SR, Burns TL, Sonka M. Automated 3-D intraretinal layer segmentation of macular spectral-domain optical coherence tomography images. *IEEE Trans Med Imaging.* 2009;28(9):1436-1447.
16. Demirkaya N, Cohen S, Wit FW, et al. Retinal Structure and Function in Perinatally HIV-Infected and cART-Treated Children: A Matched Case-Control Study. *Invest Ophthalmol Vis Sci.* 2015;56(6):3945-3954.
17. Demirkaya N, van Dijk HW, van Schuppen SM, et al. Effect of age on individual retinal layer thickness in normal eyes as measured with spectral-domain optical coherence tomography. *Invest Ophthalmol Vis Sci.* 2013;54(7):4934-4940.

18. Su T, Wit FW, Caan MW, et al. White matter hyperintensities in relation to cognition in HIV-infected men with sustained suppressed viral load on combination antiretroviral therapy. *AIDS.* 2016;30(15):2329-2339.
19. Ashburner J, Friston KJ. Unified segmentation. *Neuroimage.* 2005;26(3):839-851.
20. Ong YT, Hilal S, Cheung CY, et al. Retinal neurodegeneration on optical coherence tomography and cerebral atrophy. *Neurosci Lett.* 2015;584:12-16.
21. Blokhuis C, Doeleman S, Cohen S, et al. Inflammatory and Neuronal Biomarkers Associated With Retinal Thinning in Pediatric HIV. *Invest Ophthalmol Vis Sci.* 2017;58(13):5985-5992.

Neuroretinal changes in HIV-infected children: The NOVICE Study

CHAPTER 6

Retinal structure and function in perinatally HIV-infected and cART-treated children: a matched case-control study

Nazli Demirkaya
Sophie Cohen
Ferdinand W.N.M. Wit
Michael D. Abramoff
Reinier O. Schlingemann
Taco W. Kuijpers
Peter Reiss
Dasja Pajkrt
Frank D. Verbraak

on behalf of the NOVICE Study Group
Published in: IOVS, 2015 Jun 1; 56(6):3945-54.

ABSTRACT

Purpose

Subtle structural and functional neuroretinal changes have been described in HIV-infected adults without retinitis treated with combination antiretroviral therapy (cART). However, studies on this subject in HIV-infected children are scarce. This study aims to assess the presence of (neuro)retinal functional and structural differences between a group of perinatally HIV-infected children on cART and age, gender, ethnicity and socioeconomically-matched healthy controls.

Methods

All participants underwent an extensive ophthalmological examination, including functional tests as well as optical coherence tomography to measure individual retinal layer thicknesses. Multivariable mixed linear regression models were used to assess possible associations between HIV status (and other HIV-related parameters) and ocular parameters, while accounting for the inclusion of both eyes and several known confounders.

Results

Thirty-three HIV-infected children (median age 13.7 years (IQR 12.2-15.8), median $CD4^+$ T-cell count 760 cells/mm^3, 82% with an undetectable HIV viral load (VL)) and 36 controls (median age 12.1 years (IQR 11.5-15.8)) were included. Contrast sensitivity was significantly lower in the HIV-infected group (1.74 vs 1.76 logCS; *P*=0.006). The patients had a significantly thinner foveal thickness (-11.2 µm, *P*=0.012), which was associated with a higher peak HIV VL (-10.3 µm per log copy/ml, *P*=0.016).

Conclusions

In this study, we found a decrease in foveal thickness in HIV-infected children, which was associated with a higher peak VL. Longitudinal studies are warranted to confirm our findings and to determine the course and clinical consequences of these foveal changes.

Keywords: HIV; SD-OCT; visual function; children; retinal layer thickness

INTRODUCTION

The spectrum of HIV-related retinal disease has changed drastically since the introduction of combination antiretroviral therapy (cART), with a major decline in incidence of opportunistic infections, such as cytomegalovirus (CMV) retinitis, as well as non-infectious ischemic HIV-retinopathy.

However, even in cART-treated individuals with well-suppressed HIV infection and absence of opportunistic infections, functional and structural retinal abnormalities have been reported, such as a subtle loss of color vision and/or contrast sensitivity, visual field deficits and a thinner retinal nerve fiber layer (RNFL) thickness.[1-10] These changes are thought to be part of a 'HIV-associated Neuroretinal Disorder' (HIV-NRD), and may be mediated by several processes, such as a long-standing microvasculopathy,[11-17] direct damage of neural tissue by HIV and/or cART,[18-20] and chronic (para)inflammation.[21]

It is unclear whether such retinal changes are also present in cART-treated HIV-infected children (without a history of ocular opportunistic infections). So far, one study group has addressed this question and reported a thinning of the peripapillary RNFL in 19 HIV-infected children as compared to 21 healthy controls,[22] as well as foveal thickening and multifocal electroretinographical (mf-ERG) abnormalities in a smaller subgroup of HIV-infected children.[23]

This study is part of an interdisciplinary observational cross-sectional study, evaluating neurological and neurocognitive disorders, neuroimaging and ophthalmic alterations in perinatally HIV-1-infected children in the Netherlands.[24] In the current study, we assessed the presence of retinal structural and functional differences between perinatally HIV-infected children on cART and a group of age, gender, ethnicity and socioeconomically matched healthy controls. This is the first study employing the *Iowa Reference Algorithm*[25,26] on SD-OCT scans in HIV-infected children, enabling the measurement of the thickness of individual retinal layers.

SUBJECTS AND METHODS

The study adhered to the tenets of the Declaration of Helsinki and approval was obtained from the investigational review board at the Academic Medical Center in Amsterdam. Written informed consent was obtained from all parents and from children aged 12 and above.

Study participants

All HIV-infected children between 8 and 18 years of age, attending the pediatric HIV outpatient clinic of the Academic Medical Center, were approached for study participation between December 2012 and January 2014. Healthy controls were recruited through parental evenings at schools, sports clubs and churches situated in areas in Amsterdam, aiming to capture an ethnically diverse population with a lower socioeconomic status (SES) than the general Dutch population, as similar as possible to patients.[27] Exclusion criteria were chronic (non-HIV associated) neurological diseases like epilepsy, (history of) intracerebral neoplasms and psychiatric disorders. Intelligence quotient (IQ) was measured using the WISC III and WAIS III for children older than 16 years of age.[28,29] Frequency matching for age, gender, ethnicity and SES was performed. SES was determined using parental education and occupational status. Parental education was scored according to the International Standard Classification of Education (ISCED). Occupational status was defined as no-, one or two caregivers with a paid job. The remaining sociodemographic data were obtained using standardized questionnaires.

HIV- and cART-related characteristics

Historical HIV VL and $CD4^+$ T-cell counts, Center for Disease Control (CDC) clinical stage category and cART treatment history were derived from the Dutch HIV Monitoring Foundation database [30]. Clinical, immunological and virological data prior to migration to the Netherlands were collected for the immigrant children, and registered as 'missing' when not traceable. Outpatient visits in our center occur every 3 months and all clinical, immunological and virological data are registered by the HIV Monitoring Foundation. The time of HIV diagnosis was defined as the first known documented positive HIV test, also using test data from the country of origin of children who were born outside the Netherlands. VL results were based on different assays used between 1995 and 2013 with decreasing detection limits (<1000 copies/mL in 1995 to <40 copies/mL in 2013). An undetectable HIV VL was defined as a VL below the detection limit of the assay used at that time. The HIV VL during study participation was determined by the Abbott Real Time HIV-1 assay. The peak HIV VL was defined as the highest VL prior to cART initiation, or the highest HIV VL due to interruption of cART or virological failure. The proportion of life spent with a detectable viral load was calculated by adding all days between two detectable HIV VL and half of the days between the last detectable and the next undetectable HIV VL, and dividing the cumulative number of days with a detectable VL by the participant's age at inclusion to this study.

To account for physiological age-related differences in CD4+ T-cell counts, all registered $CD4^+$ T-cell counts were transformed into Z-scores by subtracting the reference value for the age at the time of the $CD4^+$ T-cell measurement and dividing this by the age-related

SD. A Z-score of 0 represents the age-appropriate mean.[30] The nadir $CD4^+$ T-cell Z-score was defined as the lowest Z-score prior to cART initiation or to a maximum of 3 months after the start of cART. At inclusion, absolute $CD4^+$ T-cell counts were analysed instead of Z-scores as all children were >8 years of age. Lastly, we calculated the cumulative time with a $CD4^+$ T-cell count below 50, 100, 200, 350 and 500 cells/mm^3 by adding all days between two $CD4^+$ T-cell measurements of <500 cells/mm^3 to half of the days between two $CD4^+$ T-cell measurements with one < 500 cells/mm^3 and one >500 cells/mm^3.

Ophthalmic examination

Ophthalmic exclusion criteria were high refractive errors (SE> +5.5 or > −8.5 D), visual acuity below 0.1 logMAR, intraocular pressure (IOP) higher than 21 mm Hg, significant media opacities and a history of ocular surgery or ocular disease. One patient with a history of cytomegalovirus retinitis in both eyes and one control with a refractive error > +5D were excluded for not meeting the inclusion criteria. In addition, 2 left eyes of 2 HIV-infected children were excluded from analysis due to the presence of uveitis and congenital toxoplasmosis lesions, respectively.

Visual acuity was measured using a modified ETDRS chart with Sloan letters (Lighthouse, NY) at 4 meters. Visual acuity (VA) was recorded in logMAR units. IOP was measured by air-puff tonometry (computerized tonometer, CT80; Topcon Medical Systems, Inc.). All subjects underwent pupil dilation (0.5% Tropicamide and 5% Phenylephrine) and a standard ophthalmic examination, including slit-lamp biomicroscopy with a handheld lens, as well as fundus photography.

Mars contrast sensitivity (CS) charts

All children were tested with the Mars Letter CS Test (Mars Perceptrix, Chappaqua, NY), a portable chart measuring 23 × 36 cm, consisting of 48 letters arranged in eight rows of six Sloan letters each. The Mars test letters subtend 2° (at 50 cm), the change in contrast between successive letters is 0.04 log units, and ranges from 0.04 to 1.92 log CS. The Mars test has test-retest reliability equal to/better than the Pelli Robson test and has proven to be a useful and practical alternative to the Pelli Robson CS chart.[23,31-34]

Lanthony D-15 color vision panel test

Color vision was determined using the Lanthony Desaturated 15-hue (D-15) color vision test.[35] This test is more sensitive to subtle color discrimination deficiencies and is easier to perform and score than the Farnsworth-Munsell 100-hue test (FM-100).[36] Testing was performed under standard illuminant conditions and repeated once when errors were made. Color confusion index (CCI), as described by Vingrys and King-Smith,[37] was

determined for each eye. Errorless performance is scored with a CCI of 1.0 and higher values indicate a worse test result. The best outcome per eye was used for analysis.

Rarebit Perimetry and Rarebit Fovea Test

The Rarebit Perimetry (RBP) and Rarebit Fovea Test (RFT) are visual function tests developed to detect subtle central visual field damage and have been described extensively elsewhere.[38,39] The RBP (inner and outer tests) evaluates the central 30° visual field, while the RFT evaluates the central 4° visual field. The results of the Rarebit test are presented as mean hit rate (MHR), a percentage of the stimuli seen by the subject.

SD-OCT and Retinal Layer Segmentation

OCT images of the subjects were obtained with SD-OCT (Topcon 3D OCT-1000; Topcon Inc., Paramus, NJ) using the 3D macular and disc volume scan protocols. Only high-quality images with a Topcon image quality factor (QF) >60 were used. From each 3D macular volume, individual retinal layers were segmented automatically by *The Iowa Reference Algorithm*,[25,26] which uses an extensively validated, robust fully three-dimensional graph search approach (**Figure 1A**). The *Iowa Reference Algorithm*[25,26] allows for the calculation of the thickness of all individual retinal layers for each of the nine ETDRS-grid defined regions (**Figure 1B-E**).

In addition, peripapillary RNFL thickness measurements were acquired from the 3D optic nerve head OCT's using the same *Iowa Reference Algorithm*.[25,26] The peripapillary ring was centered manually if needed, with the center of the ring coinciding with the center of the optic disc.

Statistical Analysis

Demographic characteristics were compared between groups using the Unpaired T-Test, the Mann-Whitney *U* test or the χ^2 test. Univariable and multivariable linear regression models with mixed effects were used to explore associations between HIV-status and ocular variables in all study participants, while accounting for the inclusion of both eyes and potential confounders (age at study visit,[40-44] gender,[41-43] intelligence quotient (IQ; corrected for in the function test analyses), OCT quality factor (QF)[40,44-46] and spherical equivalent (SE)[44,47] (corrected for in the OCT analyses). Covariates with a *P*-value<0.2 in univariable analysis were incorporated in the multivariable models. In the multivariable models the level of significance was set at a *P*-value<0.05.

The outcome variables that were significantly different between HIV-infected and healthy children in the models described above, were further investigated in the HIV-infected group only, again using multivariable mixed linear regression models. Associa-

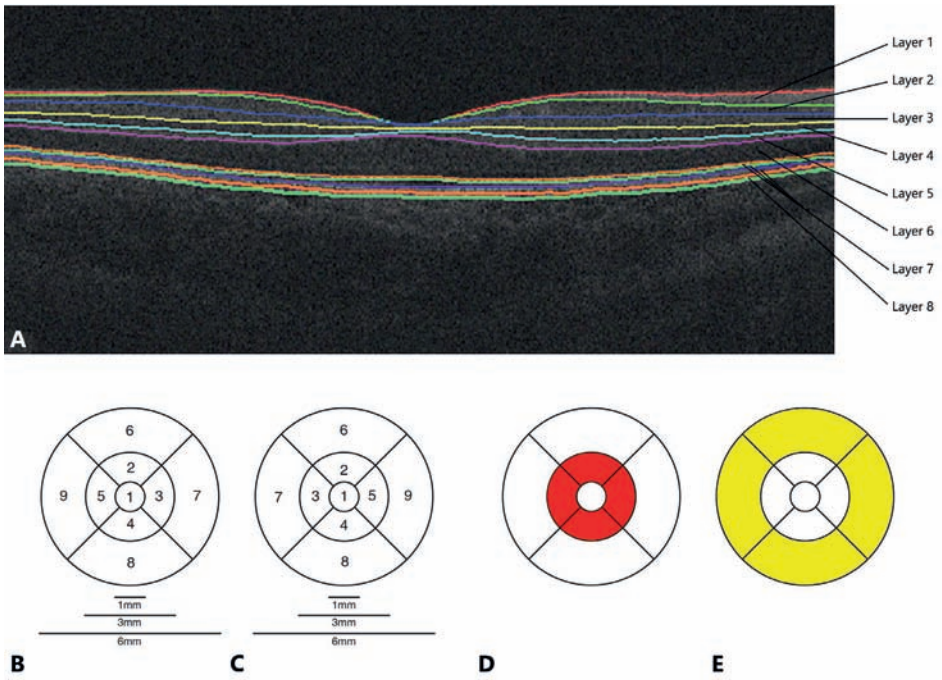

FIGURE 1. A. Macular SD-OCT B-scan with intraretinal surfaces as indicated by the colored lines and segmented using the *Iowa Reference Algorithm*.[25,26] In this study, the highly reflective layer between inner and outer segments, and the outer segments up to the retinal pigment layer were taken together as one layer, the outer segment layer (OSL), ignoring the line ascribed to the cone outer segments.[63] Corresponding retinal layers: 1/ retinal nerve fiber layer, 2/ ganglion cell layer, 3/ inner plexiform layer, 4/ inner nuclear layer, 5/ outer plexiform layer, 6/ outer nuclear layer + inner segments (photoreceptors), 7/ outer segments (photoreceptors), 8/ retinal pigment epithelium.**B-E**. ETDRS grid. Nine subfields of the 9 ETDRS regions in each eye. (**B**) Right eye. (**C**) Left eye. For each retinal layer, three areas were defined using this ETDRS grid: the fovea, the central circle with a diameter of 1 mm (depicted as 1 in Figures 1B-C); the pericentral ring, a donut-shaped ring centered on the fovea with an inner diameter of 1 mm and an outer diameter of 3 mm (Figure 1**D**); and the peripheral ring, with an inner diameter of 3 mm and outer diameter of 6 mm (Figure 1**E**). Thickness measurements of the pericentral and peripheral rings were estimated by averaging the thickness measurements of the four corresponding quadrant areas (segments 2 to 5 for the pericentral ring and segments 6 to 9 for the peripheral ring).

tions between the specified parameters and 1) disease-related factors (HIV VL at time of study visit, peak HIV VL, the proportion of life spent with a detectable VL, nadir $CD4^+$ T-cell Z-score, duration of $CD4^+$ T-cell counts <500 cells/mm^3, CDC clinical category) and 2) cART-related factors (age at cART initiation, duration of cART use, current cART use and duration of exposure to didanosine and/or stavudine (which can cause a toxic retinopathy[48-50]) were explored.

Furthermore, possible correlations between visual function test results and retinal layer thickness were assessed, in particular focusing on the significant parameters.

Data entry and management was performed using OpenClinica© open source software. Statistical analyses were carried out using Stata Statistical Software, release 12 (StataCorp LP, College Station, TX, USA).

RESULTS

Demographic and clinical characteristics

Table 1 shows the demographic and clinical characteristics of all study participants. In total, 33 HIV-infected children (median age 12.1; IQR 11.5-15.8) and 36 healthy controls were included (median age 13.7; IQR 12.2-15.8). Most children were of black (HIV: 79%; healthy: 75%) or mixed black (HIV:12%; healthy:17%) ethnicity. Although mean spherical equivalent, intra-ocular pressure and visual acuity differed significantly between the two groups, all values were within a normal range. Among the HIV-infected children, 32 (97%) had ever received cART, and 28 (85%) were using cART at time of the study assessment, among which 27 (96%) had an undetectable plasma HIV VL. The median $CD4^+$ T-cell count was 760 cells/mm^3 at the time of assessment.

Visual function tests

No significant differences in color vision and central visual field were detected between both groups (**Table 2**). Contrast sensitivity was significantly lower in the HIV-infected children, although the difference was only half a letter (1.74 vs 1.76 logCS, *P*-value=0.006).

Thickness of individual retinal layers

Multivariable mixed linear regression analyses (adjusted for age, gender, OCT quality factor and spherical equivalent) were performed to detect differences between the HIV-infected and healthy groups. Mean retinal layer thicknesses (individual retinal layers, peripapillary RNFL and total retinal thickness) for patients and controls are shown in **Table 3**. HIV-infected children had a significantly thinner total foveal thickness (-11.2 µm, *P*-value=0.012), predominantly due to a thinner foveal outer nuclear layer and inner segments (ONL-IS; -6.2 µm, *P*-value=0.011).

TABLE 1. Participant characteristics

Demographic characteristics		HIV-infected children (nr=33)	Healthy controls (nr=36)	*P*-value
Male gender		17 (52)	17 (47)	0.807
Age		12.1 (11.5-15.8)	13.7 (12.2-15.8)	0.170
Country of birth	Netherlands	10 (30)	34 (94)	**<0.001**
	Sub Saharan Africa	18 (55)	2 (6)	
	Suriname	1 (3)	0 (0)	
	Other	4 (12)	0 (0)	
Ethnicity	Black	26 (79)	27 (75)	0.358
	Mixed black	4 (12)	6 (17)	
	Caucasian	0 (0)	3 (8)	
	Other	3 (9)	0 (0)	
Education child	Primary School	9 (27)	19 (53)	**0.036**
	High school	10 (30)	13 (36)	
	Special school	9 (27)	1 (3)	
	Other	5 (15)	3 (8)	
Country of birth, parent (m/f)	Netherlands	1 (3)/ 4 (12)	6 (17)/ 8 (22)	**<0.001**
	Sub Saharan Africa	25 (76)/ 18 (55)	8 (22)/ 5 (14)	
	Surinam	2 (6)/ 3 (9)	19 (53)/ 19 (53)	
	Other	5 (15)/ 6 (18)	3 (8)/ 4 (11)	
ISCED educational level parent[*]		5 (4-6)	5 (5-6)	0.245
One parent employed		16 (62)	24 (67)	0.468
Two parents employed		5 (19)	9 (25)	0.798
HIV- and cART related characteristics				
Clinical				
Age at HIV diagnosis (y)		2.3 (0.7-4.9)	-	-
CDC category	N	4 (12)	-	-
	A	6 (18)	-	-
	B	15 (46)	-	-
	C	8 (24)	-	-
Cerebral HIV/AIDS[†]		2 (6)	-	-
$CD4^+$ T-cell and HIV viral load				
Peak HIV viral load (log copies/mL)		5.54 (5.10-5.92)	-	-
Nadir $CD4^+$ Z-score		-0.7 (-1.4- -0.4)	-	-
HIV viral load at eye exam	Detectable	6 (18)	-	-
	Undetectable	27 (82)	-	-
$CD4^+$ T-cell count at eye exam ($*10^6$/L)		760 (580-950)	-	-
$CD4^+$ Z-score at eye exam		-0.1 (-0.3- 0.2)	-	-
Time living with a detectable viral load (y)		2.4 (1.4-5.8)	-	-

TABLE 1. Participant characteristics (continued)

Demographic characteristics	**HIV-infected children (nr=33)**	**Healthy controls (nr=36)**	***P*-value**
Time with $CD4^+$ T-cell count <500 ($*10^6$/L) (m)	18.3 (11.0-94.1)	-	-
cART			
Age at cART initiation (y)	2.6 (1.0-6.2)	-	-
Current cART use	28 (85)	-	-
Duration cART use (y)	10.7 (7.1-14.4)	-	-
Mono- or dual therapy treatment before cART	3 (9)	-	-
Duration of exposure to didanosine (y) (n=15)	2.2 (0.8-4.4)	-	-
Duration of exposure to stavudine (y) (n=12)	4.6 (3.9-5.6)	-	-
Ocular features	**mean ± SD, Range**	**mean ± SD, Range**	***P*-value**
Spherical equivalent refraction, D	-0.86 ±1.6 (-5.9-1,3)	-1.6±2.2 (-7,1-0,8)	**0.033**
Intra-ocular pressure, mm Hg	14.1±2.4 (10-19)	16.2±3.1 (10-24)	**<0.001**
Visual acuity, LogMar	-0.02±0.06 (-0.2-0,1)	-0.05±0.05 (-0.18-0.06)	**0.008**
Topcon image quality factor, macula scan	85.6±6.9 (60.0-100.6)	85.3±7.2 (68.7-101.9)	0.771
Topcon image quality factor, disc scan	84.7±7.2 (66.6-94.9)	86.0±5.3 (73.6-96.5)	0.247

HIV=Human Immunodeficiency Virus. (y)=years. (m)= months. (m/f)= mother/father. ISCED: International Standard Classification of Education. cART=combination antiretroviral therapy. CDC= Centre for Disease Control and Prevention. Values are expressed ad N (%), median (IQR) or as mean ± standard deviation (SD). [*]: Most educated parent. [†]: HIV-encephalopathy (n=2) and CMV encephalitis (n=1). *P*-values in bold are P <0.05.

TABLE 2. Visual function test results in HIV patients and controls

Visual function test	**HIV-infected children (nr=33)**				**Healthy controls (nr=36)**				**Coef-ficient**	***P*-value**
	n	**mean**	**SD**	**range**	**n**	**mean**	**SD**	**range**		
Lanthony D15 test; CCI	64	1.18	0.23	1-2.12	70	1.15	0.19	1-1.87	-0.0379	0.315
Mars CS; logCS	63	1.74	0.03	1.64-1.80	72	1.76	0.03	1.72-1.92	-0.0192	**0.006**
RBP Outer Test; MHR	60	79.5	13.3	47-99	71	83.8	11.6	43-100	-2.44	0.379
RBP Inner Test; MHR	60	93.6	11.1	44-100	72	94.8	7.4	63-100	0.0158	0.993
Rarebit Fovea Test; MHR	60	88.6	17.3	38-100	72	93.9	9.8	50-100	-2.0372	0.476

P-values derived from multivariable linear mixed model and adjusted for age at assessment, gender and total IQ. n=number of eyes. *P*-value in bold is P <0.05.

TABLE 3. OCT individual retinal layer thicknesses in HIV patients and controls

Macular layer	HIV-infected children (nr=33)				Healthy controls (nr=36)				Coeffi-cient	*P*-value
	n	mean	SD	range	n	mean	SD	range		
RNFL										
Fovea	64	3.4	1.5	0.8-8.5	70	4.0	1.8	1.1-11.3	-0.6162	0.068
Pericentral ring	64	20.3	1.8	15.6-24.7	70	21.3	1.9	15.6-25.1	-0.9317	**0.015**
Peripheral ring	64	33.1	3.4	24.1-42.7	70	34.3	3.3	26.5-41.0	-1.009	0.153
GCL										
Fovea	64	10.9	3.3	4.1-18.4	70	14.4	5.1	5.5-31.3	-3.1545	**0.001**
Pericentral ring	64	51.8	5.6	31.2-63.1	70	53.3	4.8	41.7-66.2	-2.0811	0.094
Peripheral ring	64	32.0	3.9	26.0-43.4	70	31.7	2.7	25.3-38.5	0.0480	0.951
IPL										
Fovea	64	20.3	3.8	14.0-29.9	70	22.1	4.4	14.5-31.2	-1.5397	0.103
Pericentral ring	64	39.6	3.5	33.9-49.9	70	40.4	3.0	34.1-46.7	-0.9592	0.217
Peripheral ring	64	40.6	3.5	31.4-49.3	70	40.4	2.7	34.9-47.7	-0.0580	0.937
INL										
Fovea	64	16.9	3.6	11.2-27.6	70	19.3	4.1	11.5-32.1	-1.9766	**0.026**
Pericentral ring	64	38.3	3.8	30.8-47.0	70	39.0	2.8	33.8-45.4	-0.9530	0.225
Peripheral ring	64	34.0	3.2	27.7-42.0	70	33.4	2.4	25.2-39.6	0.2916	0.656
OPL										
Fovea	64	23.6	4.4	14.7-37.4	70	23.2	4.0	15.0-33.3	0.4933	0.562
Pericentral ring	64	27.6	3.7	19.9-37.9	70	27.9	3.9	22.2-40.0	-0.2125	0.795
Peripheral ring	64	25.2	1.6	22.2-28.9	70	24.8	1.4	21.6-28.4	0.3330	0.309
ONL + IS										
Fovea	64	107.1	11.9	82.1-135.1	70	112.4	9.6	92.4-130.2	-6.2414	**0.011**
Pericentral ring	64	95.5	8.9	81.6-116.7	70	96.3	8.4	73.6-111.1	0.2998	0.507
Peripheral ring	64	81.7	6.9	70.0-96.6	70	82.8	5.6	70.4-94.9	-1.9953	0.311
OSL										
Fovea	64	50.9	2.6	44.5-56.8	70	49.0	3.9	29.6-54.5	1.8653	**0.010**
Pericentral ring	64	43.7	2.7	37.6-51.7	70	41.2	4.1	20.8-46.9	2.1511	**0.006**
Peripheral ring	64	38.8	2.8	32.7-46.0	70	37.0	3.1	30.3-42.5	1.1224	0.088
RPE										
Fovea	64	16.9	2.1	14.2-23.1	70	17.3	1.8	14.0-22.9	-0.3441	0.425
Pericentral ring	64	17.4	2.2	12.8-22.0	70	18.7	2.3	14.7-23.7	-0.9706	0.063
Peripheral ring	64	19.5	2.8	12.5-23.7	70	20.7	2.1	16.4-24.0	-0.9117	0.113
Total foveal RT	64	233.2	18.3	198.2-279.4	70	244.4	19.3	208.5-279.7	-11.2368	**0.012**
Total pericentral RT	64	316.9	16.5	283.4-348.8	70	319.3	14.1	287.1-345.1	-5.0431	0.162
Total peripheral RT	64	285.5	16.0	248.2-317.5	70	284.4	12.3	258.3-310.7	-0.8588	0.798
Peripapillary RNFL	63	112.1	15.8	81.0-143.9	67	111.2	9.5	91.4-129.8	0.8840	0.772

SD=standard deviation. n= number of eyes. RNFL=retinal nerve fibre layer. GCL=ganglion cell layer. IPL= inner plexiform layer. INL=inner nuclear layer. OPL=outer plexiform layer. ONL-IS=outer nuclear layer- inner segments. OSL=outer segment layer. RPE=retinal pigment epithelium. RT=retinal thickness. *P*-values derived from multivariable linear mixed model and adjusted for age, gender, OCT quality factor and spherical equivalent. *P*-values in bold are P <0.05.

Multivariable analyses within the HIV-infected group

Visual function and OCT parameters that differed significantly between HIV-infected and healthy children were further investigated in the HIV-infected group, to identify potential associations between these parameters and HIV- and/or cART related variables.

Multivariable mixed regression analysis showed an inverse association between total foveal retinal thickness and peak HIV VL (-10.7 µm per log copy/ml, *P*-value=0.016, **FIGURE 2**); a similar relationship was observed between the foveal outer nuclear layer and inner segments and peak HIV VL (-7.1 µm per log copy/ml, *P*-value=0.013). No other associations were found between visual function, OCT parameters and HIV or cART-related parameters.

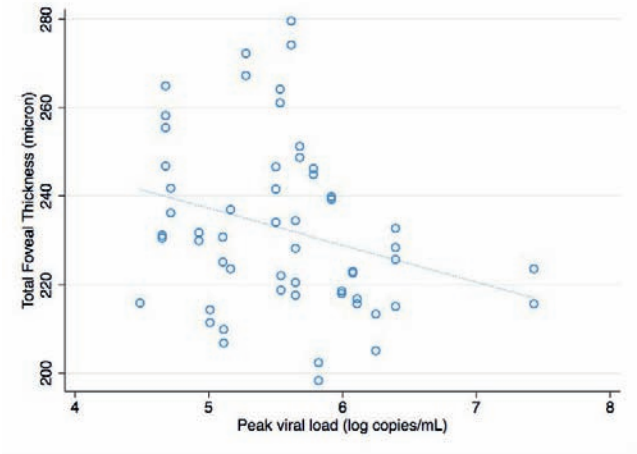

FIGURE 2. Correlation between total foveal thickness and peak HIV viral load.

Structure-function relationships

Finally, we explored potential correlations between visual function test results (color vision, contrast sensitivity and central visual field) and OCT retinal layer thickness in HIV-infected children. No associations were observed (data not shown).

DISCUSSION

This study aimed to assess retinal structure and visual function in a group of perinatally HIV-infected children, compared to a group of matched healthy controls. Subtle structural retinal changes and visual dysfunction, termed 'HIV- Associated Neuroretinal Disorder' (HIV-NRD), have been described in HIV-infected adults on cART without infectious retinitis,[1-10,14,16,17,51-59] however data on this subject in HIV-infected children are

limited and derived from one study group.[22,23] This is the first study assessing individual retinal layer thicknesses and exploring associations between various HIV-and cART-related factors and ocular parameters in HIV-infected children.

Our findings indicate that HIV-infected children have a thinner foveal retinal thickness than healthy controls, while having a comparable peripapillary RNFL thickness and visual function outcomes.

We found no significant differences in peripapillary RNFL thickness between HIV-infected children and age-, gender-, ethnicity- and socioeconomically matched controls, which is not in line with the previous pediatric study by Moschos et al.[22] They reported a thinner peripapillary RNFL thickness in a group of 19 HIV-infected children compared to a group of 21 age-matched healthy children.[22] Of note, however, in our study we used Spectral-Domain OCT, which is more accurate in measuring retinal and RNFL thickness than Time-Domain OCT.[60] Furthermore, in our assessment of peripapillary RNFL thickness, we adjusted for known confounders such as age,[40-44] gender,[41-43] spherical equivalent[40,44,47] and OCT quality factor.[40,44,46] In addition, we applied multilevel mixed linear modelling to take correlations between right and left eyes into account.

In their second study, Moschos et al. found an increase in foveal thickness as well as multifocal ERG abnormalities in a subgroup, consisting of 10 eyes (the number of children was not stated) in their cohort.[23] We observed the opposite in our study with a significantly lower total foveal thickness in the group of HIV-infected children, predominantly due to a thinner outer nuclear layer and inner segments of the photoreceptors as well as thinner inner retinal layers. Since we are the first group measuring individual OCT retinal layer thicknesses in HIV-infected children, comparison of our findings to other studies in children is not yet attainable. In HIV-infected adults however, it is thought that damage (caused by HIV and/or other factors) to the optic nerve leads to thinning of the peripapillary RNFL.[1,7,9] Multiple adult studies indeed reported a decrease in peripapillary RNFL thickness, particularly in patients with (a history of) low (<100 cells/mm^3) CD4$^+$ T-cell counts.[4,52,57-59] Since the axons of the ganglion cell layer make up the optic nerve for a large part, a decrease in peripapillary RNFL implies that a decrease in ganglion cell layer thickness (and possibly other inner retinal layers) would also be expected, but no study has reported on this. If we extrapolate this hypothesis of HIV-associated neuroretinal degeneration to HIV-infected children, a decrease of peripapillary RNFL thickness and inner retinal layers (especially in the pericentral retinal area, where the ganglion cell layer is thickest) would be expected in this group. Surprisingly, we detected a thinner *foveal* thickness and no other OCT differences in the HIV-infected children as compared to the controls.

However, the consequences of chronic HIV-infection in perinatally infected children are likely to be different from adults because their infection occurs during- rather than after- (neuronal) development. This may result in different findings between adults and children. Of all foveal layers, the outer nuclear layer shows the most distinct increase during foveal maturation (from infancy to 16 years of age), creating a bulge.[61] Therefore, if we speculate that HIV-infection may interrupt this maturation, this would be mostly reflected in the outer nuclear layer. This may explain the significantly thinner fovea – in particular the outer nuclear layer and inner segments- we detected in the HIV-infected children in our study. Supporting this hypothesis was the significant association we observed between a higher peak HIV VL and thinner foveal outer nuclear layer and inner segments.

A recent study in 22 perinatally HIV-infected children (median age 16.6 years) on cART with nadir CD4 counts > 200 cells/mm^3, reported an absence of vision-threatening disease, but a high prevalence (18%) of strabismus,[62] which is thought to be a developmental disorder, again suggesting that HIV-infection may hamper the development of the visual system.

We did not detect any correlations between retinal structure and visual function in HIV-infected children. This was to be expected, considering the high inter-individual variability in retinal layer thickness and functional test outcomes, and the small changes observed.

Strengths of our study are the inclusion of an age, gender, ethnicity and socioeconomically matched control group, and the adjustment for relevant potentially confounding factors in our statistical analyses. Of note, we found IQ to be an important confounder when analyzing the functional test outcomes, with a strong positive association between test results and total IQ. Nonetheless, there are some limitations. Despite being the largest ophthalmological study in clinically stable HIV-infected children without retinitis at present, the relatively small sample size may have hampered the detection of some potential associations. Secondly, a cross-sectional study of parameters known to have a high inter-individual variability is less able to detect small changes in retinal structure and function than a longitudinal study.

Although we aimed to capture a control population, as similar as possible to the patients, by matching for age, gender and socio-economic status, there is a possibility that some of the variability in the results we detected was caused by non-HIV related factors.

The visual function tests we used are psychophysical techniques and involve an element of subjectivity; however we used standardized protocols (i.e. lightning conditions, test-

ing distance) to minimize this problem. A more objective method for evaluating retinal function is multifocal-electroretinography (mf-ERG), but needs adequate cooperation and can therefore be challenging to perform in children. Lastly, we did not measure peripapillary RNFL thickness in quadrants, therefore it is possible that there were quadrantal changes in RNFL thickness in our patients, while the average peripapillary RNFL thickness was not different between the two groups.

In summary, our findings indicate that HIV-infected children have a thinner foveal retinal thickness compared to matched controls, while having a comparable peripapillary RNFL thickness and visual function outcomes. Our results do not confirm the results of Moschos et al.,[22,23] however they are in accordance with some recent studies in HIV-infected adults, observing similar average peripapillary RNFL thickness between patients and controls,[1,9] and little differences in contrast sensitivity.[7,9] A novel finding in our study is the decrease in foveal thickness in the group of HIV-infected children, of which the clinical significance is yet unclear, since both visual acuity and visual function were adequate. We postulate that HIV-infection may disturb foveal maturation, leading to a thinner fovea. Although our results do not support the presence of a HIV-neuroretinal disorder, it is also possible that retinal (neuro)degeneration will occur at a later time in patients' lives. The long-term effects of HIV-infection on the retina are unknown, and as life-expectancy of HIV-infected patients is increasing with the global roll-out of cART, vision loss might become more prevalent and symptomatic with time. Therefore, longitudinal studies are warranted to investigate the effect of chronic HIV-infection and long-term cART on the retinal structure and visual function of both HIV-infected adults and children.

AUTHORS' CONTRIBUTIONS

ND contributed to study design, data collection and interpretation and wrote the manuscripted in cooperation with SC, under supervision of DP and FDV.

SC contributed to study design, data collection, statistical analysis and writing of the manuscript. FWNMW contributed to study design, supervised the statistical analysis, contributed to data interpretation and edited and revised the manuscript.

MDA invented and provided the Iowa Reference Algorithms, contributed to data interpretation and revised the manuscript. ROS edited and revised the manuscript. TWK edited and revised the manuscript. PR edited and revised the manuscript. DP and FDV contributed to study design, data interpretation, supervised and edited the manuscript.

REFERENCES

1. Arantes TE, Garcia CR, Tavares IM, Mello PA, Muccioli C. Relationship between retinal nerve fiber layer and visual field function in human immunodeficiency virus-infected patients without retinitis. *Retina*. 2012;32:152-159.
2. Falkenstein I, Kozak I, Kayikcioglu O, et al. Assessment of retinal function in patients with HIV without infectious retinitis by multifocal electroretinogram and automated perimetry. *Retina*. 2006;26:928-934.
3. Falkenstein IA, Bartsch DU, Azen SP, Dustin L, Sadun AA, Freeman WR. Multifocal electroretinography in HIV-positive patients without infectious retinitis. *Am J Ophthalmol*. 2008;146:579-588.
4. Faria E Arantes TE, Garcia CR, Mello PA, Muccioli C. Structural and functional assessment in HIV-infected patients using optical coherence tomography and frequency-doubling technology perimetry. *Am J Ophthalmol*. 2010;149:571-576.
5. Freeman WR, Van Natta ML, Jabs D, et al. Vision function in HIV-infected individuals without retinitis: report of the Studies of Ocular Complications of AIDS Research Group. *Am J Ophthalmol*. 2008;145:453-462.
6. Goldbaum MH, Falkenstein I, Kozak I, et al. Analysis with support vector machine shows HIV-positive subjects without infectious retinitis have mfERG deficiencies compared to normal eyes. *Trans Am Ophthalmol Soc*. 2008;106:196-204.
7. Kalyani PS, Holland GN, Fawzi AA, Arantes TE, Yu F, Sadun AA. Association between retinal nerve fiber layer thickness and abnormalities of vision in people with human immunodeficiency virus infection. *Am J Ophthalmol*. 2012;153:734-42, 742.
8. Kozak I, Sample PA, Hao J, et al. Machine learning classifiers detect subtle field defects in eyes of HIV individuals. *Trans Am Ophthalmol Soc*. 2007;105:111-118.
9. Pathai S, Lawn SD, Weiss HA, Cook C, Bekker LG, Gilbert CE. Retinal Nerve Fibre Layer Thickness and Contrast Sensitivity in HIV-Infected Individuals in South Africa: A Case-Control Study. *PLoS One*. 2013;8:e73694.
10. Shah KH, Holland GN, Yu F, Van NM, Nusinowitz S. Contrast sensitivity and color vision in HIV-infected individuals without infectious retinopathy. *Am J Ophthalmol*. 2006;142:284-292.
11. Dadgostar H, Holland GN, Huang X, et al. Hemorheologic abnormalities associated with HIV infection: in vivo assessment of retinal microvascular blood flow. *Invest Ophthalmol Vis Sci*. 2006;47:3933-3938.
12. Dejaco-Ruhswurm I, Kiss B, Rainer G, et al. Ocular blood flow in patients infected with human immunodeficiency virus. *Am J Ophthalmol*. 2001;132:720-726.
13. Furrer H, Barloggio A, Egger M, Garweg JG. Retinal microangiopathy in human immunodeficiency virus infection is related to higher human immunodeficiency virus-1 load in plasma. *Ophthalmology*. 2003;110:432-436.
14. Gangaputra S, Kalyani PS, Fawzi AA, et al. Retinal vessel caliber among people with acquired immunodeficiency syndrome: relationships with disease-associated factors and mortality. *Am J Ophthalmol*. 2012;153:434-444.
15. Kim A, Dadgostar H, Holland GN, et al. Hemorheologic abnormalities associated with HIV infection: altered erythrocyte aggregation and deformability. *Invest Ophthalmol Vis Sci*. 2006;47:3927-3932.

16. Pathai S, Weiss HA, Lawn SD, et al. Retinal arterioles narrow with increasing duration of anti-retroviral therapy in HIV infection: a novel estimator of vascular risk in HIV? *PLoS One.* 2012;7:e51405.
17. Tan PB, Hee OK, Cheung C, et al. Retinal vascular parameter variations in patients with human immunodeficiency virus. *Invest Ophthalmol Vis Sci.* 2013;54:7962-7967.
18. Kaul M, Garden GA, Lipton SA. Pathways to neuronal injury and apoptosis in HIV-associated dementia. *Nature.* 2001;410:988-994.
19. Kaul M, Lipton SA. Mechanisms of neuroimmunity and neurodegeneration associated with HIV-1 infection and AIDS. *J Neuroimmune Pharmacol.* 2006;1:138-151.
20. Tenhula WN, Xu SZ, Madigan MC, Heller K, Freeman WR, Sadun AA. Morphometric comparisons of optic nerve axon loss in acquired immunodeficiency syndrome. *Am J Ophthalmol.* 1992;113:14-20.
21. Xu H, Chen M, Forrester JV. Para-inflammation in the aging retina. *Prog Retin Eye Res.* 2009;28:348-368.
22. Moschos MM, Mostrou G, Psimenidou E, Spoulou V, Theodoridou M. Objective analysis of retinal function in HIV-positive children without retinitis using optical coherence tomography. *Ocul Immunol Inflamm.* 2007;15:319-323.
23. Moschos MM, Margetis I, Markopoulos I, Moschos MN. Optical coherence tomography and multifocal electroretinogram study in human immunodeficiency virus-positive children without infectious retinitis. *Clin Exp Optom.* 2011;94:291-295.
24. Cohen S, Ter Stege JA, Geurtsen GJ, et al. Poorer cognitive performance in perinatally HIV-infected children as compared to healthy socioeconomically matched controls. *Clin Infect Dis.* 2014.
25. Garvin MK, Abramoff MD, Kardon R, Russell SR, Wu X, Sonka M. Intraretinal layer segmentation of macular optical coherence tomography images using optimal 3-D graph search. *IEEE Trans Med Imaging.* 2008;27:1495-1505.
26. Garvin MK, Abramoff MD, Wu X, Russell SR, Burns TL, Sonka M. Automated 3-D intraretinal layer segmentation of macular spectral-domain optical coherence tomography images. *IEEE Trans Med Imaging.* 2009;28:1436-1447.
27. Bicknese L, Slot J. Staat van de aandachtswijken. 2009:107-118.
28. Wechsler D. Wechsler Adult Intelligence Scale Manual. In: London: The Psychological Corporation; 2000.
29. Wechsler D. Wechsler Intelligence Scale Manual. In: London.: The Psychological Corporation; 2002.
30. Comans-Bitter WM, de GR, van den Beemd R, et al. Immunophenotyping of blood lymphocytes in childhood. Reference values for lymphocyte subpopulations. *J Pediatr.* 1997;130:388-393.
31. Arditi A. Improving the design of the letter contrast sensitivity test. *Invest Ophthalmol Vis Sci.* 2005;46:2225-2229.
32. Dougherty BE, Flom RE, Bullimore MA. An evaluation of the Mars Letter Contrast Sensitivity Test. *Optom Vis Sci.* 2005;82:970-975.
33. Haymes SA, Roberts KF, Cruess AF, et al. The letter contrast sensitivity test: clinical evaluation of a new design. *Invest Ophthalmol Vis Sci.* 2006;47:2739-2745.
34. Thayaparan K, Crossland MD, Rubin GS. Clinical assessment of two new contrast sensitivity charts. *Br J Ophthalmol.* 2007;91:749-752.
35. Lanthony P. The desaturated panel D-15. *Doc Ophthalmol.* 1978;46:185-189.

36. Good GW, Schepler A, Nichols JJ. The reliability of the Lanthony Desaturated D-15 test. *Optom Vis Sci.* 2005;82:1054-1059.
37. Vingrys AJ, King-Smith PE. A quantitative scoring technique for panel tests of color vision. *Invest Ophthalmol Vis Sci.* 1988;29:50-63.
38. Frisen L. New, sensitive window on abnormal spatial vision: rarebit probing. *Vision Res.* 2002;42:1931-1939.
39. Salvetat ML, Zeppieri M, Parisi L, Brusini P. Rarebit perimetry in normal subjects: test-retest variability, learning effect, normative range, influence of optical defocus, and cataract extraction. *Invest Ophthalmol Vis Sci.* 2007;48:5320-5331.
40. Demirkaya N, van Dijk HW, van Schuppen SM, et al. Effect of age on individual retinal layer thickness in normal eyes as measured with spectral-domain optical coherence tomography. *Invest Ophthalmol Vis Sci.* 2013;54:4934-4940.
41. Ooto S, Hangai M, Tomidokoro A, et al. Effects of age, sex, and axial length on the three-dimensional profile of normal macular layer structures. *Invest Ophthalmol Vis Sci.* 2011;52:8769-8779.
42. Song WK, Lee SC, Lee ES, Kim CY, Kim SS. Macular thickness variations with sex, age, and axial length in healthy subjects: a spectral domain-optical coherence tomography study. *Invest Ophthalmol Vis Sci.* 2010;51:3913-3918.
43. Kashani AH, Zimmer-Galler IE, Shah SM, et al. Retinal thickness analysis by race, gender, and age using Stratus OCT. *Am J Ophthalmol.* 2010;149:496-502.
44. Rao HL, Kumar AU, Babu JG, Kumar A, Senthil S, Garudadri CS. Predictors of normal optic nerve head, retinal nerve fiber layer, and macular parameters measured by spectral domain optical coherence tomography. *Invest Ophthalmol Vis Sci.* 2011;52:1103-1110.
45. Huang J, Liu X, Wu Z, Sadda S. Image quality affects macular and retinal nerve fiber layer thickness measurements on fourier-domain optical coherence tomography. *Ophthalmic Surg Lasers Imaging.* 2011;42:216-221.
46. Samarawickrama C, Pai A, Huynh SC, Burlutsky G, Wong TY, Mitchell P. Influence of OCT signal strength on macular, optic nerve head, and retinal nerve fiber layer parameters. *Invest Ophthalmol Vis Sci.* 2010;51:4471-4475.
47. Lim MC, Hoh ST, Foster PJ, et al. Use of optical coherence tomography to assess variations in macular retinal thickness in myopia. *Invest Ophthalmol Vis Sci.* 2005;46:974-978.
48. Whitcup SM, Butler KM, Pizzo PA, Nussenblatt RB. Retinal lesions in children treated with dideoxyinosine. *N Engl J Med.* 1992;326:1226-1227.
49. Whitcup SM, Butler KM, Caruso R, et al. Retinal toxicity in human immunodeficiency virus-infected children treated with 2',3'-dideoxyinosine. *Am J Ophthalmol.* 1992;113:1-7.
50. Whitcup SM, Dastgheib K, Nussenblatt RB, Walton RC, Pizzo PA, Chan CC. A clinicopathologic report of the retinal lesions associated with didanosine. *Arch Ophthalmol.* 1994;112:1594-1598.
51. Barteselli G, Chhablani J, Gomez ML, et al. Visual function assessment in simulated real-life situations in HIV-infected subjects. *PLoS One.* 2014;9:e97023.
52. Besada E, Shechtman D, Black G, Hardigan PC. Laser scanning confocal ophthalmoscopy and polarimetry of human immunodeficiency virus patients without retinopathy, under antiretroviral therapy. *Optom Vis Sci.* 2007;84:189-196.
53. Cheng S, Klein H, Bartsch DU, Kozak I, Marcotte TD, Freeman WR. Relationship between retinal nerve fiber layer thickness and driving ability in patients with human immunodeficiency virus infection. *Graefes Arch Clin Exp Ophthalmol.* 2011;249:1643-1647.

54. Gomez ML, Mojana F, Bartsch DU, Freeman WR. Imaging of long-term retinal damage after resolved cotton wool spots. *Ophthalmology*. 2009;116:2407-2414.
55. Holland GN, Kappel PJ, Van Natta ML, et al. Association between abnormal contrast sensitivity and mortality among people with acquired immunodeficiency syndrome. *Am J Ophthalmol*. 2010;149:807-816.
56. Kalyani PS, Fawzi AA, Gangaputra S, et al. Retinal vessel caliber among people with acquired immunodeficiency syndrome: relationships with visual function. *Am J Ophthalmol*. 2012;153:428-433.
57. Kozak I, Bartsch DU, Cheng L, Kosobucki BR, Freeman WR. Objective analysis of retinal damage in HIV-positive patients in the HAART era using OCT. *Am J Ophthalmol*. 2005;139:295-301.
58. Kozak I, Bartsch DU, Cheng L, McCutchan A, Weinreb RN, Freeman WR. Scanning laser polarimetry demonstration of retinal nerve fiber layer damage in human immunodeficiency virus-positive patients without infectious retinitis. *Retina*. 2007;27:1267-1273.
59. Plummer DJ, Bartsch DU, Azen SP, Max S, Sadun AA, Freeman WR. Retinal nerve fiber layer evaluation in human immunodeficiency virus-positive patients. *Am J Ophthalmol*. 2001;131:216-222.
60. Ho J, Sull AC, Vuong LN, et al. Assessment of artifacts and reproducibility across spectral- and time-domain optical coherence tomography devices. *Ophthalmology*. 2009;116:1960-1970.
61. Vajzovic L, Hendrickson AE, O'Connell RV, et al. Maturation of the human fovea: correlation of spectral-domain optical coherence tomography findings with histology. *Am J Ophthalmol*. 2012;154:779-789.
62. Rutar T, Youm J, Porco T, et al. Ophthalmic manifestations of perinatally acquired HIV in a US cohort of long-term survivors. *Br J Ophthalmol*. 2014.
63. Jonnal RS, Kocaoglu OP, Zawadzki RJ, Lee SH, Werner JS, Miller DT. The cellular origins of the outer retinal bands in optical coherence tomography images. *Invest Ophthalmol Vis Sci*. 2014;55:7904-7918.

CHAPTER 7

The eye as a window to the brain: neuroretinal thickness is associated with microstructural white matter injury in HIV-infected children

Charlotte Blokhuis*
Nazli Demirkaya*
Sophie Cohen
Ferdinand W.N.M. Wit
Henriëtte J. Scherpbier
Peter Reiss
Michael D. Abramoff
Matthan W.A. Caan
Charles B.L.M. Majoie
Frank D. Verbraak
Dasja Pajkrt

* **These authors contributed equally to the manuscript.**

on behalf of the NOVICE Study Group
Published in: IOVS, 2016 Jul 1;57(8):3864-3871

ABSTRACT

Purpose

Despite combination antiretroviral therapy (cART), perinatal HIV-infection can cause decreased gray and white matter volume, microstructural white matter injury and retinal structural abnormalities. As neuroretinal tissue is directly connected to the brain, these deficits may have a shared pathogenesis. We aimed to assess associations between neuroretinal thickness and cerebral injury in cART-treated perinatally HIV-infected children and healthy controls.

Methods

This cross-sectional observational study included 29 cART-treated perinatally HIV-infected children and 35 matched healthy controls. All participants underwent 3.0 Tesla MRI, determining gray and white matter volumes from T1-weighted sequences, and white matter diffusivity using diffusion tensor imaging (DTI). Regional individual and total neuroretinal layer thickness was quantified using Spectral-Domain Optical Coherence Tomography. We explored associations between retinal and cerebral parameters using multivariable linear regression analysis.

Results

In HIV-infected children, lower foveal and pericentral neuroretinal thickness was associated with damaged white matter microstructure, in terms of lower fractional anisotropy and higher mean and radial diffusivity. In healthy controls only, neuroretinal thickness was associated with gray and white matter volume.

Conclusions

Decreased neuroretinal thickness is associated with microstructural white matter injury, but not with lower cerebral volume in HIV-infected children. This suggests that HIV-induced retinal thinning and microstructural white matter injury may share a common pathogenesis, and longitudinal assessment of neuroretinal alterations in parallel with MRI and neuroinflammatory markers may further our insight into the pathogenesis of HIV-induced cerebral injury in children.

Key words: Perinatally HIV-infected children; cerebral injury; magnetic resonance imaging; diffusion tensor imaging; retina; optical coherence tomography.

INTRODUCTION

The prevalence of severe central nervous system (CNS) abnormalities in HIV-infected children, such as HIV-encephalopathy, has decreased drastically since combination antiretroviral therapy (cART).[1] Nevertheless, cART treated HIV-infected children still encounter neurological and cognitive problems with macro- and microstructural cerebral damage that can occur subclinically.[2,3] Recently, we demonstrated lower brain volumes, increased white matter (WM) hyperintensities, and increased WM diffusivity in perinatally HIV-infected children on cART, as compared to matched healthy controls.[4] The observed cerebral injury was associated with poorer cognitive performance in multiple neurocognitive domains.[4,5] Retinal thickness (RT) analysis using Spectral Domain optical coherence tomography (SD-OCT) revealed a decrease in foveal thickness in the HIV-infected children compared to controls.[6] As the retina shares developmental, physiological and anatomical features with the brain,[7] these retinal and cerebral deficits may have a shared pathogenesis, which could include HIV-induced impeded maturation or persistent neuroinflammation and neurodegeneration. The associations between a higher peak HIV viral load and both retinal and cerebral injury support this theory.[4,6]

Here, we examined associations of RT with cerebral volume and WM microstructural alterations in HIV-infected children and matched controls, using SD-OCT and advanced MRI techniques, including diffusion tensor imaging (DTI). Further, we evaluated whether the relationship between retinal and cerebral structure is affected by pediatric HIV-infection.

As OCT has been successfully used to link retinal and intracerebral pathology in other neuroinflammatory and neurodegenerative diseases,[7–11] evaluating neuroretinal structure may increase our understanding of the pathogenesis of pediatric HIV-induced cerebral injury.

METHODS

This study is part of an interdisciplinary observational cross-sectional case-control study, evaluating neurological and neurocognitive disorders, neuroradiological and ophthalmic alterations in perinatally HIV-infected children as compared to age, gender ethnicity and socio-economic status (SES) matched healthy controls in the Netherlands (NOVICE study, Dutch Trial Registry ID NTR4074).[4–6] The study adhered to the tenets of the Declaration of Helsinki and was approved by the investigational review board of

the Academic Medical Center (AMC) in Amsterdam, the Netherlands. Written informed consent was obtained from all parents and from children aged 12 years and above.

Study participants

The NOVICE study participants consisted of perinatally HIV-infected children aged 8-18 years, recruited from the AMC outpatient clinic, Amsterdam, and healthy controls, matched for age, gender, ethnicity and SES as described previously.[5] Exclusion criteria for study participation were chronic HIV-unrelated neurological disease, (history of) intracerebral neoplasms, traumatic brain injury, psychiatric disorders and MRI contra-indications. Additional ophthalmic exclusion criteria were high refractive errors (spherical equivalent [SE] exceeding +5.5 or −8.5 D), visual acuity below 0.1 on the logMAR chart, intraocular pressure higher than 21 mmHg, significant media opacities and a history of ocular surgery or ocular disease.

Spectral-Domain Optical Coherence Tomography and Retinal Layer Segmentation

SD-OCT images were obtained with the Topcon 3D OCT-1000 (Topcon Inc., Paramus, NJ) using the 3D macular and disc volume scan protocols. Only high-quality images with a Topcon image quality factor (QF)>60 were used. From each 3D macular volume, individual neuroretinal layers were segmented automatically using the validated *Iowa Reference Algorithms*, allowing for all individual retinal layers thickness calculations for each of the nine macular regions as defined by the Early Treatment of Diabetic Retinopathy Study (ETDRS; as shown in **Supplemental Figure 1**).[12,13] We selected foveal, pericentral and peripheral ETDRS rings, as in previous studies.[6,14,15] Peripapillary retinal nerve fiber layer (RNFL) thickness measurements were acquired from the 3D optic nerve head OCT's using the same *Iowa Reference Algorithms.*[12,13] The peripapillary ring was centered manually if needed, with the center of the ring coinciding with the center of the optic disc.

MRI data acquisition and data processing

Brain scans were obtained using a 3.0 Tesla MRI scanner (Intera, Philips Healthcare, Best, the Netherlands) as previously described in further detail.[4] A non-linear least squares estimation of diffusion tensors was used to compute fractional anisotropy (FA), mean diffusivity (MD), axial diffusivity (AD) and radial diffusivity (RD) maps, which were averaged over the entire skeleton to obtain whole brain WM DTI measures. T1-weighted images were automatically segmented (Freesurfer Image Analysis Suite v5.0.17, Charlestown, MA, USA) and manually checked for inaccuracies. White matter hyperintensity (WMH) prevalence and volume were derived from Fluid-Attenuated Inversion Recovery images using a semi-automated technique.

Statistical analysis

Statistical analyses were performed using Stata Statistical Software, release 13 (StataCorp LP, College Station, TX, USA). Demographic/clinical characteristics were compared between the two groups using the Mann-Whitney-U test or the ^{2} test, as appropriate. Group differences in RT were assessed by age-, gender- and spherical equivalent-adjusted mixed linear models, taking into account within-subject inter-eye correlations.[6] Group differences in MRI parameters were assessed using linear regression, adjusted for age and gender, and additionally for intracranial volume (ICV) in case of volumetric measurements.

Multivariable linear regression was used to assess associations between OCT (independent) and MRI (dependent) parameters, focusing on the macular regions and layers that differed between the two groups, as shown previously (foveal and pericentral total retina, inner retinal layers, and outer nuclear layer + inner segments [ONL+IS]).[6] Additionally, we explored the peripapillary retinal nerve fiber layer (RNFL), as RT in this area has previously been associated with MRI abnormalities in patients with dementia and multiple sclerosis.[16–18] Prior to analysis, RT values obtained from both eyes were averaged, and DTI values were multiplied by 100 to obtain easier-to-read coefficients. All analyses were corrected for age, gender and SE, and additionally for ICV in case of volumetric outcomes. Correction for OCT scan quality factor (QF) was not applied, as mean QF was high and did not differ significantly between groups (median QF: HIV-infected=85.78; controls=86.37; *P*-value=0.710). Considering the relatively small sample size, we performed only pooled analyses with HIV-status as a covariable to generate more statistical power as compared to stratifying by HIV-status.

We used a two-step analysis approach to evaluate the relationship between OCT and MRI parameters in our cohort. We first evaluated the associations between OCT and MRI parameters separately for HIV-infected and healthy participants, by stratifying only RT between the two groups and adding the two resulting variables (RT of HIV-infected participants and RT of healthy controls) to the basic model described above. In a separate analysis, we assessed whether being HIV-infected exerted a significant influence on the potential association between RT and cerebral injury (i.e., if the predictive value of RT on cerebral injury differed between groups), by including RT and a HIV-RT interaction term in the basic model.

In line with the exploratory nature of this study, adjustment for multiple comparisons was not performed and statistical significance was set at a two-sided *P*-value<.05.

RESULTS

Participant characteristics

The NOVICE cohort consisted of 35 HIV-infected children and 37 healthy controls. Four HIV-infected children did not undergo MRI examination due to dental braces (n=2), claustrophobia (n=1), or lack of consent for the scan (n=1). Two patients (one with a history of cytomegalovirus retinitis in both eyes; one that did not consent to OCT examination) and two controls (one with refractive error > +5.5D; one with fixation problems) were excluded from OCT. In addition, two left eyes of two HIV-infected children were excluded from analysis due to the presence of uveitis and congenital toxoplasmosis lesions, respectively.

Consequently, 29 HIV-infected children (median age 13.1; IQR 11.5-15.8) and 35 healthy controls (median age 12.1; IQR 11.5-15.7) were analyzed. Demographical data, clinical characteristics, and relevant OCT and MRI findings are displayed in **Table 1**. Age, gender, ethnicity and parental employment did not differ significantly between groups. In the HIV-infected group, parental education level was slightly lower and more children were immigrants. Among HIV-infected children, 25 (86%) were on cART at time of study assessment, all of whom had undetectable plasma HIV viral loads. Median $CD4^+$ T-cell count was 800 cells/µl at time of assessment. With OCT, a significantly lower total foveal RT was detected in HIV-infected children, most prominently due to a thinner ONL+IS (median ONL+IS thickness: HIV-infected=107.0µm; controls=111.8µm; *P*-value=.02). On MRI scans, HIV-infected participants had a significantly lower total gray matter (GM) volume, as well as poorer WM integrity, as indicated by higher MD, RD, and AD, and lower FA.

Retinal thickness and white matter diffusivity

Associations between OCT and DTI parameters in HIV-infected and healthy children are described in **Table 2** (and displayed in further detail in **Supplemental Tables 1 and 2**). Multiple correlations were found between RT and DTI parameters in HIV-infected children. A thinner RT (total retina as well as individual layers) was associated with higher MD and RD, and lower FA (**Figure 1**); these findings were more pronounced in the foveal region. No significant correlations were observed between RT and AD in HIV-infected children. In healthy children, a thinner RT (foveal ONL+IS and pericentral total RT) was associated with lower AD (**Supplemental Table 1**). No significant associations were detected between peripapillary RNFL thickness and any DTI parameters for both HIV-positive children and controls.

TABLE 1. Participant characteristics.

Demographic characteristics			HIV-infected (n=29)	Healthy controls (n=35)	*P*-value
Male gender			16 (55)	16 (45)	*.567*
Age at OCT (y)			13.1 (11.5-15.8)	12.1 (11.5-15.7)	*.377*
Ethnicity (black)			22 (76)	24 (69)	*.238*
Immigrant	*child*		19 (66)	2 (6)	***<.001****
	one or both parents		10 (34)	31 (88)	
Socio-economic status	*parental employment*		1 (0-1)	1 (0-1)	*.449*
	parental education (ISCED)		5 (4-6)	5 (5-6)	***.030****
HIV-characteristics		*n*			
Age at HIV-diagnosis (y)		29	1.2 (0.6-4.2)	-	-
CDC stage (n)	N/A	29	9 (31)	-	-
	B		12 (41)	-	-
	C		8 (28)	-	-
HIV-encephalopathy (n)		29	2 (7)	-	-
Nadir $CD4^+$ T-cell Z-score		27	-0.7 (-1.5 - -0.4)	-	-
Peak viral load (log copies/mL)		26	5.5 (5.1-5.9)	-	-
$CD4^+$ T-cell count at study inclusion ($*10^6$/L)		28	800 (590-980)	-	-
Undetectable viral load (n)		29	25 (86)	-	-
Current cART use (n)		29	25 (86)	-	-
Duration of cART use (y)		26	11.3 (7.1-14.7)	-	-
Optical Coherence Tomography					
Macula	Foveal retinal thickness		232.1 (218.1-245.7)	245.2 (228.4-256.3)	***.020****
	Pericentral retinal thickness		315.2 (310.1-327.2)	319.2 (312.6-328.3)	*.171*
	Peripheral retinal thickness		288.2 (270.5-295.6)	286.0 (274.7-292.1)	*.688*
Peripapillary RNFL thickness			107.4 (99.4-122.1)	111.7 (101.8-118.2)	*.760*
Magnetic Resonance Imaging					
T1-weighted	Suitable for assessment		26 (89)	35 (100)	*.051*
	Total gray matter volume (cm^3)		656 (640-708)	706 (627-755)	***.029****
	Total white matter volume (cm^3)		436 (400-442)	439 (424-480)	*.168*
FLAIR	Suitable for assessment		25 (86)	33 (94)	*.270*
	WMH prevalence		16 (64)	6 (18)	***<.001****
	WMH volume† (cm^3)		52.3 (0-124.5)	0 (0-0)	***<.001****
DTI	Suitable for assessment		27 (93)	35 (100)	*.114*
	Fractional anisotropy		0.43 (0.41-0.44)	0.44 (0.42-0.47)	***.026****

TABLE 1. Participant characteristics. (continued)

Demographic characteristics	HIV-infected (n=29)	Healthy controls (n=35)	*P*-value
Mean diffusivity (*10^3)	0.79 (0.77-0.82)	0.77 (0.76-0.79)	***<.001****
Radial diffusivity (*10^3)	0.59 (0.57-0.63)	0.57 (0.54-0.59)	***<.001****
Axial diffusivity (*10^3)	1.19 (1.17-1.21)	1.17 (1.16-1.18)	***<.001****

All data are presented as median (IQR) or n (%). Non-black ethnicity includes creol, hispanic, caucasian and mixed (i.e., black/caucasian, asian/caucasian). Group differences in demographical data were assessed using χ^2 or Fisher's exact tests for categorical data and the Mann-Whitney-U test for continuous data. Group differences in retinal thickness were assessed using linear regression with mixed effects, adjusted for age, gender, and spherical equivalent. Group differences in neuroimaging outcomes were assessed as follows: volumetric measurements using linear regression adjusted for age and gender, and intracranial volume; WMH prevalence using logistic regression adjusted for age and gender; DTI using linear regression adjusted for age and gender.
Abbreviations: OCT: optical coherence tomography; ISCED: international standard classification of education; CDC: Centers for Disease Control and Prevention; HIV: human immunodeficiency virus; cART: combination antiretroviral therapy; mo: months; y: years; RNFL: retinal nerve fiber layer; FLAIR: fluid-attenuated inversion recovery; WMH: white matter hyperintensities; DTI: diffusion tensor imaging.
*: P-value <.05.
† Median and IQR for all participants in each group

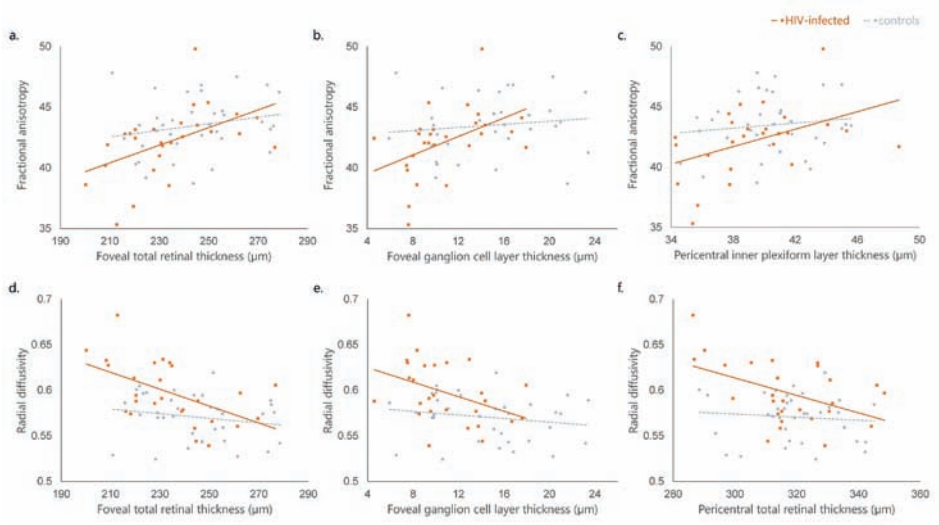

FIGURE 1. Associations between retinal thickness and white matter microstructure in HIV-infected children and healthy controls.
Univariable scatter and linear fit plots illustrating the associations between retinal thickness and fractional anisotropy (a, b, c) and radial diffusivity (d, e, f) in HIV-infected children (solid line), which were absent in healthy controls (dashed line). Furthermore, the associations between retinal thickness in pericentral regions (c, f) and white matter diffusivity were significantly different between the two participant groups (i.e., the interaction between HIV status and pericentral retinal thickness was significantly associated with white matter diffusivity outcomes).

TABLE 2. Associations between retinal thickness and white matter diffusivity.

		Fractional anisotropy		*Mean diffusivity*		*Radial diffusivity*	
FOVEAL LAYERS		coefficient	*P*-value	coefficient	*P*-value	coefficient	*P*-value
Total RT	*HIV-infected*	0.062	***.010****	-0.057	***.004****	-0.079	***.002****
	healthy	0.039	*.073*	-0.018	*.310*	-0.036	*.109*
GCL	*HIV-infected*	0.338	***.012****	-0.211	*.059*	-0.344	***.016****
	healthy	0.127	*.152*	-0.105	*.154*	-0.155	*.101*
IPL	*HIV-infected*	0.299	***.014****	-0.186	*.063*	-0.304	***.018****
	healthy	0.131	*.177*	-0.105	*.196*	-0.156	*.131*
INL	*HIV-infected*	0.431	***.000****	-0.253	***.012****	-0.427	***.001****
	healthy	0.171	*.087*	-0.130	*.133*	-0.198	*.065*
ONL+IS	*HIV-infected*	0.069	*.073*	-0.057	*.075*	-0.085	***.040****
	healthy	0.069	*.131*	0.012	*.758*	-0.030	*.533*
PERICENTRAL LAYERS							
Total RT	*HIV-infected*	0.047	*.110*	-0.066	***.005****	-0.080	***.010****
	healthy	0.033	*.276*	0.019	*.404*	-0.004	*.908*
GCL	*HIV-infected*	0.195	***.029****	-0.200	***.005****	-0.275	***.003****
	healthy	0.061	*.485*	0.073	*.293*	0.020	*.825*
IPL	*HIV-infected*	0.360	***.008****	-0.259	***.020****	-0.400	***.005****
	healthy	0.094	*.499*	0.066	*.564*	-0.004	*.976*
INL	*HIV-infected*	0.156	*.186*	-0.140	*.141*	-0.199	*.111*
	healthy	0.033	*.829*	0.143	*.249*	0.091	*.573*
ONL+IS	*HIV-infected*	-0.019	*.725*	-0.024	*.594*	-0.014	*.809*
	healthy	0.044	*.416*	0.032	*.462*	0.002	*.979*

Results of the pooled regression analysis evaluating the relationship between retinal layer thickness and white matter diffusivity. The regression model included retinal layer thickness, which was stratified between HIV-infected children and controls (as displayed in the table), and covariables HIV-status, age, gender, and spherical equivalent (not shown). Coefficients represent the change in white matter diffusivity outcomes ($x10^{-2}$) per micron increase in RT.

Abbreviations: HIV: human immunodeficiency virus; RT: retinal thickness; GCL: ganglion cell layer; IPL: inner plexiform layer; INL: inner nuclear layer; ONL+IS: outer nuclear layer + inner segments; RNFL: retinal nerve fiber layer.

*: P-value<.05.

The association between RT and WM diffusivity was significantly different between HIV-infected and healthy children (i.e. HIV-RT interaction terms with *P*-values<.05 (**Supplemental Table 2**) for several pericentral layers (total RT, ganglion cell layer [GCL] and inner plexiform layer [IPL] with MD; GCL with RD; total RT with AD), but not for foveal layers.

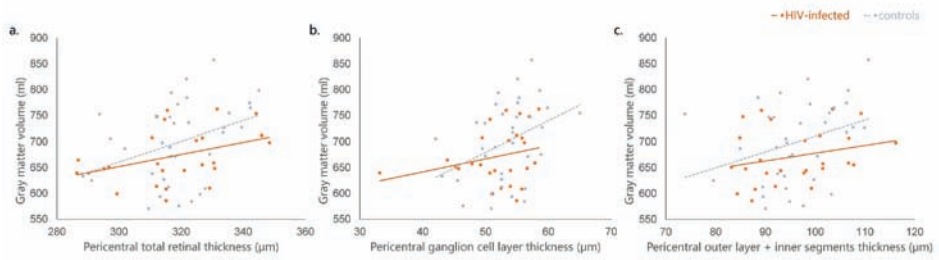

FIGURE 2. Associations between retinal thickness and gray matter volume in HIV-infected children and healthy controls.
Univariable scatter and linear fit plots illustrating the relationships between gray matter volume and retinal thickness in healthy controls (dashed line), which were less pronounced – and not statistically significant – in HIV-infected children (solid line).

Retinal thickness and cerebral volumes

Results of the regression analysis of RT and cerebral volume measurements are summarized in **Table 3** (and displayed in detail in **Supplemental Tables 3 and 4**). In healthy children, positive associations were found between thickness of several foveal and pericentral retinal layers and GM volume (**Figure 2**). Furthermore, foveal GCL thickness was positively correlated with WM volume. However, we found no significant associations between peripapillary RNFL and cerebral volume in either group (**Supplemental Table 3**) or between RT and cerebral volume in the HIV-infected group. The HIV-RT interaction term was not significant for any of the detected associations between RT and cerebral volume (**Supplemental Table 4**).

RT was not associated with WMH volume, although we detected a borderline significant association between thickness of the pericentral ONL+IS and WMH volume (*P*-value=.051).

DISCUSSION

In the current study, we assessed associations between RT and WM integrity and cerebral volume in perinatally HIV-infected children stable on cART, as compared to a group-wise matched healthy control group. Our findings indicate that RT is strongly associated with WM microstructure in HIV-infected children, and correlates with cerebral volume in healthy children. To our knowledge, this is the first study exploring RT as a potential tool to help elucidate the pathogenesis of cerebral injury in HIV, which hampers comparison of our findings to other studies.

TABLE 3. Associations between retinal thickness and cerebral volume

		Gray matter volume		*White matter volume*		*WMH volume (log)*	
FOVEAL LAYERS		coefficient	*P*-value	coefficient	*P*-value	coefficient	*P*-value
Total RT	*HIV-infected*	0.393	*.361*	-0.260	*.471*	0.003	*.827*
	healthy	1.020	***.011****	0.649	*.052*	-0.007	*.485*
GCL	*HIV-infected*	-0.827	*.738*	0.398	*.846*	-0.005	*.934*
	healthy	4.561	***.005****	3.408	***.011****	-0.010	*.818*
IPL	*HIV-infected*	0.221	*.920*	-1.461	*.423*	-0.023	*.674*
	healthy	2.936	*.106*	1.507	*.311*	-0.001	*.985*
INL	*HIV-infected*	1.029	*.656*	-1.833	*.331*	-0.051	*.384*
	healthy	3.950	***.048****	3.053	*.060*	-0.014	*.784*
ONL+IS	*HIV-infected*	0.915	*.192*	-0.307	*.609*	0.026	*.170*
	healthy	1.859	***.024****	0.612	*.378*	-0.020	*.326*
PERICENTRAL LAYERS							
Total RT	*HIV-infected*	0.557	*.257*	0.064	*.879*	0.002	*.856*
	healthy	1.286	***.015****	0.443	*.318*	-0.016	*.257*
GCL	*HIV-infected*	0.174	*.916*	1.240	*.369*	-0.042	*.304*
	healthy	3.620	***.023****	1.857	*.157*	-0.030	*.492*
IPL	*HIV-infected*	0.373	*.881*	1.113	*.591*	-0.091	*.149*
	healthy	3.370	*.200*	0.600	*.781*	-0.077	*.248*
INL	*HIV-infected*	3.160	*.176*	-0.680	*.728*	-0.050	*.403*
	healthy	4.394	*.108*	1.911	*.403*	-0.051	*.467*
ONL+IS	*HIV-infected*	0.982	*.295*	-0.005	*.995*	0.046	*.051*
	healthy	1.819	***.050****	0.533	*.492*	-0.006	*.799*

Results of the pooled regression analysis evaluating the relationship between retinal layer thickness and cerebral volume. The regression model included retinal layer thickness, which was stratified between HIV-infected children and controls (as displayed in the table), and covariables HIV-status, age, gender, spherical equivalent and intracranial volume (not shown). Coefficients represent changes in volume (cm^3) per micron increase in RT.

Abbreviations: WMH: white matter hyperintensities; HIV: human immunodeficiency virus; RT: retinal thickness; GCL: ganglion cell layer; IPL: inner plexiform layer; INL: inner nuclear layer; ONL+IS: outer nuclear layer + inner segments; RNFL: retinal nerve fiber layer.

*: *P*-value<.05.

HIV-infected children had a significantly lower FA, higher RD and higher MD compared to the healthy group, all indicative of reduced WM integrity.[4] In a previous report comparing these same two groups, we described a significant decrease in foveal RT (and to a lesser degree pericentral RT) in the HIV-infected group, mostly caused by thinner neuroretinal layers and ONL+IS.[6] In the current study, the thickness of these retinal layers proved to be strongly associated with DTI outcomes in the HIV-infected group. The directions of associations between RT and WM diffusivity were shown to be consistent

with our hypothesis that retinal structural alterations occur in parallel with cerebral injury, as reflected by lower FA, higher MD, and higher RD.[4]

Our results are suggestive of a shared pathogenesis of observed WM microstructural alterations and retinal thinning, which could include HIV-induced impeded maturation of the retina and WM, and/or persistent neuroinflammation and neurodegeneration.[2] Interestingly, a significant influence of HIV on the relationship between RT and WM diffusivity was only apparent in the pericentral retinal region, but not in the foveal region (as shown in **Supplemental Table 2**). Foveal RT and WM diffusivity were both affected in HIV-infected children. Conversely, pericentral RT did not differ between cases and controls. Despite this, associations between pericentral RT and WM diffusivity were found exclusively in HIV-infected children, who had higher WM diffusivity as compared to controls. This results in a different predictive value of pericentral RT for WM diffusivity in HIV-infected children, as reflected by the significant HIV-RT interaction term. These findings may imply that pericentral RT is affected by HIV infection via similar mechanisms that underlie foveal and WM diffusivity changes, yet to a lesser degree, that does not lead to a detectable group difference.

Significant associations between RT and cerebral volume (in particular GM volume) were detected in healthy children only, implying a physiological relationship between RT and GM volume. This seems plausible, since both retina and GM largely consist of unmyelinated neuronal cells.[7] A previous study also described a correlation between GM volume and inner retinal layer thickness (ganglion cell-inner plexiform layer) in healthy participants without glaucoma or clinical retinal disease, although this was a study assessing neurodegeneration in elderly individuals (with patients over 60 years of age),[18] limiting comparability to our pediatric study population. Nonetheless, currently there are no other studies comparing MRI and OCT in healthy individuals or children.

In HIV-infected children, the relationship between RT and cerebral volume for the most part paralleled that of healthy children, but without reaching statistical significance, even though both RT[6] and cerebral volume[4] were significantly reduced in the HIV-infected children of our cohort. This might indicate that a physiological relationship between RT and cerebral volume – as detected in healthy children – is disturbed in HIV-infected children. However, a difference between HIV-infected children and controls in the association between RT and cerebral volume was only detected for a single retinal layer (as shown in **Supplemental Table 4**), which may partly be caused by lack of statistical power for the associations for the other retinal layers due to the relatively low number of subjects.

The absence of an association between RT and cerebral volume in HIV-infected children contrasts with the presence of multiple associations between RT and WM diffusivity in HIV-infected children. This may suggest a difference in the pathogenesis of the microstructural retinal and WM changes on the one hand, and of macrostructural cerebral volume changes on the other hand. Firstly, this distinction could reflect different timing of the impact of HIV infection on retinal and cerebral structures, i.e., progressive ongoing injury versus stable injury or delayed maturation as residual effects of (unsuppressed) HIV infection early in life. Previously detected associations of cerebral and retinal impairments with historical HIV disease markers, such as lower nadir $CD4^+$ T-cell count, higher peak HIV viral load, and an Acquired Immunodeficiency Syndrome (AIDS) diagnosis, provide substantial support for the relevance of lingering HIV-induced damage in the pathogenesis of all observed changes.[4,6] However, the course of retinal and neurostructural abnormalities over time in the context of potent cART can only be evaluated in a longitudinal setting. There may also be different contributions of underlying HIV-related pathogenic mechanisms, e.g., direct HIV neurotoxicity, chronic HIV-induced neuroinflammation, vascular dysfunction, cerebral perfusion changes, or (long-term) cART toxicity, that can exert different effects on the various cells and systems within the brain, resulting in different types of injury.[2]

Unmeasured factors unrelated to the HIV-infection itself might also have been at play, such as detrimental early life circumstances that may have hindered normal brain development.[19–21] Indeed, early life malnutrition has been linked to cortical atrophy,[20] which may have occurred more frequently among HIV-infected participants, due to a larger proportion of immigrants in that group. Furthermore, we did not have reliable information regarding prematurity of these children, which might have affected both retinal and cerebral development.[22,23]

Despite being the largest and first combined OCT/MRI study in cART-treated HIV-infected children without retinitis to date, using a highly similar control group, this study is subject to several limitations. First, the modest sample size may have limited our power to detect potentially clinically relevant associations. Second, as this was an exploratory study, we did not adjust for multiple comparisons. Nonetheless, we detected a substantial number of significant associations, and the overall pattern and direction of the observed associations between RT and WM diffusivity in HIV-infected children, and RT and GM volume in healthy children, was consistent with our predictions and pathophysiological models, making it unlikely that our findings were spurious. Third, a detailed assessment of specific brain areas might reveal stronger associations with RT than the global MRI measures we currently used. Finally, this cross-sectional study does

not explain the mechanisms underlying the associations observed between retinal and cerebral changes.

To conclude, in this cross-sectional study we observed that RT is correlated with WM microstructural alterations, but not with cerebral volume in perinatally HIV-infected children on cART. These findings support OCT as a non-invasive, rapid and relatively inexpensive adjuvant tool to assess white matter changes in this population, and provide a rationale for conducting longitudinal studies assessing retinal and cerebral changes and relations over time. To explore how different HIV-related pathogenic mechanisms contribute to retinal structural abnormalities and different types of cerebral injury, future studies should assess the relationship of these OCT and MRI outcomes with markers of inflammation, immune activation, vascular endothelial function, and neurodegeneration in cerebrospinal fluid and blood. Furthermore, comparing retinal and cerebral abnormalities between perinatally HIV-infected children and individuals who acquired HIV as adults may further contribute to our understanding of the role of brain maturation, early life exposure to HIV, and lifelong cART in the pathogenesis of pediatric HIV-induced retinal and cerebral injury.

FUNDING

Supported by Bayer Healthcare's Global Ophthalmology Awards Program 2012 and the Emma Foundation (Grant 11.001). These funding bodies had no role in the design or conduct of the study, nor in the analysis or interpretation of the results.

MA's institution received research grants (NIH, NSF, JDRF). PR's institution has received research grants (Gilead Sciences, ViiV Healthcare, Janssen Pharmaceutica, Bristol Myers Squibb, and Merck). DP's institution has received research grants from Emma Foundation, AIDS Fonds, and ViiV Healthcare.

DISCLOSURES

C. Blokhuis, None; N. Demirkaya, None; S. Cohen, None; F.W.N.M. Wit, None; H.J. Scherpbier, None; P. Reiss, None; M.D. Abramoff, IDxLLC (C, S), University of Iowa (F, R) P; M.W.A. Caan, None; C.B.L.M. Majoie, None; F.D. Verbraak, Bayer (C, R), Novartis (C); D. Pajkrt, None.

AUTHORS' CONTRIBUTIONS

CB performed statistical analysis, contributed to data interpretation and co-wrote the manuscript, together with ND. ND contributed to study design, data collection, data interpretation and co-wrote the manuscript with CB. SC contributed to study design and coordination, data collection and revised the manuscript.

FWNMW supervised the statistical analysis, contributed to data interpretation and revised the manuscript. HJS contributed to study design and revised the manuscript. PR contributed to/ supervised study design and revised the manuscript. MDA invented and provided the Iowa Reference Algorithms, contributed to data interpretation and revised the manuscript. MWAC and CBLMM conceptualized the MRI imaging protocol, supervised MRI scanning, and revised the manuscript. FDV and DP contributed to study design and data interpretation and revised the manuscript.

SUPPLEMENTARY TABLE S1: ASSOCIATIONS BETWEEN RETINAL THICKNESS AND WHITE MATTER DIFFUSIVITY IN HIV-INFECTED CHILDREN AND HEALTHY CONTROLS.

		FRACTIONAL ANISOTROPY			MEAN DIFFUSIVITY			RADIAL DIFFUSIVITY			AXIAL DIFFUSIVITY		
		coef	P-value	R^2	coef	P-value	R^2	coef	P-value	R^2	coef	P-value	R^2
FOVEAL TOTAL RT	HIV-infected	0.062	.010		-0.057	.004		-0.079	.002		-0.014	.577	
	controls	0.039	.073		-0.018	.310		-0.036	.109		0.018	.436	
HIV status		-6.633	.382		11.880	.059		12.770	.108		10.110	.231	
				0.350			0.554			0.514			0.316
FOVEAL GCL	HIV-infected	0.338	.012		-0.211	.059		-0.344	.016		0.055	.706	
	controls	0.127	.152		-0.105	.154		-0.155	.101		-0.007	.941	
HIV status		-3.590	.077		3.643	.033		4.674	.031		1.581	.474	
				0.334			0.522			0.480			0.306
FOVEAL IPL	HIV-infected	0.299	.014		-0.186	.063		-0.304	.018		0.050	.696	
	controls	0.131	.177		-0.105	.196		-0.156	.131		-0.003	.979	
HIV status		-5.750	.038		4.644	.054		6.569	.028		0.793	.804	
				0.327			0.517			0.474			0.306
FOVEAL INL	HIV-infected	0.431	.000		-0.253	.012		-0.427	.001		0.094	.474	
	controls	0.171	.087		-0.130	.133		-0.198	.065		0.006	.959	
HIV status		-4.882	.136		4.303	.116		5.859	.093		1.191	.738	
				0.416			0.546			0.532			0.311
FOVEAL ONL+IS	HIV-infected	0.069	.073		-0.057	.075		-0.085	.040		-0.001	.983	
	controls	0.069	.131		0.012	.758		-0.030	.533		0.095	.046	
HIV status		-1.323	.838		10.260	.061		8.835	.206		13.100	.055	
				0.296			0.501			0.443			0.353
PERICENTRAL TOTAL RT	HIV-infected	0.047	.110		-0.066	.005		-0.080	.010		-0.037	.206	
	controls	0.033	.276		0.019	.404		-0.004	.908		0.065	.031	

HIV status		-6.129	.637		29.790	.005		27.300	.045		34.770	.009	
				0.274			0.547			0.464			0.380
PERICENTRAL GCL	HIV-infected	0.195	.029		-0.200	.005		-0.275	.003		-0.050	.576	
	controls	0.061	.485		0.073	.293		0.020	.825		0.178	.051	
HIV status		-8.468	.198		17.010	.002		18.320	.008		14.390	.037	
				0.297			0.549			0.484			0.354
PERICENTRAL IPL	HIV-infected	0.360	.008		-0.259	.020		-0.400	.005		0.022	.877	
	controls	0.094	.499		0.066	.564		-0.004	.976		0.208	.166	
HIV status		-12.070	.120		15.690	.016		18.620	.025		9.816	.237	
				0.325			0.523			0.474			0.329
PERICENTRAL INL	HIV-infected	0.156	.186		-0.140	.141		-0.199	.111		-0.023	.847	
	controls	0.033	.829		0.143	.249		0.091	.573		0.247	.117	
HIV status		-6.354	.396		13.760	.025		14.230	.074		12.810	.095	
				0.250			0.503			0.425			0.335
PERICENTRAL ONL+IS	HIV-infected	-0.019	.725		-0.024	.594		-0.014	.809		-0.043	.430	
	controls	0.044	.416		0.032	.462		0.002	.979		0.093	.084	
HIV status		4.357	.547		8.213	.167		4.614	.550		15.410	.036	
				0.236			0.478			0.395			0.350
PERIPAPILLARY RNFL	HIV-infected	0.041	.192		-0.025	.335		-0.044	.186		0.014	.669	
	controls	-0.005	.916		0.021	.585		0.020	.687		0.023	.637	
HIV status		-6.752	.282		7.883	.127		10.180	.128		3.298	.610	
				0.249			0.482			0.415			0.309

Results of the pooled regression analysis evaluating the relationship between retinal layer thickness and white matter diffusivity. The model included retinal layer thickness, which was stratified between HIV-infected children and controls, and HIV status (as shown), and covariables age, gender, and spherical equivalent (not shown). Retinal thickness coefficients represent the change in white matter diffusivity measure outcome ($x10^2$) per micron increase in retinal thickness. The HIV status coefficient represents the intercept. Abbreviations: HIV: human immunodeficiency virus; RT: retinal thickness; GCL: ganglion cell layer; IPL: inner plexiform layer; INL: inner nuclear layer; ONL+IS: outer nuclear layer + inner segments; RNFL: retinal nerve fiber layer. *: P-value<.05.

SUPPLEMENTARY TABLE S2: THE INFLUENCE OF HIV STATUS ON ASSOCIATIONS BETWEEN RETINAL THICKNESS AND WHITE MATTER DIFFUSIVITY.

	FRACTIONAL ANISOTROPY			MEAN DIFFUSIVITY			RADIAL DIFFUSIVITY			AXIAL DIFFUSIVITY		
	coef	P-value	R^2	coef	P-value	R^2	coef	P-value	R^2	coef	P-value	R^2
FOVEAL												
TOTAL RT	0.039	.073		-0.018	.310		-0.036	.109		0.018	.436	
HIV status	-6.633	.382		11.880	.059		12.770	.108		10.110	.231	
HIV-RT interaction	0.023	.472		-0.040	.130		-0.043	.195		-0.033	.352	
			0.350			0.554			0.514			0.316
FOVEAL												
GCL	0.127	.152		-0.105	.154		-0.155	.101		-0.007	.941	
HIV status	-3.590	.077		3.643	.033		4.674	.031		1.581	.474	
HIV-RT interaction	0.211	.189		-0.106	.430		-0.189	.267		0.062	.726	
			0.334			0.522			0.480			0.306
FOVEAL												
IPL	0.131	.177		-0.105	.196		-0.156	.131		-0.003	.979	
HIV status	-5.750	.038		4.644	.054		6.569	.028		0.793	.804	
HIV-RT interaction	0.167	.274		-0.081	.526		-0.148	.362		0.053	.750	
			0.327			0.517			0.474			0.306
FOVEAL												
INL	0.171	.087		-0.130	.133		-0.198	.065		0.006	.959	
HIV status	-4.882	.136		4.303	.116		5.859	.093		1.191	.738	
HIV-RT interaction	0.261	.086		-0.123	.346		-0.229	.158		0.088	.614	
			0.416			0.546			0.532			0.311
FOVEAL												
ONL+IS	0.069	.131		0.012	.758		-0.030	.533		0.095	.046	
HIV status	-1.323	.838		10.260	.061		8.835	.206		13.100	.055	

SUPPLEMENTARY TABLE S2: THE INFLUENCE OF HIV STATUS ON ASSOCIATIONS BETWEEN RETINAL THICKNESS AND WHITE MATTER DIFFUSIVITY. (continued)

	FRACTIONAL ANISOTROPY			MEAN DIFFUSIVITY			RADIAL DIFFUSIVITY			AXIAL DIFFUSIVITY		
	coef	P-value	R^2	coef	P-value	R^2	coef	P-value	R^2	coef	P-value	R^2
HIV-RT interaction	0.000	.999		-0.069	.161		-0.055	.380		-0.096	.116	
			0.296			0.501			0.443			0.353
P ERICENTRAL												
TOTAL RT	0.033	.276		0.019	.404		-0.004	.908		0.065	.031	
HIV status	-6.129	.637		29.790	.005		27.300	.045		34.770	.009	
HIV-RT interaction	0.014	.724		-0.085	.009		-0.077	.073		-0.102	.015	
			0.274			0.547			0.464			0.380
P ERICENTRAL												
GCL	0.061	.485		0.073	.293		0.020	.825		0.178	.051	
HIV status	-8.468	.198		17.010	.002		18.320	.008		14.390	.037	
HIV-RT interaction	0.134	.282		-0.273	.007		-0.295	.024		-0.229	.079	
			0.297			0.549			0.484			0.354
P ERICENTRAL												
IPL	0.094	.499		0.066	.564		-0.004	.976		0.208	.166	
HIV status	-12.070	.120		15.690	.016		18.620	.025		9.816	.237	
HIV-RT interaction	0.267	.168		-0.325	.045		-0.395	.056		-0.186	.369	
			0.325			0.523			0.474			0.329
P ERICENTRAL												
INL	0.033	.829		0.143	.249		0.091	.573		0.247	.117	
HIV status	-6.354	.396		13.760	.025		14.230	.074		12.810	.095	
HIV-RT interaction	0.123	.522		-0.283	.070		-0.290	.155		-0.270	.170	
			0.250			0.503			0.425			0.335
P ERICENTRAL												

SUPPLEMENTARY TABLE S2: THE INFLUENCE OF HIV STATUS ON ASSOCIATIONS BETWEEN RETINAL THICKNESS AND WHITE MATTER DIFFUSIVITY. (continued)

	FRACTIONAL ANISOTROPY			MEAN DIFFUSIVITY			RADIAL DIFFUSIVITY			AXIAL DIFFUSIVITY		
	coef	P-value	R^2	coef	P-value	R^2	coef	P-value	R^2	coef	P-value	R^2
ONL+IS	0.044	.416		0.032	.462		0.002	.979		0.093	.084	
HIV status	4.357	.547		8.213	.167		4.614	.550		15.410	.036	
HIV-RT interaction	-0.063	.402		-0.056	.361		-0.016	.844		-0.136	.072	
			0.236			0.478			0.395			0.350
P ERIPAPILLARY												
RNFL	-0.005	.916		0.021	.585		0.020	.687		0.023	.637	
HIV status	-6.752	.282		7.883	.127		10.180	.128		3.298	.610	
HIV-RT interaction	0.046	.416		-0.045	.323		-0.064	.285		-0.009	.875	
			0.249			0.482			0.415			0.309

Results of the pooled regression analysis evaluating the influence of HIV status on the relationship between retinal layer thickness and white matter diffusivity. The model included retinal thickness, HIV status, and the interaction between these two variables (as shown), and covariables age, gender, and spherical equivalent (not shown). Retinal thickness coefficients represent the change in white matter diffusivity outcome ($x10^2$) per micron increase in retinal thickness. The HIV status coefficient represents the intercept. The interaction term between HIV status and retinal thickness shows whether associations between retinal thickness and white matter diffusivity outcomes in HIV-infected children are different from those in controls. Abbreviations: HIV: human immunodeficiency virus; RT: retinal thickness; GCL: ganglion cell layer; IPL: inner plexiform layer; INL: inner nuclear layer; ONL+IS: outer nuclear layer + inner segments; RNFL: retinal nerve fiber layer. *: P-value<.05.

SUPPLEMENTARY TABLE S3: ASSOCIATIONS BETWEEN RETINAL THICKNESS AND CEREBRAL VOLUMES IN HIV-INFECTED CHILDREN AND HEALTHY CONTROLS.

		FRACTIONAL ANISOTROPY			MEAN DIFFUSIVITY			RADIAL DIFFUSIVITY		
		coef	P-value	R^2	coef	P-value	R^2	coef	P-value	R^2
FOVEAL TOTAL RT	HIV-infected	0.393	.361		-0.260	.471		0.003	.827	
	controls	1.020	.011		0.649	.052		-0.007	.485	
HIV status		119.900	.388		203.100	.085		-1.443	.707	
				0.686			0.612			0.235
FOVEAL GCL	HIV-infected	-0.827	.738		0.398	.846		-0.005	.934	
	controls	4.561	.005		3.408	.011		-0.010	.818	
HIV status		36.810	.318		27.750	.363		0.898	.384	
				0.690			0.627			0.228
FOVEAL IPL	HIV-infected	0.221	.920		-1.461	.423		-0.023	.674	
	controls	2.936	.106		1.507	.311		-0.001	.985	
HIV status		23.330	.701		47.010	.351		1.440	.355	
				0.657			0.592			0.230
FOVEAL										
INL	HIV-infected	1.029	.656		-1.833	.331		-0.051	.384	
	controls	3.950	.048		3.053	.060		-0.014	.784	
HIV status		20.830	.703		73.400	.103		1.587	.267	
				0.666			0.613			0.240
FOVEAL ONL+IS	HIV-infected	0.915	.192		-0.307	.609		0.026	.170	
	controls	1.859	.024		0.612	.378		-0.020	.326	
HIV status		74.370	.523		86.130	.391		-4.076	.182	
				0.681			0.587			0.271
PERICENTRAL TOTAL RT	HIV-infected	0.557	.257		0.064	.879		0.002	.856	
	controls	1.286	.015		0.443	.318		-0.016	.257	

SUPPLEMENTARY TABLE S3: ASSOCIATIONS BETWEEN RETINAL THICKNESS AND CEREBRAL VOLUMES IN HIV-INFECTED CHILDREN AND HEALTHY CONTROLS. (continued)

		FRACTIONAL ANISOTROPY			MEAN DIFFUSIVITY			RADIAL DIFFUSIVITY		
		coef	P-value	R^2	coef	P-value	R^2	coef	P-value	R^2
HIV status		199.200	.370		105.700	.581		-4.960	.414	
				0.684			0.587			0.247
PERICENTRAL GCL	HIV-infected	0.174	.916		1.240	.369		-0.042	.304	
	controls	3.620	.023		1.857	.157		-0.030	.492	
HIV status		147.900	.220		19.290	.847		1.548	.627	
				0.673			0.601			0.251
PERICENTRAL IPL	HIV-infected	0.373	.881		1.113	.591		-0.091	.149	
	controls	3.370	.200		0.600	.781		-0.077	.248	
HIV status		84.640	.560		-35.410	.768		1.474	.688	
				0.651			0.582			0.278
PERICENTRAL INL	HIV-infected	3.160	.176		-0.680	.728		-0.050	.403	
	controls	4.394	.108		1.911	.403		-0.051	.467	
HIV status		14.840	.913		84.700	.459		0.885	.801	
				0.667			0.586			0.245
PERICENTRAL ONL+IS	HIV-infected	0.982	.295		-0.005	.995		0.046	.051	
	controls	1.819	.050		0.533	.492		-0.006	.799	
HIV status		45.990	.710		36.390	.730		-3.904	.200	
				0.671			0.583			0.286
PERIPAPILLARY RNFL	HIV-infected	-0.007	.991		-0.058	.902		0.003	.844	
	controls	-0.135	.872		1.257	.063		-0.007	.716	
HIV status		-50.770	.659		130.900	.153		-0.187	.948	
				0.640			0.606			0.230

of the pooled regression analysis evaluating the relationship between retinal layer thickness and measures of cerebral volume. The model included retinal layer thickness, which was stratified between HIV-infected children and controls, and HIV status (as shown), and covariables age, gender, spherical equivalent and intracranial volume (not shown). Coefficients represent changes in volume (cm3) per micron increase in retinal thickness. The HIV status coefficient represents the intercept. Abbreviations: WMH: white matter hyperintensities; HIV: human immunodeficiency virus; RT: retinal thickness; GCL: ganglion cell layer; IPL: inner plexiform layer; INL: inner nuclear layer; ONL+IS: outer nuclear layer + inner segments; RNFL: retinal nerve fiber layer. *: P-value<.05.

SUPPLEMENTARY TABLE S4: THE INFLUENCE OF HIV STATUS ON ASSOCIATIONS BETWEEN RETINAL THICKNESS AND CEREBRAL VOLUMES.

	GREY MATTER VOLUME			WHITE MATTER VOLU ME			WMH VOLIME (LOG)		
	coef	P-value	R^2	coef	P-value	R^2	coef	P-value	R^2
FOVEAL									
TOTAL RT	1.020	.011		0.649	.052		-0.007	.485	
HIV status	-0.627	.282		-0.909	.066		0.010	.532	
HIV-RT interaction	119.900	.388		203.100	.085		-1.443	.707	
			0.686			0.612			0.235
FOVEAL									
GCL	4.561	.005		3.408	.011		-0.010	.818	
HIV status	-5.387	.070		-3.010	.217		0.005	.955	
HIV-RT interaction	36.810	.318		27.750	.363		0.898	.384	
			0.690			0.627			0.228
FOVEAL									
IPL	2.936	.106		1.507	.311		-0.001	.985	
HIV status	-2.716	.342		-2.968	.209		-0.022	.754	
HIV-RT interaction	23.330	.701		47.010	.351		1.440	.355	
			0.657			0.592			0.230
FOVEAL									
INL	3.950	.048		3.053	.060		-0.014	.784	
HIV status	-2.921	.331		-4.886	.049		-0.037	.634	
HIV-RT interaction	20.830	.703		73.400	.103		1.587	.267	
			0.666			0.613			0.240
FOVEAL									
ONL+IS	1.859	.024		0.612	.378		-0.020	.326	
HIV status	-0.944	.370		-0.919	.311		0.046	.096	

SUPPLEMENTARY TABLE S4: THE INFLUENCE OF HIV STATUS ON ASSOCIATIONS BETWEEN RETINAL THICKNESS AND CEREBRAL VOLUMES. (continued)

	GREY MATTER VOLUME			WHITE MATTER VOLU ME			WMH VOLIME (LOG)		
	coef	P-value	R^2	coef	P-value	R^2	coef	P-value	R^2
HIV-RT interaction	74.370	.523		86.130	.391		-4.076	.182	
			0.681			0.587			0.271
PERICENTRAL									
TOTAL RT	1.286	.015		0.443	.318		-0.016	.257	
HIV status	-0.729	.296		-0.379	.529		0.019	.331	
HIV-RT interaction	199.200	.370		105.700	.581		-4.960	.414	
			0.684			0.587			0.247
PERICENTRAL									
GCL	3.620	.023		1.857	.157		-0.030	.492	
HIV status	-3.446	.133		-0.617	.745		-0.012	.836	
HIV-RT interaction	147.900	.220		19.290	.847		1.548	.627	
			0.673			0.601			0.251
PERICENTRAL IPL	3.370	.200		0.600	.781		-0.077	.248	
HIV status	-2.997	.410		0.513	.864		-0.014	.877	
HIV-RT interaction	84.640	.560		-35.410	.768		1.474	.688	
			0.651			0.582			0.278
PERICENTRAL									
INL	4.394	.108		1.911	.403		-0.051	.467	
HIV status	-1.234	.724		-2.591	.380		0.001	.988	
HIV-RT interaction	14.840	.913		84.700	.459		0.885	.801	
			0.667			0.586			0.245
PERICENTRAL									
ONL+IS	1.819	.050		0.533	.492		-0.006	.799	

SUPPLEMENTARY TABLE S4: THE INFLUENCE OF HIV STATUS ON ASSOCIATIONS BETWEEN RETINAL THICKNESS AND CEREBRAL VOLUMES. (continued)

	GREY MATTER VOLUME			WHITE MATTER VOLU ME			WMH VOLIME (LOG)		
	coef	P-value	R^2	coef	P-value	R^2	coef	P-value	R^2
HIV status	-0.837	.515		-0.538	.622		0.051	.106	
HIV-RT interaction	45.990	.710		36.390	.730		-3.904	.200	
			0.671			0.583			0.286
PERIPAPILLARY									
RNFL	-0.135	.872		1.257	.063		-0.007	.716	
HIV status	0.128	.900		-1.315	.108		0.011	.681	
HIV-RT interaction	-50.770	.659		130.900	.153		-0.187	.948	
			0.640			0.606			0.230

Results of the pooled regression analysis evaluating the influence of HIV status on relationship between retinal layer thickness and cerebral volume. The model included retinal thickness, HIV status, and the interaction between these two variables (as shown), and covariables age, gender, spherical equivalent and intracranial volume (not shown). Coefficients represent changes in volume (cm3) per micron increase in retinal thickness. The HIV status coefficient represents the intercept. The interaction term between HIV status and retinal thickness shows whether associations between retinal thickness and cerebral volume in HIV-infected children are different from those in controls. Abbreviations: WMH: white matter hyperintensities; HIV: human immunodeficiency virus; RT: retinal thickness; GCL: ganglion cell layer; IPL: inner plexiform layer; INL: inner nuclear layer; ONL+IS: outer nuclear layer + inner segments; RNFL: retinal nerve fiber layer. *: P-value

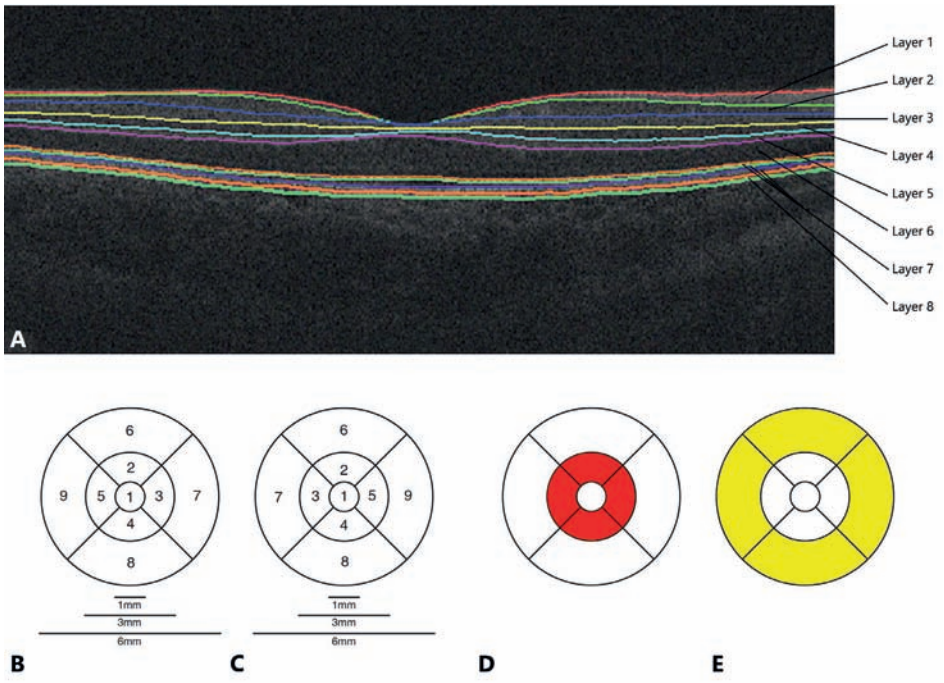

SUPPLEMENTARY FIGURE 1: OPTICAL COHERENCE TOMOGRAPHY

A. Macular SD-OCT B-scan with intraretinal surfaces as indicated by the colored lines and segmented using the Iowa Reference Algorithm.[12,13] In this study, the highly reflective layer between inner and outer segments, and the outer segments up to the retinal pigment layer were taken together as one layer, the outer segment layer (OSL), ignoring the line ascribed to the cone outer segments. Corresponding retinal layers: 1: retinal nerve fiber layer; 2: ganglion cell layer; 3: inner plexiform layer; 4: inner nuclear layer; 5: outer plexiform layer; 6: outer nuclear layer + inner segments (photoreceptors); 7: outer segments (photoreceptors); 8: retinal pigment epithelium. **B-E**. Early Treatment of Diabetic Retinopathy Study (ETDRS)-grid. Nine subfields of the ETDRS regions in each eye. (**B**) Right eye. (**C**) Left eye. For each retinal layer, three areas were defined using this ETDRS grid: the fovea, the central circle with a diameter of 1mm (depicted as 1 in **B-C**); the pericentral ring, a donut-shaped ring centered on the fovea with an inner diameter of 1mm and an outer diameter of 3mm (**D**); and the peripheral ring, with an inner diameter of 3 mm and outer diameter of 6mm (**E**). Thickness measurements of the pericentral and peripheral rings were estimated by averaging the thickness measurements of the four corresponding quadrant areas (segments 2 to 5 for the pericentral ring and segments 6 to 9 for the peripheral ring).

REFERENCES

1. Patel K, Ming X, Williams PL, Robertson KR, Oleske JM, Seage GR. Impact of HAART and CNS-penetrating antiretroviral regimens on HIV encephalopathy among perinatally infected children and adolescents. *AIDS*. 2009;23(14):1893-1901.
2. Blokhuis C, Kootstra NA, Caan MW, Pajkrt D. Neurodevelopmental delay in pediatric HIV/AIDS: current perspectives. *Neurobehav HIV Med*. 2016;7(1):1-13.
3. Hoare J, Ransford GL, Phillips N, Amos T, Donald K, Stein DJ. Systematic review of neuroimaging studies in vertically transmitted HIV positive children and adolescents. *Metab Brain Dis*. 2014;29(2):221-229.
4. Cohen S, Caan MWA, Mutsaerts HJ, et al. Cerebral injury in perinatally HIV-infected children compared to matched healthy controls. *Neurology*. 2016;86(1):19-27.
5. Cohen S, Stege JA, Geurtsen GJ, et al. Poorer Cognitive Performance in Perinatally HIV-Infected Children Versus Healthy Socioeconomically Matched Controls. *Clin Infect Dis*. 2015;60(7):1111-1119.
6. Demirkaya N, Cohen S, Wit FWNM, et al. Retinal Structure and Function in Perinatally HIV-Infected and cART-Treated Children: A Matched Case-Control Study. *Invest Ophthalmol Vis Sci*. 2015;56(6):3945-3954.
7. London A, Benhar I, Schwartz M. The retina as a window to the brain-from eye research to CNS disorders. *Nat Rev Neurol*. 2013;9(1):44-53.
8. Balk LJ, Petzold A. Current and future potential of retinal optical coherence tomography in multiple sclerosis with and without optic neuritis. *Neurodegener Dis Manag*. 2014;4(2014):165-176.
9. Ikram MK, Cheung CY, Wong TY, Chen CPLH. Retinal pathology as biomarker for cognitive impairment and Alzheimer's disease. *J Neurol Neurosurg Psychiatry*. 2012;83(9):917-922.
10. Sari ES, Koc R, Yazici A, Sahin G, Ermis SS. Ganglion Cell-Inner Plexiform Layer Thickness in Patients With Parkinson Disease and Association With Disease Severity and Duration. *J Neuroophthalmol*. 2014;(6).
11. Schönfeldt-Lecuona C, Kregel T, Schmidt A, et al. From Imaging the Brain to Imaging the Retina: Optical Coherence Tomography (OCT) in Schizophrenia. *Schizophr Bull*. 2016;42(1):9-14.
12. Garvin MK, Abramoff MD, Kardon R, Russell SR, Wu X, Sonka M. Intraretinal layer segmentation of macular optical coherence tomography images using optimal 3-D graph search. *IEEE Trans Med Imaging*. 2008;27(10):1495-1505.
13. Garvin MK, Abràmoff MD, Wu X, Russell SR, Burns TL, Sonka M. Automated 3-D intraretinal layer segmentation of macular spectral-domain optical coherence tomography images. *IEEE Trans Med Imaging*. 2009;28(9):1436-1447.
14. Demirkaya N, van Dijk HW, van Schuppen SM, et al. Effect of age on individual retinal layer thickness in normal eyes as measured with spectral-domain optical coherence tomography. *Invest Ophthalmol Vis Sci*. 2013;54(7):4934-4940.
15. van Dijk HW, Verbraak FD, Kok PHB, et al. Decreased retinal ganglion cell layer thickness in patients with type 1 diabetes. *Invest Ophthalmol Vis Sci*. 2010;51(7):3660-3665.
16. Gordon-Lipkin E, Chodkowski B, Reich DS, et al. Retinal nerve fiber layer is associated with brain atrophy in multiple sclerosis. *Neurology*. 2007;69(16):1603-9.
17. Grazioli E, Zivadinov R, Weinstock-Guttman B, et al. Retinal nerve fiber layer thickness is associated with brain MRI outcomes in multiple sclerosis. *J Neurol Sci*. 2008;268(1-2):12-17.

18. Ong Y-T, Hilal S, Cheung CY, et al. Retinal neurodegeneration on optical coherence tomography and cerebral atrophy. *Neurosci Lett.* 2015;584:12-16.
19. Behnke M, Smith VC. Prenatal Substance Abuse: Short- and Long-term Effects on the Exposed Fetus. *Pediatrics.* 2013;131(3):e1009-e1024.
20. Potchen MJ, Kampondeni SD, Mallewa M, Taylor TE, Birbeck GL. Brain imaging in normal kids: a community-based MRI study in Malawian children. *Trop Med Int Health.* 2013;18(4):398-402.
21. van Harmelen AL, van Tol M, van der Wee NJA, et al. Reduced medial prefrontal cortex volume in adults reporting childhood emotional maltreatment. *Biol Psychiatry.* 2010;68(9):832-838.
22. Nosarti C, Nam KW, Walshe M, et al. Preterm birth and structural brain alterations in early adulthood. *NeuroImage Clin.* 2014;6:180-191.
23. Vajzovic L, Rothman AL, Tran-Viet D, Cabrera MT, Freedman SF, Toth CA. Delay in retinal photoreceptor development in very preterm compared to term infants. *Invest Ophthalmol Vis Sci.* 2015;56(2):908-913.

CHAPTER 8 General discussion and summary

Subtle structural and functional retinal abnormalities, termed 'HIV-associated Neuroretinal Disorder (HIV-NRD)', have been reported in HIV patients receiving combination antiretroviral therapy (cART) and without a history of infectious retinitis or any apparent fundus abnormalities otherwise. As reviewed in **Chapter 2**, most studies assessing HIV-NRD in the cART era focused predominantly on patients with (prior) severe immunedeficiency; e.g. with nadir CD4 counts <100 cells/µl and/or a clinical AIDS diagnosis.[1]

There is a lack of literature on the prevalence and risk factors of HIV-NRD in HIV patients with higher nadir CD4 counts (> 350 cells/µl) and well-suppressed HIV-infection, who constitute a growing part of the (Western) HIV-infected population as current HIV treatment guidelines strongly emphasize the importance of diagnosing HIV-infection as early as possible and quickly initiating cART irrespective of the CD4 cell count.[2]

The main aims of this thesis were to assess whether HIV-infected patients receiving long-term cART with systemically well-controlled infection (both adults and children), remain at risk for retinal neurodegeneration/HIV-neuroretinal disorder (HIV-NRD), assessed with retinal structural and functional tests, and to determine the value of retinal thickness (measured with SD-OCT) as a potential biomarker for (micro)structural brain abnormalities in HIV-infected patients. We summarize and review the key findings in this chapter.

ASSOCIATIONS BETWEEN AGE AND RETINAL LAYER THICKNESS

When studying changes in retinal thickness, it is essential to distinguish disease processes from physiological age-related changes. In **Chapter 3** we explored associations of age with the thickness of individual retinal layers, as measured with the use of automated segmentation of SD-OCT images, in a population of 120 healthy individuals.[3] Our results indicate that the thickness of the peripapillary RNFL, pericentral GCL, peripheral IPL and foveal OSL decrease significantly and that foveal RPE thickness increases significantly with increasing age. These findings should be taken into account while interpreting retinal layer and RNFL thickness variation in studies evaluating the effects of disease on the retina.

NEURORETINAL CHANGES IN HIV-INFECTED ADULTS

HIV-infected adults with prolonged suppressed viremia are NOT at risk for neuroretinal loss

In **Chapter 4** we assessed the prevalence and possible risk factors of retinal functional and structural loss by means of contrast sensitivity and retinal layer thickness measurements, comparing a group of HIV-infected men (n=92) with prolonged suppressed viremia on cART with a group of HIV-uninfected men (n=63), all aged 45 years or above and participating in the AGE_hIV neuroretinal substudy[4] (the AGE_hIV study population is described further in **Chapter 1**).

Pelli Robson (PR) contrast sensitivity was significantly reduced in HIV-infected patients (1.89 vs 1.93 logCS, P-value: 0.001), although the loss corresponded to only one letter and was likely not clinically relevant. In addition, only one (1.3%) patient had an abnormal Pelli Robson score of 1.5 (cut-off value used by several previous studies to define HIV-NRD). Surprisingly, instead of an expected neuroretinal *thinning*, we observed a slightly *increased* retinal thickness in the HIV-infected group (+4.6 µm, P-value: 0.029), predominantly due to an increase in the thickness of the inner nuclear layer (+1.04 µm, P-value: 0.006) and outer plexiform layer (+0.95 µm, P-value: 0.006). A similar increase in INL and OPL thickness has also been described by studies assessing retinal layer thickness in multiple sclerosis,[5,6] a disease characterized by neuro-inflammation and- degeneration, processes both believed to occur in HIV-associated neurocognitive and-retinal changes as well. The authors of these studies speculated that these changes might reflect low grade inflammatory activity, which could perhaps also be relevant in the HIV-infected population. However, we did not find any associations between systemic markers of inflammation and immune activation and retinal layer thickness in the examined HIV-infected population (**Chapter 4**). At present we do not have access to such markers in the cerebrospinal fluid.

Applying multivariable regression analysis, we did not find any associations between indicators of (past) HIV disease severity (nadir or current CD4 counts, prior AIDS diagnosis or pre-ART plasma VL) and any of the visual function/OCT parameters tested. In summary, our results provide little evidence for neuroretinal loss in individuals with well-suppressed HIV-infection. Only a statistical, but not clinically relevant, decrease in Pelli Robson contrast sensitivity was detected, and a complete absence of significant neuroretinal thinning. Surprisingly, if anything a slight increase in RT was measured.[4]

Retinal thickness a potential biomarker to assess brain alterations in HIV-infection?

In addition to retinal (micro)structural alterations, subtle brain alterations have been reported in patients with well-suppressed HIV-infection.[7,8] We hypothesized that these abnormalities may have a shared pathophysiology, as neuroretinal tissue can be considered to be an extension of the brain. In recent years, combined OCT/MRI studies have explored retinal thickness (RT) as a potential proxy for brain dysfunction in several neurodegenerative conditions,[9] but similar comparative imaging studies on HIV-related neuroretinal degeneration were thus far lacking. In **Chapter 5** we demonstrate that RT, and in particular thickness of inner retinal layers, is associated with WM microstructure (measured with DTI), as well as cerebral volume in *both* HIV-infected patients and HIV-uninfected controls (*manuscript in preparation*), providing no support for our hypothesis that OCT might be a useful biomarker to monitor HIV-related neurodegeneration. Our results are in line with a recent report of the *Rotterdam Study* showing that thinner RNFL, GCL and IPL (assessed with a similar Topcon OCT device and the same *Iowa Reference Algorithms* as applied in our study) were associated with smaller gray- and white-matter volume, as well as disturbed white matter microstructure, in a population of 2124 elderly participants (mean age 67.0 years).[10] The underlying pathophysiology of these correlations remains unclear, and several explanatory mechanisms have been proposed: inner retinal thinning might reflect degradation of brain structure in normal aging, simultaneous retinal and cerebral neuronal loss might be caused by a common neurodegenerative process, or on the other hand, damage to the retina might correlate with cerebral damage or vice versa (e.g. retrograde versus anterograde neurodegeneration). In our study, the detected correlations were quite parallel between the HIV-infected and –uninfected group ; i.e. HIV-status did not influence the associations between MRI and OCT parameters (as reflected by non-significant HIV-RT interaction terms), suggesting that potential physiological retina-brain relationships are not disrupted in patients with well-controlled HIV-infection.

NEURORETINAL CHANGES IN HIV-INFECTED CHILDREN

A decrease in foveal thickness is associated with a higher peak viral load

In **Chapter 6** we explored the potential (neuro)retinal functional and structural differences between a group of 33 perinatally HIV-infected children on cART and 36 age, gender, ethnicity and socioeconomically-matched healthy controls (NOVICE study cohort; **Chapter 1**).[11] No significant differences in color vision (Lanthony D-15 test) and central visual field (Rarebit Perimetry) were detected between both groups. Contrast

sensitivity (Mars charts) was significantly lower in the HIV-infected children, although the difference was only half a letter (1.74 vs 1.76 logCS, *P*-value=0.006).

Interestingly, HIV-infected children had a significantly thinner total foveal thickness (= central subfield ETDRS grid) (-11.2 µm, *P*-value=0.012), predominantly due to thinner foveal outer nuclear layer and inner segments (ONL-IS; -6.2 µm, *P*-value=0.011). Multivariable mixed regression analysis showed an inverse association between total foveal retinal thickness and peak HIV VL (-10.7 µm per $\log_{10}$ copy/ml, *P*-value=0.016); a similar relationship was observed between the foveal outer nuclear layer and inner segments and peak HIV VL (-7.1 µm per log copy/ml, *P*-value=0.013).[11] We postulated that perinatal HIV-infection may disturb foveal maturation, mostly reflected in the outer nuclear layer, which of all foveal layers shows the most distinct increase during foveal maturation.[12] The clinical significance of this decrease in foveal thickness is yet unclear; since both visual acuity and visual function were adequate in HIV-infected children.

Retinal thickness is associated with microstructural white matter injury in HIV-infected children

Subsequently, in **Chapter 6** we assessed associations between RT and WM integrity and cerebral volume in (nearly) the same group of HIV-infected children (n=29) and matched controls (n=35).[13] Our findings indicate that RT is strongly associated with WM microstructure in HIV-infected children, and correlates with cerebral volume in healthy children. HIV-infected children had a significantly lower FA, higher RD and higher MD compared to the healthy group, all indicative of reduced WM integrity. We also observed a significant decrease in foveal RT in the HIV-infected group, mostly caused by thinner ONL+IS (and to a lesser degree inner retinal layers).[11] The thickness of these retinal layers proved to be strongly associated with DTI outcomes in the HIV-infected group. The directions of associations between RT and WM diffusivity were shown to be consistent with our hypothesis that retinal structural alterations occur in parallel with cerebral injury, as reflected by lower FA, higher MD, and higher RD.

Significant associations between RT and cerebral volume (in particular GM volume) were detected in healthy children only. In HIV-infected children, the relationship between RT and cerebral volume for the most part paralleled that of healthy children, but without reaching statistical significance, even though both RT and cerebral volume were significantly reduced in the HIV-infected children of our cohort. This might indicate that a physiological relationship between RT and cerebral volume – as detected in healthy children – is disturbed in HIV-infected children. The absence of an association between RT and cerebral volume in HIV-infected children contrasts with the presence of multiple associations between RT and WM diffusivity in HIV-infected children. This may suggest

a difference in the pathogenesis of the microstructural retinal and WM changes on the one hand, and of macrostructural cerebral volume changes on the other hand. There may be different contributions of underlying HIV-related pathogenic mechanisms, e.g. direct HIV neurotoxicity, chronic HIV-induced neuro-inflammation, cerebral perfusion changes or long-term cART toxicity, that can exert different effects on the various cells and systems within the brain, resulting in different types of injury.[14]

The discrepancy in findings between HIV-infected adults and perinatally HIV-infected children that we report in this thesis may be explained by several factors, in particular time of infection. As children are still in development, (unsuppressed) HIV-infection in their early years may disrupt or delay retinal and/or cerebral maturation. Previously detected associations of cerebral and retinal impairments in the NOVICE patients with historical HIV disease markers, such as lower nadir $CD4^+$ T-cell count, higher peak HIV viral load, and an Acquired Immunodeficiency Syndrome (AIDS) diagnosis, provide substantial support for the relevance of lingering HIV-induced damage in the pathogenesis of all observed changes in the NOVICE patients.[11,15] Unmeasured factors unrelated to the HIV-infection itself might also have been at play, such as detrimental early life circumstances that may have hindered normal brain, and eye development.[16-18] Indeed, early life malnutrition has been linked to cortical atrophy,[17] which may have occurred more frequently among the HIV-infected children in the NOVICE cohort, due to a larger proportion of immigrants in that group. Furthermore, we did not have reliable information regarding prematurity of these children, which might have affected both retinal and cerebral development.[12,19]

In conclusion, it is difficult to extrapolate the findings in HIV-infected children to adults and vice versa. To explore how different HIV-related pathogenic mechanisms contribute to retinal structural abnormalities and different types of cerebral injury, future longitudinal studies should assess the relationship of these OCT and MRI outcomes with markers of inflammation, immune activation, vascular endothelial function, and neurodegeneration in cerebrospinal fluid and blood. A subsequent analysis of the *NOVICE* pediatric HIV cohort data revealed significant associations between neuroretinal thinning and inflammatory and neuronal injury biomarkers[20]; the presence/absence of similar potential associations in the *AGE_hIV* cohort will be explored in a future study.

CONCLUDING REMARKS

The findings in this thesis suggest that HIV-infected adult patients with prolonged well-suppressed viremia on cART are not at risk for developing HIV-neuroretinal disorder (e.g. neuroretinal loss)[4] and that physiological retina-brain correlations are not disrupted in this group.

The clinical significance of a thinner fovea in perinatally HIV-infected children is as yet unclear, as these children displayed a normal vision.[11] While our findings indicate and confirm that retinal OCT can indeed provide information on neurodegeneration in the brain,[13] at this time we cannot conclude whether it is a useful biomarker indicating specific HIV-related neurodegeneration based on our cross-sectional data only. Ongoing longitudinal studies will provide more information on the effect of chronic HIV infection and long-term cART on the retinal and cerebral structure and function of both HIV-infected adults and children.

REFERENCES

1. Demirkaya N, Wit F, Schlingemann R, Verbraak F. Neuroretinal Degeneration in HIV Patients Without Opportunistic Ocular Infections in the cART Era. *AIDS Patient Care STDS.* 2015;29(10):519-532.
2. IeDea, Collaborations CC. Global Trends in CD4 Cell Count at the Start of Antiretroviral Therapy: Collaborative Study of Treatment Programs. *Clin Infect Dis.* 2018.
3. Demirkaya N, van Dijk HW, van Schuppen SM, et al. Effect of age on individual retinal layer thickness in normal eyes as measured with spectral-domain optical coherence tomography. *Invest Ophthalmol Vis Sci.* 2013;54(7):4934-4940.
4. Demirkaya N, Wit FW, van Den Berg TJ, et al. HIV-Associated Neuroretinal Disorder in Patients With Well-Suppressed HIV-Infection: A Comparative Cohort Study. *Invest Ophthalmol Vis Sci.* 2016;57(3):1388-1397.
5. Saidha S, Sotirchos ES, Ibrahim MA, et al. Microcystic macular oedema, thickness of the inner nuclear layer of the retina, and disease characteristics in multiple sclerosis: a retrospective study. *Lancet Neurol.* 2012;11(11):963-972.
6. Knier B, Berthele A, Buck D, et al. Optical coherence tomography indicates disease activity prior to clinical onset of central nervous system demyelination. *Mult Scler.* 2015.
7. Schouten J, Cinque P, Gisslen M, Reiss P, Portegies P. HIV-1 infection and cognitive impairment in the cART era: a review. *AIDS.* 2011;25(5):561-575.
8. Su T, Caan MW, Wit FW, et al. White matter structure alterations in HIV-1-infected men with sustained suppression of viraemia on treatment. *AIDS.* 2016;30(2):311-322.
9. London A, Benhar I, Schwartz M. The retina as a window to the brain-from eye research to CNS disorders. *Nat Rev Neurol.* 2013;9(1):44-53.
10. Mutlu U, Bonnemaijer PWM, Ikram MA, et al. Retinal neurodegeneration and brain MRI markers: the Rotterdam Study. *Neurobiol Aging.* 2017;60:183-191.
11. Demirkaya N, Cohen S, Wit FW, et al. Retinal Structure and Function in Perinatally HIV-Infected and cART-Treated Children: A Matched Case-Control Study. *Invest Ophthalmol Vis Sci.* 2015;56(6):3945-3954.
12. Vajzovic L, Rothman AL, Tran-Viet D, Cabrera MT, Freedman SF, Toth CA. Delay in retinal photoreceptor development in very preterm compared to term infants. *Invest Ophthalmol Vis Sci.* 2015;56(2):908-913.
13. Blokhuis C, Demirkaya N, Cohen S, et al. The Eye as a Window to the Brain: Neuroretinal Thickness Is Associated With Microstructural White Matter Injury in HIV-Infected Children. *Invest Ophthalmol Vis Sci.* 2016;57(8):3864-3871.
14. Blokhuis C, Kootstra NA, Caan MWA, Pajkrt D. Neurodevelopmental delay in pediatric HIV/AIDS: current perspectives. *Neurobehavioral HIV Medicine.* 2015.
15. Cohen S, Caan MWA, Mutsaerts H, et al. Cerebral injury in perinatally HIV-infected children compared to matched healthy controls. *Neurology.* 2015.
16. Behnke M, Smith VC. Prenatal substance abuse: short- and long-term effects on the exposed fetus. *Pediatrics.* 2013;131(3):e1009-e1024.
17. Potchen MJ, Kampondeni SD, Mallewa M, Taylor TE, Birbeck GL. Brain imaging in normal kids: a community-based MRI study in Malawian children. *Trop Med Int Health.* 2013;18(4):398-402.

18. van Harmelen AL, van Tol MJ, van der Wee NJ, et al. Reduced medial prefrontal cortex volume in adults reporting childhood emotional maltreatment. *Biol Psychiatry.* 2010;68(9):832-838.
19. Nosarti C, Nam KW, Walshe M, et al. Preterm birth and structural brain alterations in early adulthood. *Neuroimage Clin.* 2014;6:180-191.
20. Blokhuis C, Doeleman S, Cohen S, et al. Inflammatory and Neuronal Biomarkers Associated With Retinal Thinning in Pediatric HIV. *Invest Ophthalmol Vis Sci.* 2017;58(13):5985-5992.

APPENDICES

NEDERLANDSE SAMENVATTING

Introductie

Met de introductie van combinatie antiretrovirale therapie (cART) in 1996 is de incidentie van Humaan Immunodeficiëntie Virus (HIV)-gerelateerde opportunistische ooginfecties, waaronder cytomegalovirus (CMV)-retinitis, sterk gedaald.[1] Tegelijkertijd is ook de incidentie van zowel HIV-gerelateerde dementie als andere ernstige afwijkingen van het centraal zenuwstelsel afgenomen.[2] Desondanks worden ook bij adequaat behandelde HIV-patiënten subtiele functionele en structurele hersen- en retina-afwijkingen beschreven, die respectievelijk de termen *HIV-associated neurocognitive disorder* (HAND)[3] en *HIV-associated neuroretinal disorder* (HIV-NRD)[4] hebben gekregen. Aangezien de retina beschouwd kan worden als een verlengde van het brein, bestaat de mogelijkheid dat er aan deze degeneratieve afwijkingen dezelfde onderliggende mechanismen ten grondslag liggen, bijvoorbeeld directe HIV neurotoxiciteit, HIV-geïnduceerde immuunactivatie en/of neuro-inflammatie.[3,4] De precieze pathofysiologie is vooralsnog niet opgehelderd.

Hoewel het met de huidige Magnetische Resonantie Imaging (MRI)-technieken mogelijk is om de cerebrale structuren en fysiologie zeer gedetailleerd in vivo te bestuderen, komt echter niet iedere patiënt in aanmerking voor een MRI onderzoek en kost het maken van een MRI scan veel tijd en geld. Beeldvormend onderzoek van de retina met optische coherentie tomografie (OCT), is daarentegen relatief eenvoudig uit te voeren en duurt slechts enkele seconden en is niet belastend voor de patiënt. OCT kan de retinale structuren weergeven met een diepte resolutie van ongeveer 5 µm en een laterale resolutie van 15 µm.

De afgelopen jaren zijn meerdere vergelijkende OCT/MRI studies uitgevoerd om te exploreren of meting van de retinadikte (of individuele retinale laagdiktes) gebruikt kan worden als een biomarker voor hersenafwijkingen en dysfunctie bij verschillende neurodegeneratieve aandoeningen, waaronder Morbus Parkinson, Alzheimer Dementie en Multipele Sclerosis.[5-8]

Soortgelijke gecombineerde imaging studies naar HIV-gerelateerde neuroretinale degeneratie en hersenafwijkingen waren echter tot op heden niet uitgevoerd en zijn onderwerp van dit proefschrift.[9]

DOELSTELLINGEN PROEFSCHRIFT

Het doel van dit proefschrift was tweeledig: enerzijds wilden wij door middel van zowel structurele als functionele retinale methoden evalueren of HIV-NRD ook voorkomt bij HIV-patiënten (zowel volwassenen als kinderen) onder langdurige behandeling met cART met een adequate onderdrukking van het HIV-virus; anderzijds wilden wij bepalen of retinadikte (gemeten met Spectral-Domain Optische Coherentie Tomografie [SD-OCT]) een geschikte biomarker is voor (micro)structurele hersenafwijkingen bij HIV-patienten.

Onze studiepopulatie bestond respectievelijk uit deelnemers van de neuro-substudie binnen de AGEhIV Cohort Studie (volwassenen)[10-14] en deelnemers van de NOVICE studie (kinderen)[9,15-18] (**Hoofdstuk 1** gaat dieper in op deze studies).

Hoofdstuk 2 geeft een overzicht van HIV-NRD bij HIV-patiënten zonder opportunistische ooginfecties onder behandeling met cART, en is een meer gedetailleerde introductie voor de studies opgenomen in dit proefschrift.[19] Uit dit overzicht komt naar voren dat de meeste voorgaande studies zich voornamelijk hebben gericht op patiënten met eerder doorgemaakte ernstige immuundeficiëntie (nadir CD4 getal <100 cellen/µl) en/of een klinische AIDS diagnose en de vraag is daarbij onbeantwoord gebleven of HIV-NRD ook voorkomt bij patiënten met een hoger nadir CD4 getal (>350 cellen/µl) en een langdurige onderdrukking van het HIV-virus. Dit is relevant om te weten, aangezien deze groep patiënten een steeds groter percentage vormt binnen de Westerse HIV-geïnfecteerde populatie, sinds tegenwoordig alle richtlijnen behandeling van HIV voorschrijven direct na diagnose en onafhankelijk van de mate van immuundeficiëntie.[20] In **Hoofdstuk 4** proberen wij antwoord te geven op deze vraag.[19]

ASSOCIATIES TUSSEN LEEFTIJD EN RETINALE LAAGDIKTEN

Bij het analyseren van veranderingen in retinale laagdikten, is het belangrijk om een onderscheid te maken tussen effect van de ziekte zelf en fysiologische leeftijdsgebonden veranderingen. In **Hoofdstuk 3**[21] hebben wij daarom associaties onderzocht tussen leeftijd en de dikte van afzonderlijke retinale lagen, door middel van geautomatiseerde segmentatie van SD-OCT scans, in een groep van 120 gezonde deelnemers variërend in leeftijd tussen de 18 en 81 jaar. De intraretinale lagen die met behulp van deze automatische segmentatie geïdentificeerd kunnen worden zijn respectievelijk de zenuwvezellaag (RNFL), ganglion cel laag (GCL), binnenste plexiform laag (OPL), binnenste nucleaire laag (INL), buitenste plexiform laag (OPL), buitenste nucleaire laag (ONL)+ bin-

nenste segment van de fotoreceptoren (IS), buitenste segment van de fotoreceptoren (OS) en het retinale pigment epitheel (RPE). Onze resultaten tonen dat de diktes van de peripapillaire RNFL, pericentrale GCL, perifere IPL en foveale OS significant verdunnen met het ouder worden. De foveale RPE wordt juist dikker met de jaren. Op de overige retinalagen had leeftijd geen significante invloed.[21]

NEURORETINALE VERANDERINGEN BIJ HIV-GEINFECTEERDE VOLWASSENEN

De resultaten in **Hoofdstuk 4**[19] tonen aan dat oudere HIV-patienten (n=92) met langdurige onderdrukking van de infectie onder cART *geen* verhoogde kans hebben op neuroretinale degeneratie/HIV-associated neuroretinal disorder in vergelijking met gezonde controles (n=63). Alhoewel de Pelli Robson contrast gevoeligheid significant verlaagd was in de patienten groep, was het verschil met de controles slechts 1 letter en niet klinisch relevant. Daarnaast had slechts 1 (1.3%) patient een Pelli Robson score van 1.5 (afkapwaarde gebruikt door voorgaande studies om HIV-NRD vast te stellen). In plaats van een verwachte *verdunning*, was de retina in de HIV-geinfecteerde groep juist significant iets *dikker* (+4.6 µm), voornamelijk door een dikkere INL (+1.04 µm) en OPL (+0.95 µm). Follow-up analyses zullen mogelijk meer inzicht geven in de klinische betekenis/relevantie van deze bevinding. Multivariabele regressie analyse toonde geen significante associaties tussen ernst van de HIV infectie (nadir/huidig CD4 getal, eerdere AIDS diagnose en pre-ART plasma viral load) en de retinale parameters.

OCT-MRI correlaties bij HIV-geinfecteerde volwassenen en controles

Hoofdstuk 5 demonstreert dat retinadikte, en in het bijzonder de dikte van de binnenste retinale lagen, significant geassocieerd is met witte stof integriteit (gemeten door middel van diffusie-gewogen MRI; oftewel Diffusion Tensor Imaging [DTI]) en hersenvolume (met name de grijze stof) bij *zowel* HIV-patiënten als niet geïnfecteerde controles (*manuscript in preparatie*). Dit suggereert dat een fysiologische relatie bestaat tussen retina en hersenen welke niet verstoord lijkt te zijn bij patiënten met een adequaat behandelde HIV-infectie. Onze hypothese dat retinadikte/OCT een geschikte biomarker zou kunnen zijn om HIV-gerelateerde cerebrale neurodegeneratie te onderzoeken, wordt echter door deze resultaten helaas **niet** ondersteund.

NEURORETINALE VERANDERINGEN BIJ HIV-GEINFECTEERDE KINDEREN

In **hoofdstuk 6** hebben wij gekeken of er retinale functionele en structurele verschillen waren tussen perinataal HIV-geinfecteerde kinderen (n=33) onder combinatiethera-

pie, en gezonde controles die vergelijkbaar waren qua leeftijd, geslacht, ethniciteit en socioeconomische status (n=36) (NOVICE studie).[15] Het kleurenzien en centrale gezichtsveld was niet verschillend tussen beide groepen; contrastgevoeligheid (Mars kaarten) was significant verminderd bij de HIV-geïnfecteerde kinderen, alhoewel het verschil slechts een halve letter was en niet klinisch relevant. De patiënten hadden een significant dunnere totale foveale dikte (-11.2 µm), voornamelijk door een dunnere buitenste nucleaire laag + binnenste segment van de fotoreceptoren (ONL-IS; ; -6.2 µm). Bij verdere analyse bleek de dikte van deze laag omgekeerd geassocieerd te zijn met de peak viral load. Daarop postuleerden wij dat de foveale maturatie verstoord wordt door perinatale HIV-infectie, wat het meest tot uitdrukking komt in de buitenste nucleaire laag, die van alle foveale lagen het meest toeneemt in dikte tijdens de maturatie fase.[22] De klinische relevantie van een dunnere fovea bij perinataal HIV-geinfecteerde kinderen is vooralsnog onduidelijk, aangezien de visus/visuele functie niet verminderd was bij deze groep.

OCT-MRI correlaties bij perinataal HIV-geinfecteerde kinderen en controles

In **Hoofdstuk 7**[9] staat het onderzoek naar een mogelijk verband tussen verdunning van de retina en MRI afwijkingen bij dezelfde studiepopulatie beschreven. We vonden geen relatie tussen retinadikte en hersenvolume of witte stofafwijkingen, maar verdunning van verschillende retinale lagen bleek wel significant gerelateerd aan een verminderde integriteit van de witte stof bij perinataal HIV-geïnfecteerde kinderen. Dit zou kunnen betekenen dat deze afwijkingen door een vergelijkbaar mechanisme worden veroorzaakt. Het blijft vooralsnog de vraag of het gaat om een verstoring van de normale ontwikkeling, later ontstane schade, of een combinatie van beide.

HIV-GEÏNFECTEERDE VOLWASSENEN VERSUS PERINATAAL HIV-GEÏNFECTEERDE KINDEREN

De verschillen in uitkomsten tussen HIV-geïnfecteerde volwassenen en perinataal HIV-geïnfecteerde kinderen, die wij in dit proefschrift beschrijven, kunnen mogelijk verklaard worden door verschillende factoren, in het bijzonder leeftijd ten tijde van infectie. De gevolgen van chronische HIV-infectie voor perinataal geïnfecteerde kinderen zijn waarschijnlijk anders dan voor volwassenen, omdat de infectie tijdens– in plaats van ná – de (neurale) ontwikkeling optreedt, en daarbij mogelijk de retinale en/of hersenontwikkeling verstoort.[23] Eerder gedetecteerde associaties bij de NOVICE patiënten tussen zowel hersen en retinale afwijkingen met historische HIV ziekte markers, zoals een lager nadir CD4 getal, hogere piek virale load en een AIDS diagnose, ondersteunen de relevantie van sluimerend voortschrijdende HIV-geïnduceerde schade.[15,16] Daarnaast

kunnen ongemeten, niet HIV-gerelateerde factoren, zoals slechte levensomstandigheden in de vroege jaren, ook nadelig zijn geweest voor een normale hersen- en retinale ontwikkeling.[24-26] Zo is bijvoorbeeld ondervoeding c.q. malnutritie in de eerste levensjaren gelinkt aan corticale atrofie,[25] en de mogelijkheid bestaat dat hier ook sprake van was bij een deel van de NOVICE patiënten bestaande uit immigranten. Verder hadden wij geen informatie over eerdere prematuriteit bij deze kinderen, wat mogelijk ook van invloed is geweest op de ontwikkeling van de hersenen en het oog.[22,27]

CONCLUSIES

De resultaten van de onderzoeken beschreven in dit proefschrift suggereren dat volwassen patienten met langdurig adequaat onderdrukte HIV-infectie onder combinatietherapie geen risico hebben op het krijgen van *HIV-associated Neuroretinal Disorder* (neuroretinaal verlies)[19] en dat fysiologische retina-hersen correlaties niet verstoord zijn in deze groep (**Hoofdstuk 5**, *manuscript in preparatie*).

De klinische betekenis van een dunnere fovea bij HIV-geïnfecteerde kinderen is vooralsnog onduidelijk, aangezien deze kinderen een normale visus hadden.[15]

Hoewel onze resultaten indiceren en bevestigen dat retinale OCT inderdaad informatie kan geven over neurodegeneratie in het brein[9](**Hoofstukken 5 en 7**), kunnen we op basis van deze cross-sectionale data nog niet concluderen dat het een bruikbare biomarker is voor specifieke HIV-gerelateerde neurodegeneratie.

Toekomstige analyse van de inmiddels lopende longitudinale studies zullen ons hopelijk meer inzicht geven in het effect van chronische HIV infectie en lange termijn combinatietherapie op de structuur en functie van de retina en het brein bij zowel HIV-geinfecteerde volwassenen als kinderen.

REFERENTIES

1. Goldberg DE, Smithen LM, Angelilli A, Freeman WR. HIV-associated retinopathy in the HAART era. *Retina.* 2005;25(5):633-649; quiz 682-633.
2. Sacktor N. The epidemiology of human immunodeficiency virus-associated neurological disease in the era of highly active antiretroviral therapy. *J Neurovirol.* 2002;8 Suppl 2:115-121.
3. Schouten J, Cinque P, Gisslen M, Reiss P, Portegies P. HIV-1 infection and cognitive impairment in the cART era: a review. *AIDS.* 2011;25(5):561-575.
4. Demirkaya N, Wit F, Schlingemann R, Verbraak F. Neuroretinal Degeneration in HIV Patients Without Opportunistic Ocular Infections in the cART Era. *AIDS Patient Care STDS.* 2015;29(10):519-532.
5. Doustar J, Torbati T, Black KL, Koronyo Y, Koronyo-Hamaoui M. Optical Coherence Tomography in Alzheimer's Disease and Other Neurodegenerative Diseases. *Front Neurol.* 2017;8:701.
6. London A, Benhar I, Schwartz M. The retina as a window to the brain-from eye research to CNS disorders. *Nat Rev Neurol.* 2013;9(1):44-53.
7. Balk LJ, Petzold A. Current and future potential of retinal optical coherence tomography in multiple sclerosis with and without optic neuritis. *Neurodegener Dis Manag.* 2014;4(2):165-176.
8. Sari ES, Koc R, Yazici A, Sahin G, Ermis SS. Ganglion cell-inner plexiform layer thickness in patients with Parkinson disease and association with disease severity and duration. *J Neuroophthalmol.* 2015;35(2):117-121.
9. Blokhuis C, Demirkaya N, Cohen S, et al. The Eye as a Window to the Brain: Neuroretinal Thickness Is Associated With Microstructural White Matter Injury in HIV-Infected Children. *Invest Ophthalmol Vis Sci.* 2016;57(8):3864-3871.
10. Su T, Caan MW, Wit FW, et al. White matter structure alterations in HIV-1-infected men with sustained suppression of viraemia on treatment. *AIDS.* 2016;30(2):311-322.
11. Su T, Wit FW, Caan MW, et al. White matter hyperintensities in relation to cognition in HIV-infected men with sustained suppressed viral load on combination antiretroviral therapy. *AIDS.* 2016;30(15):2329-2339.
12. Su T, Schouten J, Geurtsen GJ, et al. Multivariate normative comparison, a novel method for more reliably detecting cognitive impairment in HIV infection. *AIDS.* 2015;29(5):547-557.
13. Schouten J, Wit FW, Stolte IG, et al. Cross-sectional comparison of the prevalence of age-associated comorbidities and their risk factors between HIV-infected and uninfected individuals: the AGEhIV cohort study. *Clin Infect Dis.* 2014;59(12):1787-1797.
14. Schouten J, Su T, Wit FW, et al. Determinants of reduced cognitive performance in HIV-1-infected middle-aged men on combination antiretroviral therapy. *AIDS.* 2016;30(7):1027-1038.
15. Demirkaya N, Cohen S, Wit FW, et al. Retinal Structure and Function in Perinatally HIV-Infected and cART-Treated Children: A Matched Case-Control Study. *Invest Ophthalmol Vis Sci.* 2015;56(6):3945-3954.
16. Cohen S, Caan MWA, Mutsaerts H, et al. Cerebral injury in perinatally HIV-infected children compared to matched healthy controls. *Neurology.* 2015.
17. Cohen S, Ter Stege JA, Geurtsen GJ, et al. Poorer cognitive performance in perinatally HIV-infected children versus healthy socioeconomically matched controls. *Clin Infect Dis.* 2015;60(7):1111-1119.

18. Blokhuis C, Doeleman S, Cohen S, et al. Inflammatory and Neuronal Biomarkers Associated With Retinal Thinning in Pediatric HIV. *Invest Ophthalmol Vis Sci.* 2017;58(13):5985-5992.
19. Demirkaya N, Wit FW, van Den Berg TJ, et al. HIV-Associated Neuroretinal Disorder in Patients With Well-Suppressed HIV-Infection: A Comparative Cohort Study. *Invest Ophthalmol Vis Sci.* 2016;57(3):1388-1397.
20. IeDea, Collaborations CC. Global Trends in CD4 Cell Count at the Start of Antiretroviral Therapy: Collaborative Study of Treatment Programs. *Clin Infect Dis.* 2018.
21. Demirkaya N, van Dijk HW, van Schuppen SM, et al. Effect of age on individual retinal layer thickness in normal eyes as measured with spectral-domain optical coherence tomography. *Invest Ophthalmol Vis Sci.* 2013;54(7):4934-4940.
22. Vajzovic L, Rothman AL, Tran-Viet D, Cabrera MT, Freedman SF, Toth CA. Delay in retinal photoreceptor development in very preterm compared to term infants. *Invest Ophthalmol Vis Sci.* 2015;56(2):908-913.
23. Blokhuis C, Kootstra NA, Caan MWA, Pajkrt D. Neurodevelopmental delay in pediatric HIV/AIDS: current perspectives. *Neurobehavioral HIV Medicine.* 2015.
24. Behnke M, Smith VC. Prenatal substance abuse: short- and long-term effects on the exposed fetus. *Pediatrics.* 2013;131(3):e1009-e1024.
25. Potchen MJ, Kampondeni SD, Mallewa M, Taylor TE, Birbeck GL. Brain imaging in normal kids: a community-based MRI study in Malawian children. *Trop Med Int Health.* 2013;18(4):398-402.
26. van Harmelen AL, van Tol MJ, van der Wee NJ, et al. Reduced medial prefrontal cortex volume in adults reporting childhood emotional maltreatment. *Biol Psychiatry.* 2010;68(9):832-838.
27. Nosarti C, Nam KW, Walshe M, et al. Preterm birth and structural brain alterations in early adulthood. *Neuroimage Clin.* 2014;6:180-191.

CO-AUTHORS AND AFFILIATIONS

M.D. (MICHAEL) ABRÁMOFF, MD PHD

Department of Ophthalmology and Visual Sciences, Stephen A. Wynn Institute for Vision Research, University of Iowa, Iowa City, United States; Department of Biomedical Engineering and Department of Electrical and Computer Engineering, University of Iowa, Iowa City, United States

T.J.T.P. (THOMAS) VAN DEN BERG, PHD

Netherlands Institute for Neuroscience (NIN), Royal Academy of Sciences (KNAW), Amsterdam, The Netherlands

M.W.A. (MATTHAN) CAAN, PHD

Department of Radiology, Academic Medical Center, University of Amsterdam, The Netherlands

S. (SOPHIE) COHEN, MD PHD

Pediatric Hematology, Immunology, and Infectious Diseases, Emma Children's Hospital, Amsterdam, The Netherlands

H. W. (HILLE) VAN DIJK, MD PHD

Department of Ophthalmology, Academic Medical Center, University of Amsterdam, The Netherlands

M. K. (MONA) GARVIN, PHD

Department of Biomedical Engineering and Department of Electrical and Computer Engineering, University of Iowa, Iowa City, United States

K.W. (KATHERINE) KOOIJ, MD PHD

Department of Global Health, Academic Medical Center, University of Amsterdam, and Amsterdam Institute for Global Health and Development, The Netherlands

T.W. (TACO) KUIJPERS, MD PHD

Pediatric Hematology, Immunology, and Infectious Diseases, Emma Children's Hospital, Amsterdam, The Netherlands

C.B.L.M. (CHARLES) MAJOIE, MD PHD

Department of Radiology, Academic Medical Center, University of Amsterdam, The Netherlands

D. (DASJA) PAJKRT, MD PHD MBA

Pediatric Hematology, Immunology, and Infectious Diseases, Emma Children's Hospital, Amsterdam, The Netherlands

M. (MARIA) PRINS, MD PHD

Division of Infectious Diseases, Center for Infection and Immunity Amsterdam (CINIMA), Academic Medical Center, Amsterdam, The Netherlands; Department of Infectious Diseases Research and Prevention, Public Health Service of Amsterdam, The Netherlands

P. (PETER) REISS, MD PHD

Department of Global Health, Academic Medical Center, University of Amsterdam, and Amsterdam Institute for Global Health and Development, The Netherlands; Department of Internal Medicine, Division of Infectious Diseases, Center for Infection and Immunity Amsterdam (CINIMA), Academic Medical Center, Amsterdam, The Netherlands; HIV Monitoring Foundation, Amsterdam, The Netherlands

H.J. (HENRIËTTE) SCHERPBIER, MD PHD

Pediatric Hematology, Immunology, and Infectious Diseases, Emma Children's Hospital, Amsterdam, The Netherlands

R.O. (REINIER) SCHLINGEMANN, MD PHD

Department of Ophthalmology, Academic Medical Center, University of Amsterdam, The Netherlands; Netherlands Institute for Neuroscience (NIN), Royal Academy of Sciences (KNAW), Amsterdam, The Netherlands

S.M. (SANNE) VAN SCHUPPEN, MD

Department of Ophthalmology, Academic Medical Center, University of Amsterdam, The Netherlands

M. (MILAN) SONKA, PHD

Department of Ophthalmology and Visual Sciences and Department of Electrical and Computer Engineering, University of Iowa, Iowa City, United States

TANJA SU, PHD

Department of Radiology, Academic Medical Center, University of Amsterdam, The Netherlands

F.D. (FRANK) VERBRAAK, MD PHD

Department of Ophthalmology, Academic Medical Center, University of Amsterdam, The Netherlands; Department of Biomedical Engineering and Physics, Academic Medical Center, University of Amsterdam, The Netherlands

F.W.N.M. (FERDINAND) Wit, MD PhD

Department of Global Health, Academic Medical Center, University of Amsterdam, and Amsterdam Institute for Global Health and Development, The Netherlands; Department of Internal Medicine, Division of Infectious Diseases, Center for Infection and Immunity Amsterdam (CINIMA), Academic Medical Center, Amsterdam, The Netherlands; HIV Monitoring Foundation, Amsterdam, The Netherlands

LIST OF PUBLICATIONS

INFLAMMATORY AND NEURONAL BIOMARKERS ASSOCIATED WITH RETINAL THINNING IN PEDIATRIC HIV
C. Blokhuis, S. Doeleman, S. Cohen, **N. Demirkaya**, H.J. Scherpbier, N.A. Kootstra, J. Kuhle, C.E. Teunissen, F.D. Verbraak, D. Pajkrt
Invest Ophthalmol Vis Sci. 2017 Nov 1;58(13):5985-5992.

THE EYE AS A WINDOW TO THE BRAIN: NEURORETINAL THICKNESS IS ASSOCIATED WITH MICROSTRUCTURAL WHITE MATTER INJURY IN HIV-INFECTED CHILDREN
C. Blokhuis*, **N. Demirkaya***, S. Cohen, F.W.N.M. Wit, H.J. Scherpbier, P. Reiss, M.D. Abramoff, M.W.A. Caan, C.B.L.M. Majoie, F.D. Verbraak, D. Pajkrt
Invest Ophthalmol Vis Sci. 2016 Jul 1;57(8):3864-71.
* denotes equal contributors

RETINAL NEURODEGENERATION MAY PRECEDE MICROVASCULAR CHANGES CHARACTERISTIC OF DIABETIC RETINOPATHY IN DIABETES MELLITUS
E.H. Sohn, H.W. van Dijk, C. Jiao, P.H.B. Kok, W. Jeong, **N. Demirkaya**, A. Garmager, F.W.N.M. Wit, M. Kucukevcilioglu, M.E. van Velthoven, J.H. DeVries, R.F. Mullins, M.H. Kuehn, R.O. Schlingemann, M. Sonka, F.D. Verbraak, M.D. Abràmoff
P*roc Natl Acad Sci U S A. 2016 May 10;113(19):E2655-64.*

HIV-ASSOCIATED NEURORETINAL DISORDER IN PATIENTS WITH WELL-SUPPRESSED HIV-INFECTION: A COMPARATIVE COHORT STUDY
N. Demirkaya, F.W.N.M. Wit, T.J.T.P. van den Berg, K.W. Kooij, M. Prins, R.O. Schlingemann, M.D. Abramoff, P. Reiss, F.D. Verbraak
Invest Ophthalmol Vis Sci. 2016 Mar;57(3):1388-97.

NEURORETINAL DEGENERATION IN HIV PATIENTS WITHOUT OPPORTUNISTIC OCULAR INFECTIONS IN THE CART ERA
N. Demirkaya, F.W.N.M. Wit, R.O. Schlingemann, F.D.Verbraak
AIDS Patient Care STDS. 2015 Oct;29(10):519-32. Review.

RETINAL STRUCTURE AND FUNCTION IN PERINATALLY HIV-INFECTED AND CART-TREATED CHILDREN: A MATCHED CASE-CONTROL STUDY
N. Demirkaya, S. Cohen, F.W.N.M. Wit, M.D. Abramoff, R.O. Schlingemann, T.W. Kuijpers, P. Reiss, D. Pajkrt, F.D. Verbraak
Invest Ophthalmol Vis Sci. 2015 Jun;56(6):3945-54.

EFFECT OF AGE ON INDIVIDUAL RETINAL LAYER THICKNESS IN NORMAL EYES AS MEASURED WITH SPECTRAL-DOMAIN OPTICAL COHERENCE TOMOGRAPHY
N. Demirkaya, H.W. van Dijk, S.M. van Schuppen, M.D. Abràmoff, M.K. Garvin, M. Sonka, R.O. Schlingemann, F.D. Verbraak
Invest Ophthalmol Vis Sci. 2013 Jul 22;54(7):4934-40.

CLINICAL AND EEG ANALYSIS OF PATIENTS WITH IDIOPATHIC GENERALIZED EPILEPSY AND PHOTOSENSITIVITY
N. Demirkaya, E.N. Vanli Yavuz, E. Altindag, B. Baykan
Journal of Neurological Sciences-Turkish. 2009. 26 (1): 26-33.

AMC GRADUATE SCHOOL FOR MEDICAL SCIENCES

PHD PORTFOLIO

Name PhD Student: Nazli Demirkaya
PhD Period: 2011 - 2018
Name PhD Supervisors: Dr. Frank D. Verbraak and Dr. Ferdinand W.M.N. Wit

PhD Training	Year	Workload (ECTS)
Courses		
Basic course in legislation and organization for clinical researchers (BROK)	2011	0.9
Oral presentation in English	2012	0.8
Practical biostatistics	2012	1.1
Clinical data management	2012	0.3
Attended (inter)national conferences		
NOG (Dutch Ophthalmology Society annual meeting); Maastricht or Groningen, the Netherlands	2012, 2013, 2014, 2015, 2016, 2017	4.5
ARVO (Association for Research in Vision and Ophthalmology); Fort Lauderdale, Seattle, Orlando and Denver, USA, respectively	2012, 2013, 2014, 2015	5.1
ISIE (International Society for Imaging in the Eye); Fort Lauderdale, Seattle, Orlando and Denver, USA; respectively	2012, 2013, 2014, 2015	1.1
Euretina (European Society of Retina Specialists); Milan, Italy	2012	1.0
DOPS (Dutch Ophthalmology PhD Students) annual meeting; Nijmegen, the Netherlands	2013, 2014	1.0
Leopoldina Symposium: 'Diabetes and Vision'; Rostock, Germany	2013	0.5
Amsterdam Retina Debate; Amsterdam, the Netherlands	2012, 2014	0.6
Course: 'Genetics in Retinal Disease'; Ghent, Belgium	2013	0.25
EACS (European AIDS Clinical Society) conference; Barcelona, Spain	2015	1.0
NCHIV; Amsterdam, the Netherlands	2015	0.25
Amsterdam Kindersymposium; Amsterdam, the Netherlands	2016	0.25
(Oral) Presentations		
NOG (Dutch Ophthalmology Society annual meeting); oral	2013, 2014, 2015, 2016	2.0
ARVO (Association for Research in Vision and Ophthalmology); poster	2012, 2013, 2014, 2015	2.0
NCHIV (Netherlands Conference on HIV Pathogenesis, Epidemiology Prevention and Treatment); poster	2015	0.5
Amsterdam Kindersymposium; oral	2016	0.5
Teaching		

Co-supervising Sanne van Schuppen, master student Research project: Effect of age on individual retinal layer thickness	2012	0.5
OCT education: AMC medical students		0.25
Other		
Attended HIV Journal Club meetings, AMC Amsterdam	2014-2015	0.3
Reviewer for scientific journals	2015-2016	0.6
Organizing committee member of the DOPS annual meeting	2014	2.0
(Co-)written research grant proposals; including awarded AIDS fonds grant nr. 2012033 and a grant received from the Global Ophthalmology Awards Program 2012 (Bayer Healthcare)	2012	1.5

DANKWOORD

Mijn dank gaat uit naar velen (ik zal ongetwijfeld een paar mensen vergeten).

Allereerst alle studiedeelnemers *(OCT & leeftijd, AGE$_h$IV, NOVICE)* die hebben bijgedragen aan de onderzoeken die beschreven zijn in dit proefschrift.

Mijn co-promotoren Dr. Frank Verbraak en Dr. Ferdinand Wit.

Beste Frank, ik had mij geen betere co-promotor kunnen wensen dan jij. Jij hebt vanaf dag 1 veel vertrouwen in mij gehad, ook wanneer ik het zelf niet meer zag zitten, en daar ben ik je zeer dankbaar voor. Je deur stond letterlijk altijd open, en ik kwam dan ook graag dagelijks 'even' buurten bij jou (eigenlijk vooral voor de gezelligheid zoals je weet, haha). Je bent een groot voorbeeld voor mij als onderzoeker en arts, mede door je bescheidenheid, gevoel voor humor en relativeringsvermogen.

Beste Ferdinand, het was zeer leerzaam om met jou samen te werken en dingen niet alleen vanuit een oogheelkundig perspectief te bekijken. Ik wil je in het bijzonder bedanken voor je uitgebreide uitleg bij het uitvoeren en analyseren van de *linear mixed models* (statistiek blijft ingewikkeld).

Mijn promotor Prof. Dr. Reinier Schlingemann. Beste Reinier, dank voor je kritische beoordeling van mijn papers. Je passie voor wetenschap is inspirerend.

De leden van de promotie-commissie, Prof. Dr. Camiel Boon, Prof. Dr. Peter Portegies, Prof. Dr. Jan Prins, Prof. Dr. Liesbeth Reneman, Dr. Henriëtte Scherpbier, Prof Dr. Caroline Klaver en Prof. Dr. Hans Vingerling wil ik hartelijk bedanken voor het kritisch beoordelen van mijn proefschrift en het plaatsnemen in mijn commissie. Caroline en Hans, mede dankzij jullie ben ik aan dit promotie-onderzoek begonnen; ik vind het dan ook een eer dat jullie aanwezig zijn bij mijn verdediging.

Ik vond het bijzonder leuk om vanuit de oogheelkunde te mogen 'aanhaken' bij de AGE$_h$IV en NOVICE studies, ik wil graag bij deze alle collega's bedanken voor de prettige en gezellige samenwerking en interessante bijeenkomsten, in het bijzonder Prof. Dr. Peter Reiss, Prof. Dr. Charles Majoie, Dr. Matthan Caan, Dr. Tanja Su, Dr. Judith Schouten, Dr. Katherine Kooij, Barbara Elsenga, Rosan van Zoest, Dr. Dasja Pajkrt, Dr. Sophie Cohen, Dr. Charlotte Blokhuis en Yvonne van Dalen.

Dr. Tom van den Berg; beste Tom, bedankt voor het ontwikkelen en uitlenen van de C-Quant en voor je bereidheid om altijd mee te denken.

Prof. Dr. Michael Abramoff en zijn team dank ik voor de ontwikkeling van het OCT segmentatie algoritme. Beste Michael, bedankt ook voor je begeleiding in Iowa.

Sanne van Schuppen: Sanne, veel dank voor je hulp bij het opzetten en uitvoeren van de OCT normaalwaarden studie. Leuk dat wij nu collega AIOS zijn!

Oculenti AMC: Hans en Corine, dank voor het rekruteren van deelnemers voor de OCT normaalwaarden studie.

Alle (oud) medewerkers van de afdeling Oogheelkunde van het AMC. Carola, je bent mijn steun en toeverlaat. Mijn buren aan het zuurstokkenplein: Carlos, dames van het secretariaat en trialbureau; dank voor het luisteren als ik weer eens een rondje bij jullie maak.

Professor Mourits (u wordt gemist!), alle stafleden, mijn collega AIOS en oud-assistenten wil ik bedanken voor de fijne samenwerking.

Hille, Pauline, Marilette: de kernleden van het *OCT-team.*

Eline, Alissa, John, Rahman, Gyan, Martin: ARVO 2013 was onvergetelijk (hilarisch) dankzij jullie.

Mijn kamergenoten Stanley en Ann-Sofie : al 7 jaar houd ik het uit met jullie☺. Stanley, leuk dat je mijn paranimf wilt zijn. Ann-Sofie, we'll always have Florence.

Keamy, mijn mede-*minion* en partner in crime. Ik ben benieuwd naar de avonturen die komen gaan.

Mo, in korte tijd zijn wij goede vrienden geworden. Je optimisme is aanstekelijk.

Mijn vrienden en familie, en in het bijzonder:

Mirjam (mijn tweede paranimf), Marlies en Karin: we kennen elkaar al ruim 20 jaar (!). Er is niet veel veranderd in onze vriendschap. Zoals ik altijd zeg: dat moeten wij blijven koesteren. Op naar vele gezellige etentjes en borrels en de jaarlijkse BBQ!

The *unigirls*: Gulhan, Sevilay en Fatma: wat hebben wij een leuke studietijd gehad. Ook al zien wij elkaar tegenwoordig niet vaak meer door onze drukke schema's (en verdwijn ik regelmatig van de radar), het is altijd weer als vanouds als wij afspreken. Bedankt voor jullie begrip en steun de afgelopen maanden.

Özlem Tapirdamaz: het is weer tijd voor een cultureel uitstapje, vind je niet?

Leyla: sorry voor de radiostilte de afgelopen maanden. Hierna heb ik gelukkig meer tijd (hoop ik).

Esma & Gülay Fitoz: bedankt dat jullie er altijd zijn als ik jullie nodig heb. Jullie zijn mijn tweede familie.

Mijn grote broers Özkan en Kerim: canim abilerim. Ik heb erg geboft met jullie en mijn lieve schoonzussen Claudia en Güler.

Mijn neefjes Altan, Arman, Ilyas en Bartu: het leven is zoveel leuker met jullie; ik weet niet meer hoe het was voordat jullie geboren waren. Kuzucuklarim, *hala* houdt heel veel van jullie!

Tot slot, mijn lieve ouders, die mij altijd hebben gestimuleerd mijzelf te blijven ontwikkelen:

Sevgili annecigim ve babacigim, sizin sevginiz ve desteginiz sayesinde bugun buralardayim. Sizin hakkinizi asla ödeyememem. Sizi cok seviyorum.

Canim babam, nurlar icinde uyu.

CURRICULUM VITAE

Nazli Demirkaya was born in 1982 in Schiedam, the Netherlands.

After graduating from the Stedelijk Gymnasium in Schiedam, she started with the Bachelor of Science (Bsc) Biology programme at Leiden University in 2000 and obtained her BSc degree in 2008. During this period, she applied for the study Medicine as well, and got accepted at the Erasmus University Medical Center (Erasmus MC) Rotterdam in 2003. In 2007, she did a research internship at the Department of Neurology (Istanbul Medical Faculty) at Istanbul University, Turkey, for a period of 5 months. In the final year of her medical studies, she followed an elective rotation in Ophthalmology at the Erasmus MC.

After graduating as a Medical Doctor in July 2010, Nazli worked for a brief period as a resident not in training at the Department of Neurology of the Amphia Hospital in Breda, before starting her PhD at the Department of Ophthalmology of the Academic Medical Center (AMC) Amsterdam in May 2011, under the supervision of Dr. Frank Verbraak (and later on Dr. Ferdinand Wit as well). Her research focused on the study of HIV-related neuroretinal degeneration and correlations between retinal and brain changes in HIV-infected adult and pediatric patients on long-term effective treatment, and an overview of the results are in part presented in this dissertation.

As of January 2016, Nazli is in training as a resident in Ophthalmology at the AMC Amsterdam; she plans to complete her residency at the end of 2020, after which she aims to combine research activities with clinical work.